THE SEPARATION OF SODIUM AND POTASSIUM BY CONTINUOUS COUNTERCURRENT ION EXCHANGE

by

C.R. Frost, M.Sc., B.Sc., D.I.C.

A thesis submitted for the degree of Doctor of Philosophy.

Department of Chemical Engineering and Chemical Technology,
Nuclear Technology Laboratory,
Imperial College, S.W.7.

Abstract

The ion exchange separation of sodium and potassium ions in the presence of hydrogen ions has been investigated using a new continuous countercurrent contacting technique.

A wide range of ion exchange operations has been carried out using trace and gross ionic fractions of the alkali metals with contactors of different numbers of stages. By applying equilibrium stage theory the operating conditions have been selected to achieve good enrichment and/or recovery of the alkali metals. In trace experiments with a 15 stage contactor a Na^+ recovery and enrichment of 46% and 9.2 respectively was achieved in the liquid product. A K^+ enrichment of 11 was achieved in the resin in another 15 stage run.

A contactor using three sections, called respectively the extraction, rectification and elution sections has been used to separate trace ionic fractions of sodium and potassium into two product streams. A 15 stage unit has given a Na^+ enrichment and recovery of 2.9 and 91% in the Na^+ rich stream and a K^+ enrichment and recovery of 5.65 and 57.4% in the K^+ rich stream with a loss in the resin waste of only 4.5% of the alkali metals in the feed.

Results have been interpreted by equilibrium stage separation theory. Over a wide range of operating conditions the calculated stage efficiency varied (a) for a glass stage design

from 36% to 70% and (b) for a perspex stage design from 60% to 110%.

It was concluded that equilibrium stage theory can be used to predict the trace ion exchange separations using the new contacting technique and also that as the number of stages is changed the ion exchange separation will be altered in a predictable way.

It was found impossible to get a good enrichment and recovery of Na^+ ions when the two alkali metals were in gross ionic fractions in the feed solution.

Results were shown to be reproducible.

Mass transfer coefficients have been calculated.

The equilibrium relations for the $Na^+/K^+/H^+$ Cl^- system with Zeo-Karb 225 were established to interpret the Na^+/K^+ continuous countercurrent separation results. In the binary Na^+/H^+ and K^+/H^+ systems it was found that the selectivity coefficients K_{NaH} and K_{KH} changed markedly as the loading of the respective alkali metals in the resin increased.

When the alkali metals were in trace ionic fractions, the Na^+/H^+ and K^+/H^+ equilibria attained in the ternary $Na^+/K^+/H^+$ system were the same as in the respective binary systems. However as the ionic fraction of the alkali metals was raised above the trace level, the Na^+/H^+ and K^+/H^+ equilibrium distributions differed increasingly from the respective binary system values.

Acknowledgements.

The author would like to thank Professor G.R. Hall for the invaluable support and encouragement given during the project. Thanks are also due to Mr. Cloete and Dr. Streat for suggesting the project and helpful suggestions in the course of the work. The assistance of the technical staff in ordering items and helping to assemble equipment is acknowledged.

Acknowledgement is also made to Permutit Co. Ltd., for the gift of Zeo-Karb 225 resin used in this work.

Finally I want to thank the UKAEA for the maintenance and equipment grant provided for the project.

CONTENTS. Page

1. Introduction

1.1. Objective of investigation 12

1.2. Review of existing countercurrent ion exchange techniques 13

1.2.1. Dense phase contactors 15

1.2.2. Dilute phase contactors 17

1.2.3. Fluidised bed contactors 19

1.2.4. Special types 20

1.3. Description of technique used 21

1.4. Scope of experimental investigation 31

2. Theory

2.1. Ion exchange equilibria 35

2.1.1. Binary systems 35

2.1.2. Ternary systems 39

2.2. The equilibrium stage concept 42

2.2.1. x - y diagrams 43

2.2.2. Extraction factors 45

2.2.3. Equilibrium stage separation theory 51

2.2.4. Calculation of the number of equivalent ideal stages in the Na^+/K^+ separation processes 56

2.3. Mass transfer 58

2.3.1. Mass transfer coefficients 58

2.3.2. Mass transfer model 60

3. Equilibrium data and other resin properties

3.1. Experimental 63

CONTENTS (Cont'd.)

	Page
3.1.1. Volume exchange capacity	63
3.1.2. Equilibrium measurements	67
3.1.3. Determination of sodium and potassium concentrations in solution	71
3.1.4. Size distribution of resin	83
3.2. Results and discussion	83
3.2.1. Volume exchange capacity	83
3.2.2. Equilibrium measurements with binary cation systems	89
3.2.3. Equilibrium measurements with the ternary $Na^+/K^+/H^+$ Cl^- system	108
3.2.4. Size distribution of resin	115
4. Hydrodynamics	
4.1. Experimental	118
4.2. Results and discussion	119
5. Countercurrent ion exchange separation of sodium and potassium	
5.1. Experimental	123
5.1.1. Single section runs	123
5.1.2. Three section runs	132
5.1.3. Design of Na^+/K^+ separation experiments	139
5.2. Trace ionic fraction results and discussion	141
5.2.1. Single section extraction runs with glass contactor	141
5.2.2. Single section elution runs with glass contactor	154
5.2.3. Single section rectification runs with glass contactor	160
5.2.4. Single section extraction runs with perspex contactor	165

CONTENTS (Cont'd)

	Page
5.2.5. Three section runs	171
5.2.6. Mass transfer calculations	195
5.3. Gross ionic fraction results and discussion	203
5.3.1. Ten stage runs	203
5.3.2. Run 22	208
5.3.3. Run 23	212
5.3.4. Run 24	213
5.3.5. Runs 25, 26, 27 and 28	213
5.3.6. Run 29	214
5.3.7. Discussion	216
6. Conclusions	228
7. References	231
8. Nomenclature	236
Appendix 1. An estimate of the errors involved in the work.	241

No. LIST OF FIGURES. Page

1. Pictorial elevation illustrating the operation of a single stage. 22

2. Typical flow cycle. 23

3. Hydrodynamic operating diagram of a stage for the resin-water system. (M5). 24

4. Glass stages used in preliminary work. 26

5. Perspex contactor components : 28

6. Method of assembly of components in a single perspex contactor stage. 29

7. Bank of ten perspex stages. 30

8. Countercurrent ion exchange separation systems. 32

   (a) Two section unit

   (b) Three section unit

9. Effect of extraction factors on distribution in a countercurrent ion exchange process. 44

10. Stagewise countercurrent separation process. 52

11. Attainment of equilibrium in $\frac{N}{1000}$ KCl - (-14 + 52) BSS 8% D.V.B. H^+ form Zeo-Karb 225 system. 69

12. EEL flame photometer calibration curves for NaCl and KCl standard solutions. 73

13. Relation between free settled and tap settled resin volumes. 88

14. Equilibrium curves for Na^+/H^+ exchange in 8% D.V.B. Zeo-Karb 225 resin. 92

15. Affinity curves for Na^+/H^+ exchange in (-14+52) BSS 8% D.V.B. Zeo-Karb 225 resin 93

16. Equilibrium curves for K^+/H^+ exchange in 8% D.V.B. Zeo-Karb resin. 97

LIST OF FIGURES

No.	(Cont'd.)	Page
17.	Affinity curves for K^+/H^+ exchange in 8% DVB. Zeo-Karb 225 resin.	98
18.	Equilibrium curve for K^+/Na^+ exchange in 8% DVB. Zeo-Karb 225 resin.	101
19.	Size distribution analysis for (-14 + 52) BSS 8% DVB. Zeo-Karb 225 resin.	117
20.	Hydrodynamic operating diagram.	120
21.	Flowsheet for single section ion exchange separation work.	124
22.	Equipment used in ion exchange separation work.	128
23.	Flowsheet for three section ion exchange separation work.	134
24.	x - y diagram for elution run 6	158
25.	x - y diagram for elution run 7	159
26.	Composite three section separation.	162
27.	Block diagrams for three section runs 14 and 15.	179
28.	x - y diagram for Na^+/H^+ exchange in three section run 14	185
29.	x - y diagram for gross ionic fraction run 16	219
30.	x - y diagram for gross ionic fraction run 17	220
31.	x - y diagram for gross ionic fraction run 18	221
32.	x - y diagram for gross ionic fraction run 19	222
33.	x - y diagram for gross ionic fraction run 20	223
34.	x - y diagram for gross ionic fraction run 21.	224

LIST OF TABLES

No.		Page
1.	Effect of centrifuging period on sodium form resin properties.	65
2.	Properties of hydrogen, sodium and potassium forms of (-14 + 52) B.S.S. Zeo-Karb 225 resin.	84
3.	Relation between free settled and tap settled H^+ form resin volumes.	87
4.	Results of equilibrium measurements on Na^+/H^+ exchange system.	90, 91
5.	Results of equilibrium measurements on K^+/H^+ exchange system.	95, 96
6.	Results of equilibrium measurements on K^+/Na^+ exchange system.	100
7.	Results of equilibrium measurements on $Na^+/K^+/H^+$ exchange system.	109, 110
8.	Size distribution analysis for (-14 + 52) BSS 8% DVB Zeo-Karb 225 resin.	116
9.	Operating conditions and results of trace continuous countercurrent ion exchange Na^+/K^+ separation runs using the glass contactor.	142-146 inc.
10.	Liquid product concentrations during trace extraction runs using the glass contactor.	147, 148
11.	Volume balance for trace extraction runs using the glass contactor.	153
12.	Liquid and resin product concentrations during trace elution and rectification runs using the glass contactor.	155
13.	Mass balances for trace elution and rectification runs using the glass contactor.	156
14.	Operating conditions and results of trace continuous countercurrent ion exchange extraction runs using the perspex contactor.	166

LIST OF TABLES

No.	(Cont'd.)	Page
15.	Liquid product concentrations during trace extraction runs in the perspex contactor.	167
16.	Volume balance for trace extraction runs in the perspex contactor.	168
17.	Operating conditions and results of continuous countercurrent trace ion exchange Na^+/K^+ separations using a three section perspex contactor.	172, 173
18.	Liquid product concentrations during three section run 13.	174
19.	Liquid product concentrations during three section run 14.	178
20.	Liquid product concentrations during three section run 15.	187
21.	Volume balance for three section runs.	189
22.	Mass balance for three section runs.	191
23.	Operating conditions and results of gross continuous countercurrent ion exchange extraction runs using the perspex contactor.	204, 205
24.	Liquid product concentrations during 10 stage gross ionic fraction runs.	206, 207
25.	Volume balance for 10 stage gross ionic fraction runs.	209
26.	Liquid product concentrations during 40 and 100 stage gross ionic fraction runs.	210, 211
27.	Liquid product concentrations during run 28.	215
28.	Volume balance for 40 and 100 stage gross ionic fraction runs.	216

1. Introduction

1.1. Objective of investigation.

Although improvements in resin properties and equipment design have led to a rapid increase in the applications and use of ion exchange since the war, until recently practically all large scale ion exchange equipment was based on the use of fixed beds where the resin and regenerant are not utilised most efficiently.

There have been many references to continuous countercurrent ion exchange in the literature. This method of operation should give maximum utilisation of the resin and regenerant because the countercurrent process provides the highest average driving force for mass transfer between the resin and the ionic species being absorbed from solution.

A new continuous countercurrent solids-fluid contacting technique has been developed(C2) in this laboratory and its hydrodynamic operating stability verified on a pilot plant scale(C3).

General principles of countercurrent separation processes, based on equilibrium stage theory, will be applied to ion exchange separations carried out with the new contacting technique. For example the extraction factors for the ions being separated will be selected to achieve a desired recovery and/or enrichment in a single multistage section contactor in a wide range

of ion exchange operations using respectively trace and gross ionic fractions of the ions. The number of stages will be varied and the separation results interpreted by equilibrium stage theory. The ternary cation system Na^+, K^+, H^+ (Cl^- anions) with a separation of the sodium and potassium has been selected for this work.

If it is established that equilibrium stage theory can be applied to ion exchange separations in a single section contactor, it will be applied to more complex countercurrent ion exchange separations.

A by-product of this programme is to develop a compact stage design which will permit separations with contactors of up to 100 stages without using bulky equipment.

The general objective of this work is to establish that fractional separations by continuous countercurrent ion exchange can be predicted and interpreted by equilibrium stage theory.

1.2. Review of existing countercurrent ion exchange techniques.

The potential advantages of continuous countercurrent ion exchange processes (i.e. smaller equipment, lower capital costs, lower resin inventory, increased regeneration efficiency, a higher degree of resin capacity utilisation and

more uniform product) have been long recognised. However there are inherent mechanical and hydraulic difficulties in obtaining satisfactory contact between a liquid and a particulate solid in countercurrent flow. The difficulties arise from the small density difference between the resin and aqueous solutions, attrition of moving resin, channelling and distribution of the two phases through the contactor and the separation of the two phases after contact.

Many types of countercurrent ion exchange contactors have been devised but many are only laboratory curiosities. Since the operating and design problems have remained largely unsolved, the continuous countercurrent ion exchange process has not been properly exploited on a large scale. The requirements of such a contactor are that it should be versatile enough to operate over a wide range of liquid and resin flowrates, and high flowrates are possible without channelling or back-mixing. In addition low pressure drops are desirable in pumping liquids into and through the contacting system. The liquid and resin phases must be separated easily and resin moved between columns or stages simply. In addition the contactor should be inexpensive, simple to operate, easy to control, and for radioactive work suitable for remote operation with minimum maintenance.

Continuous and semi-continuous countercurrent ion exchange contactors can be classified in the following groups

Dense phase contactors

Dilute phase contactors

Fluidised bed contactors

Miscellaneous types.

1.2.1 Dense phase contactors.

This type should have plug flow of the resin and liquid phases so that a high contacting efficiency is possible. The height of a transfer unit will be less than with other types of equipment and capital costs will be smaller.

Operation can be either continuous, cyclic or pulsed, with upflow or downflow of resin.

The only units which operate continuously are the Arehart, Stanton and Hiester contactors, all using downflow of resin, with the dense resin bed positively displaced countercurrent to the liquid flow. In the type[A3,S8] described by Arehart recirculated liquid is pumped at high velocity down through the top section of the bed and the whole resin bed is displaced downwards by frictional drag countercurrent to the liquid influent. With the Stanton[S7] and Hiester[H3] types there are special valves at the bottom, and top and bottom, of the columns respectively which cause attrition of the resin.

Cyclic contactors where the two phases flow alternately through the contactor in opposite directions have the advantages of higher capacity and greater flexibility since operating conditions can be controlled by the choice of cycle times. The Higgins,(H6) with upflow of resin and Porter(P6) and Asahi,(A4) with downflow of resin are of this type.

The Higgins contactor has been considered or used by the USAEC in many pilot plant scale operations (H7,H8,H9) and there are now 18 large scale plants in operation(H10). Adsorption and regeneration cycles are performed in the same unit and this does not permit optimum utilisation of the resin and regenerant. In addition the complex operating cycle and valves required lead to resin attrition and maintenance problems.

The Porter and Asahi contactors use separate columns for saturation and regeneration. The Asahi contactor has been used for large scale water processing for about 7 years in Japan where 16 units are in operation. Several processes using the Asahi contactor have been patented including the production of NaOH from sea water using $Ca(OH)_2$.(A5)

With the pulsed contactor the pulse rate and amplitude of the pulsing device control the flowrates of the two phases. Two types have been recently developed.

The Erickson contactor[E2,P4] is an upward resin flow contactor. The resin flowrate was found to drop markedly as the liquid flowrate increased and when the height of the column was increased.

The Meyer design[M3] is a downward resin flow type. Flow of liquid and resin into the contactor is controlled by ball valves. As the only moving parts in the contactor are the ball valves the system is mechanically very simple. With a 3 in. diameter column flowrates up to 200 gall/(ft^2)(hr) were used without detectable backmixing or fluidisation of resin and tests showed that the liquid moved in plug flow. This contactor design appeared to have some commercial potential.

1.2.2 Dilute phase contactors.

In this type the resin particles settle by gravity countercurrent to the liquid flow. As the specific gravity of most resins is little greater than that of water, a considerable restriction is imposed on the range of operation. Early patents of this type were by Matthieson[M2] and Nordell[N1,N2].

In the Gorshkov contactor[G6] the liquid and resin are recirculated countercurrent through two columns and a regeneration unit. The operating conditions are chosen to give a large separation factor for the cations A and B being separated. After a time pure solutions of A and B can be withdrawn from the

two columns respectively. This column has been used on a laboratory scale to separate alkali metals[G9], rare earths[G7] and lithium isotopes[G8].

In the Shulman[S4] contactor plastic tubing is looped around a tilted drum. Resin is fed to the top and liquid to the bottom of the unit through rotary joints. Rotation of the drum causes resin to move down through the tubing countercurrent to the liquid feed. It was found that resin did not fill the cross section of the plastic tube and channelling of the liquid past the resin occurred at all flowrates.

Spinner columns[O1] in which baffles attached to a rapidly rotating central rod swirl the liquid have been developed to prevent channelling of the liquid through the falling resin particles. In the Plate type contactor[A1], a scraper rotating above each plate moves the resin down a column through staggered holes countercurrent to the upflowing liquid. There is poor utilisation of resin in this type.

Although the dilute phase contactor has proved very successful for some difficult separations on the laboratory scale, the restriction of the liquid flowrate to the settling velocity of the resin particles makes it very unlikely that this type of contactor will ever have widespread commercial application.

1.2.3 Fluidised bed contactors.

This type can be either continuous, cyclic or pulsed. Although the liquid flowrate can be much greater than in the dilute phase type, because the resin particles are not settling against the upward flow of liquid, the maximum flowrate of liquid is restricted as co-current transport of the resin particles is undesirable. There is no tendency for resin bed blockage to occur with such equipment and a liquid feed with suspended solids can be treated.

Continuous units.

The concept of a multi-bed column simulating a plate fractionating column was first suggested by Perry[P3]. Recent work on this type has been described by Komarovskii[K1] and Turner.[T1] Liquid flows upwards through perforations in the plates gently fluidising the resin particles. The resin descends the column through downcomers. A disadvantage is the tendency of the liquid to flow up the downcomers rather than through the perforations in the plates, especially at start-up.

With the Selke[S1], Jigged Bed[A2] and Dorr Hydrosoftener[H5] units, the resin is fluidised in a tower. The basis of countercurrent operation is that as saturation of the resin particles proceeds they become more dense and settle from the fluidised region to the bottom of the column.

Cyclic units.

The Zsigmond contactor[Z1] consists of two concentric vessels containing resin which communicate at the top. In the saturation cycle liquid passes up through the central compartment fluidising the resin and down through the outer compartment. In elution periods the regenerant passes through the contactor in the opposite direction.

Pulsed units.

It is claimed[S9] that a rapidly pulsating liquid feed greatly improves the performance of the Perry type contactor. An expanded resin bed is formed on each plate but there is relatively little turbulence or backmixing of the resin. The bed flows like a dense fluid across the plates to the downcomers. A wider range of flowrates can also be used. The use of a bed of stainless steel balls resting on each plate has been proposed[G11] to prevent clogging of the perforations.

1.2.4 Special types.

Various methods using a continuous belt of exchanger have been suggested. The ion exchanger has been enclosed in a porous casing[M1] and moved through counterflowing feed and regenerant solutions like a string of sausages. Selke and Muendel[S2] have performed experiments with an endless belt of phosphorylated cotton. A wire mesh coated with ion exchange

resin has also been used(M4).

1.3. Description of technique used.

The work described here has been performed using a new cyclic continuous countercurrent ion exchange contactor. This design fulfills most of the requirements for a countercurrent contactor satisfactorily.

A single stage of this contactor consists of two compartments, a contactor and a retainer. Figure 1 shows a single stage in the three parts of the operating cycle. The liquid flow cycle (Figure 2) is controlled by means of two three way solenoid valves actuated by the cycle timer. During forward flow of liquid the resin in each stage is fluidised. In the no flow period, liquid flow is stopped to allow the resin particles to settle. This period is not essential if the particles settle in substantially less time than the reverse flow period. In the reverse flow period an increment of resin, W, is transferred in dense phase flow countercurrent to the net flow of liquid. The value of W is dependent only on the volume of liquid displaced in the reverse flow period i.e. $U_r t_r$. The hydrodynamic operating diagram, which defines the range of operating conditions for a typical single stage, is shown in Figure 3. A characteristic of the curves in the diagram is the maximum value, W_{max}, corresponding to all values of H above a certain value, $H_{critical}$, for any given set of conditions.

FIGURE 1 PICTORIAL ELEVATION ILLUSTRATING THE OPERATION OF A SINGLE STAGE

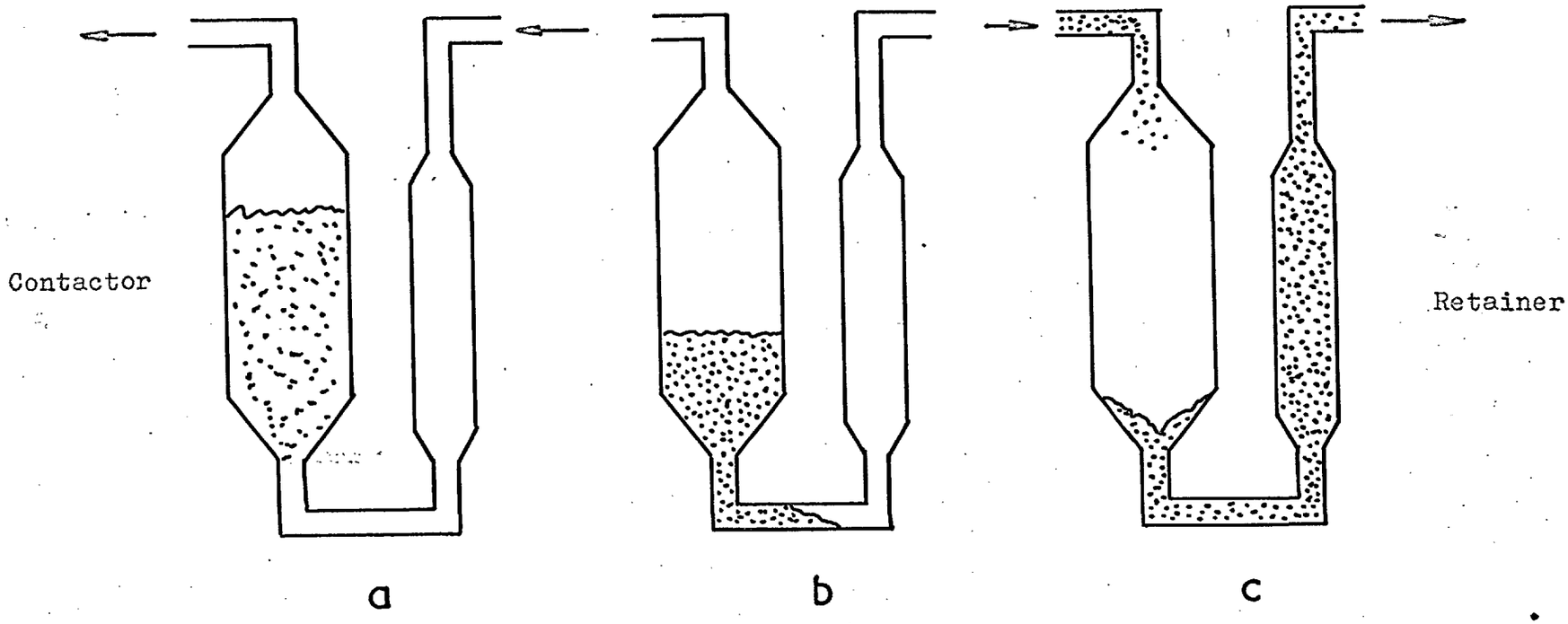

a = forward flow of fluid

b = no flow of fluid

c = reverse flow of fluid

FIGURE 2 TYPICAL FLOW CYCLE

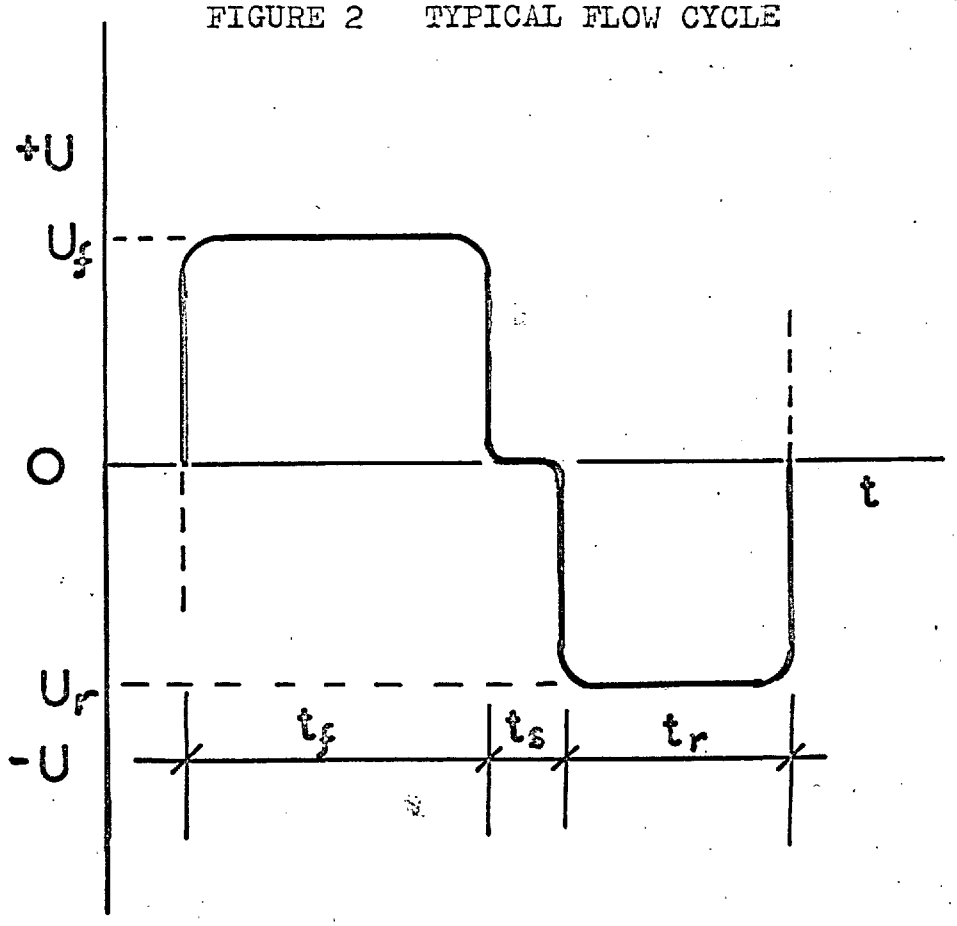

Average flowrate of solids, $S = \frac{W}{(t_f + t_s + t_r)}$

Average flowrate of liquid, $L = \frac{(U_f t_f - U_r t_r)}{(t_f + t_s + t_r)}$

FIGURE 3 HYDRODYNAMIC OPERATING DIAGRAM OF A STAGE FOR THE RESIN-WATER SYSTEM (M5)

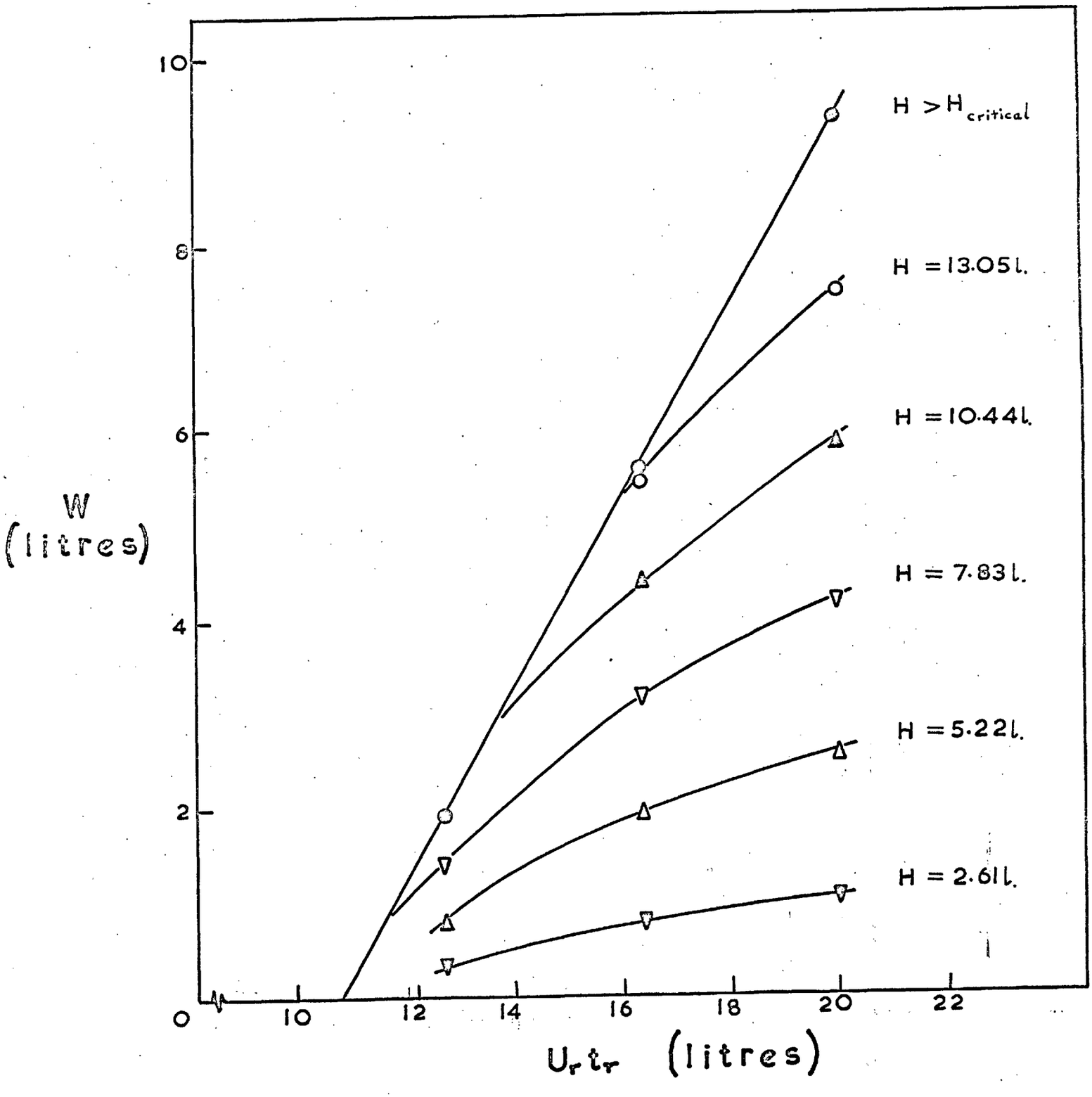

The average liquid flowrate is given by the expression

$$L = \frac{U_f t_f - U_r t_r}{t_f + t_r + t_s} \qquad (1.1)$$

and the average resin flowrate by

$$S = \frac{W}{t_f + t_r + t_s} \qquad (1.2)$$

The operation of this type of contactor is governed by a cycle timer and control of the liquid flowrate.

In a multistage contactor of this type it is possible to feed and take-off resin and liquid at intermediate points, so that the $\frac{L}{S}$ ratio can be altered, thereby adjusting the extraction factor in various sections of the contactor.

Early work was conducted with banks of three glass stages (Figure 4) connected by Quickfit ball and socket joints. Miller[M5] has recommended that the ratio of $\frac{\text{contactor}}{\text{retainer}}$ volume should be at least 1.9 for operation of this type of contactor. The volume ratio of $\frac{20.7}{11.3}$, or 1.84 for the glass stages was close to the recommended value.

The size and fragility of the glass stages would be a disadvantage in experiments using up to 100 stages, and since this was anticipated in future work a compact stage design which could be easily mass produced was developed. It was apparent

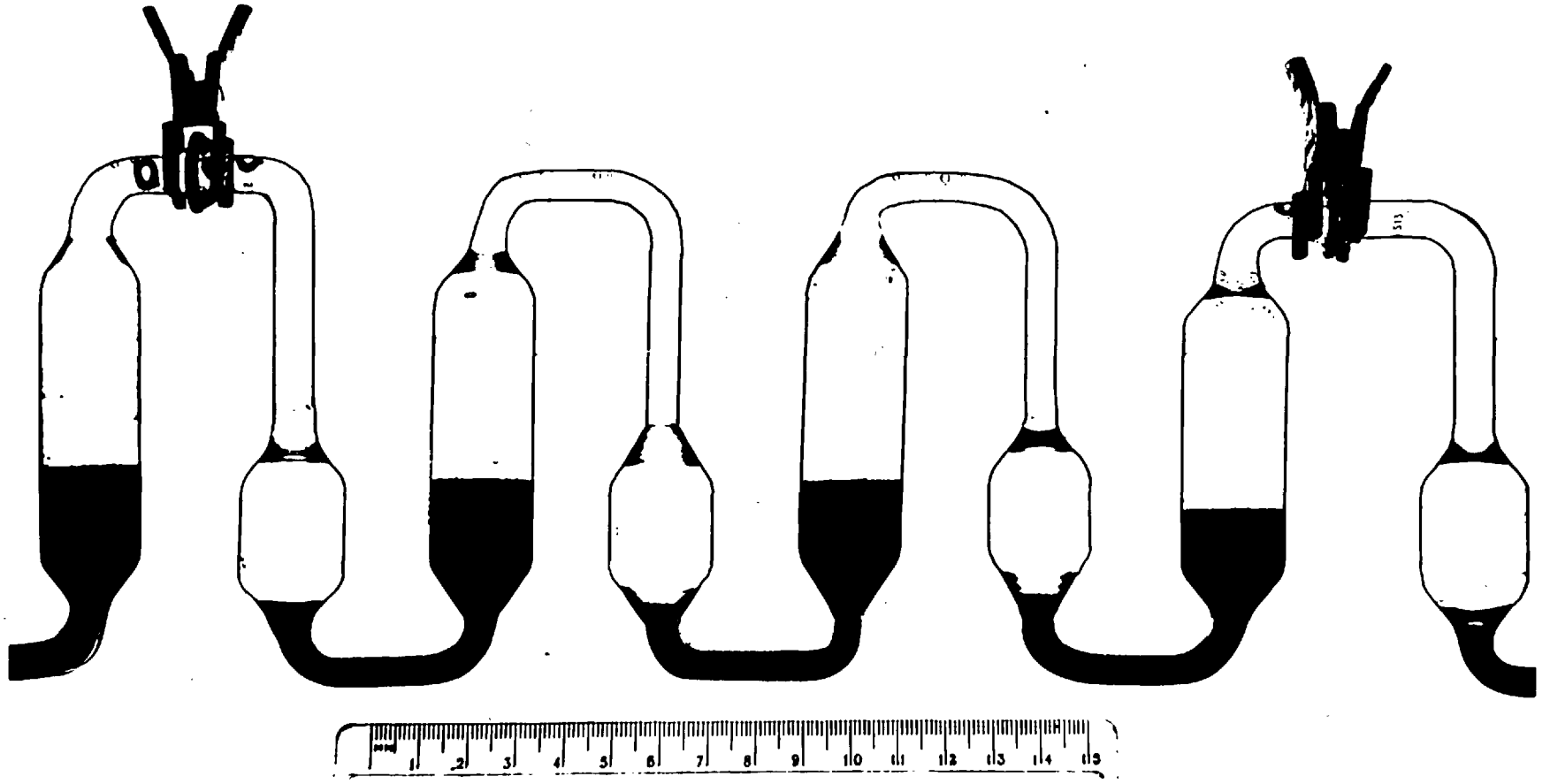

FIGURE 4 GLASS STAGES USED IN PRELIMINARY WORK

that each stage should consist of a number of components which could be machined or milled out of sheet material. Perspex was chosen as the material of construction because it is cheap, robust, easily worked, available in sheets of many thicknesses accurate to small tolerances and chemically stable in the aqueous work planned.

The new design (Figure 5) was developed after evaluating three prototypes by residence time distribution and mass transfer studies.

It is based on milled out 4in. x 2 in. perspex blanks held together like plates in a filter press. The contactor to retainer volume ratio is 2.42. As each stage is only $\frac{5}{8}$in. thick a contactor of 100 stages is only about 5 ft. long and is easily accommodated on a bench top. The method of assembly of a single stage is shown in Figure 6 and a bank of ten assembled stages in Figure 7.

FIGURE 5 PERSPEX CONTACTOR COMPONENTS

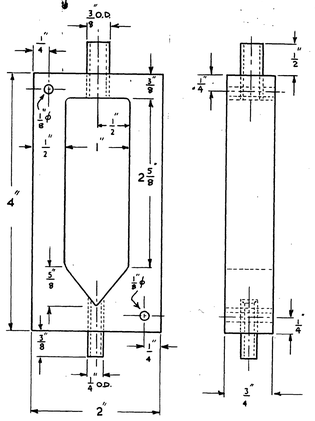

RESIN INLET

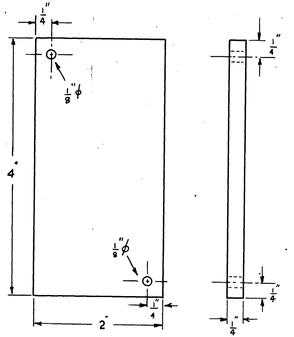

END

NOTE:-
WITH LIQUID INLET, RESIN INLET AND CONTACTOR COMPONENTS, INTERNAL CORNERS TO BE 1/8 IN. RADIUS.

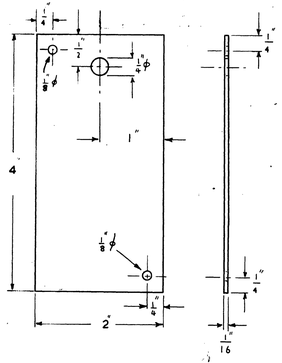

BAFFLE

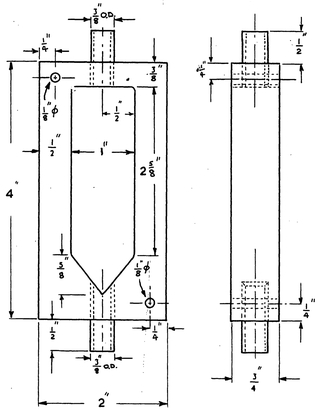

LIQUID INLET

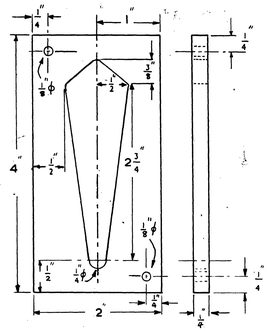

CONTACTOR

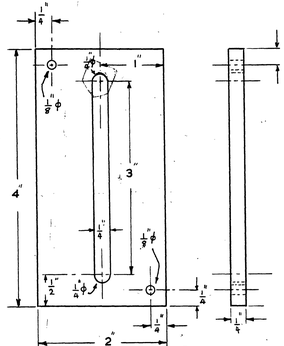

RETAINER

FIGURE 6. METHOD OF ASSEMBLY OF COMPONENTS IN A SINGLE PERSPEX CONTACTOR STAGE

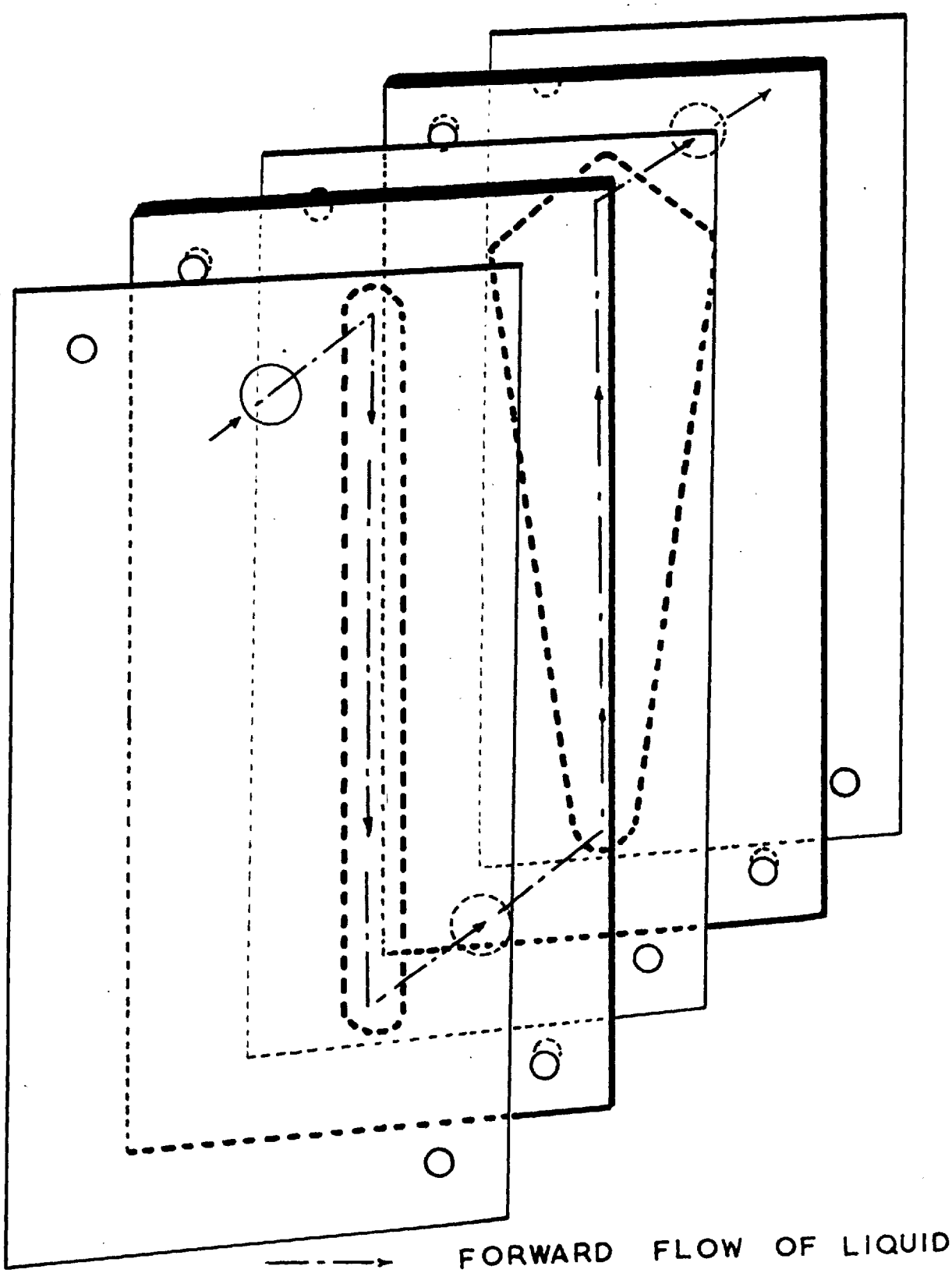

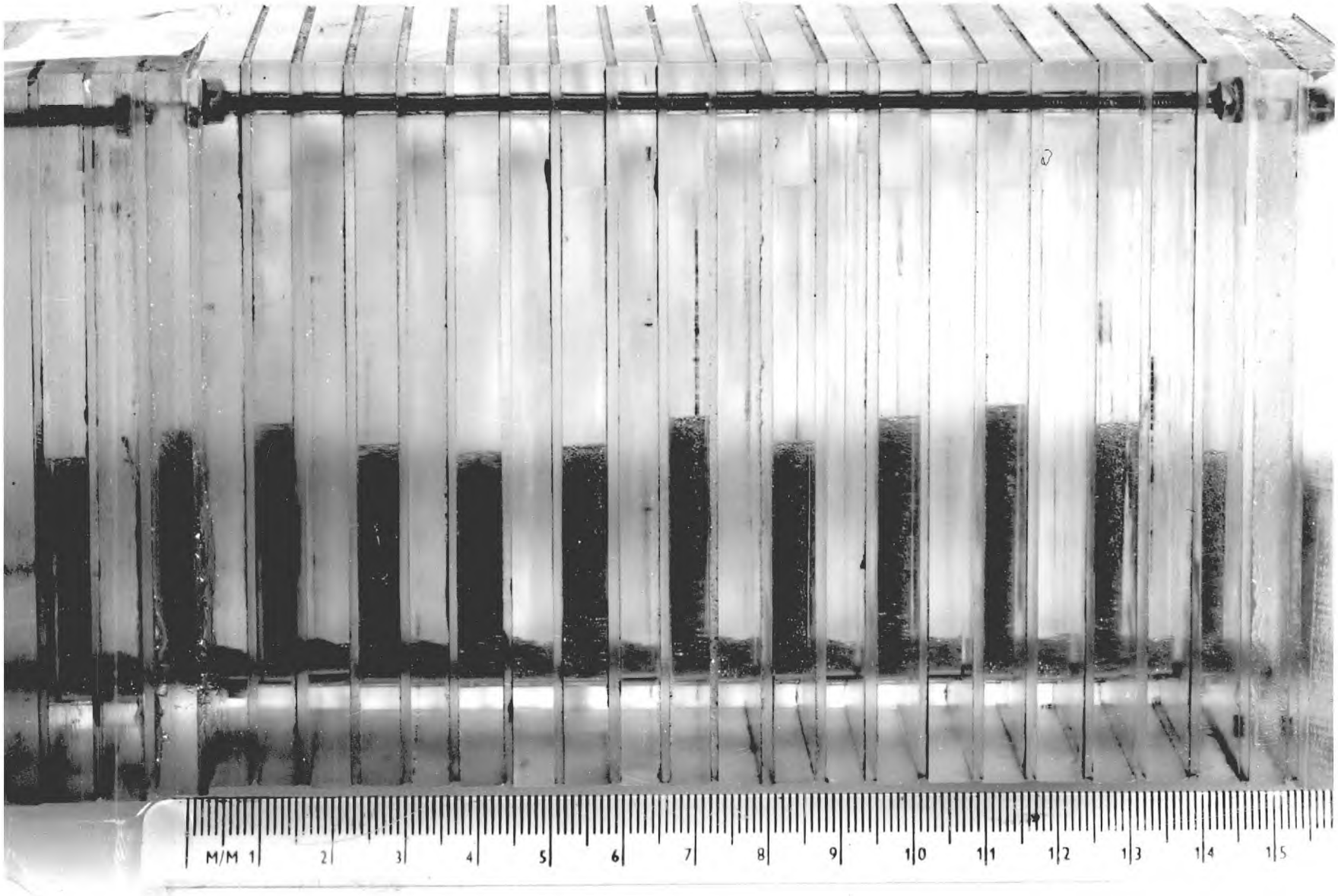

FIGURE 7 BANK OF TEN PERSPEX STAGES

1.4. Scope of experimental investigation.

An important criterion in the choice of a system to be separated was that concentrations of components could be determined accurately and, if possible, quickly. Other requirements were that all components used in the separation should be available at high purity and reasonable cost and no complexing or side reactions should occur so that operation over a wide range of conditions is possible.

The chemical system chosen was sodium and potassium using hydrogen as the third component, with chloride anions. The alkali metal concentrations can be determined by flame photometric methods and hydrogen ion concentrations are readily measured by titration. This system has the additional advantages that the ions are monovalent and equivalent and the alkali metals are known to have a separation factor, K_{KH}/K_{NaH}, of about 2, so that a measurable separation should be possible using a small number of stages.

A total cation concentration of 0.1N was chosen for this work because penetration of solute into the resin is negligibly small (section 2.1). The ion exchange resin used was the strongly acidic 8% D.V.B. Zeo-Karb 225 ((-14 + 52) B.S.S.), a sulphonated polystyrene type resin.

The simplest arrangement (Figure 8(a)) for a countercurrent separation unit consists of two sections, an

FIGURE 8 COUNTERCURRENT ION EXCHANGE SEPARATION SYSTEMS

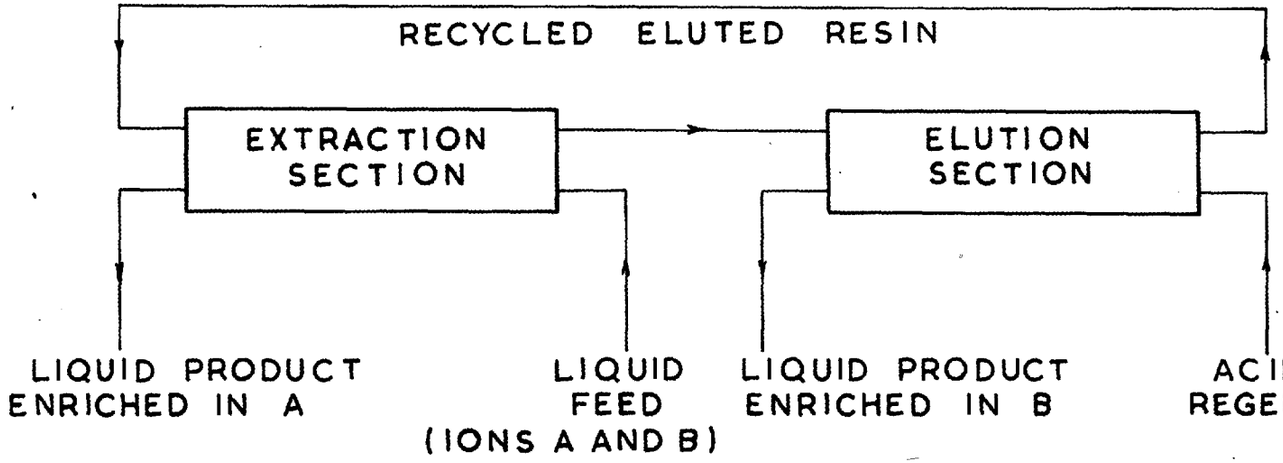

(a) TWO SECTION UNIT

(b) THREE SECTION UNIT.

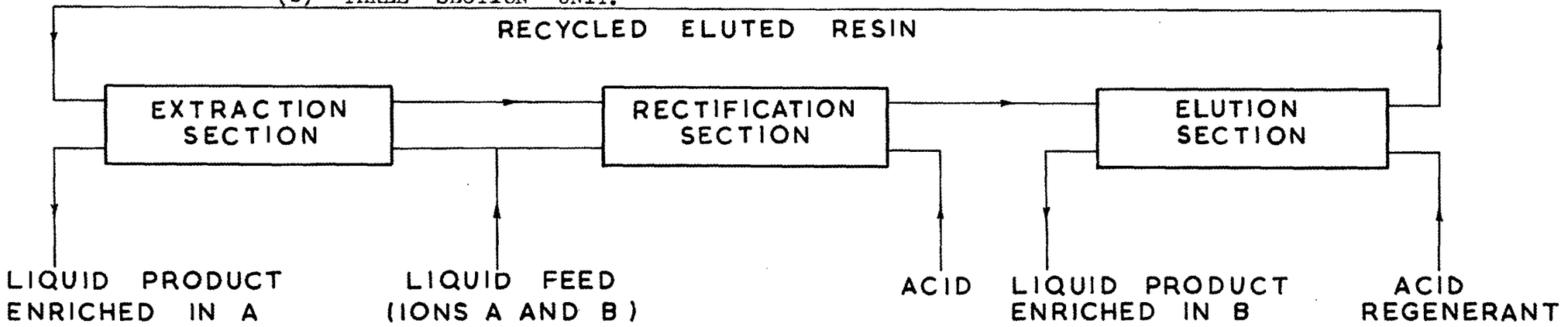

extraction section and an elution section. The feed solution containing the ions to be separated, say cations A and B, enters the extraction section. Some separation of cations A and B occurs in this section and the solution leaving is enriched in the component, say A, least strongly held by the resin. The resin containing most of B and the rest of A is reconverted to the hydrogen form in the elution section by the acid feed and is recirculated to the extraction section.

In a slightly different system two sections with an acid feed are used (Figure 8(b)). In the rectification section operating conditions are arranged so that enrichment of B occurs in the resin. The liquid product from the rectification section is circulated to the extraction section after being mixed with the feed liquid containing ionic species A and B. With almost complete regeneration of the B enriched resin, the liquid product stream from the elution section is much enriched in cation B.

A number of single section extraction, rectification and elution runs using trace ionic fractions of sodium and potassium in the liquid feed were carried out separately using the glass stages. On the basis of these results a composite three section Na^+/K^+ separation was designed and carried out with the perspex contactor.

Little work has been reported on the ion exchange separation of ions in gross ionic fractions. Using the perspex

contactor as a single section unit of up to 100 stages the separation of sodium and potassium in gross ionic fractions was investigated. A liquid feed containing equimolar concentrations of sodium and potassium (no hydrogen) and a H^+ form resin feed were used.

The aim of these experiments was to investigate the Na^+/K^+ separation performance of the new type of contactor under a wide range of operating conditions and relate this to the equilibrium stage theory.

The equilibrium relations for the $Na^+/K^+/H^+$ Cl^- - Zeo-Karb 225 resin system were required for the interpretation of the separation results. There are plenty of published equilibrium data for the K^+/H^+ (B2, G1, R3) and Na^+/H^+ (B2, D4, G1, M8, R2, R3) exchange with sulphonated polystyrene resins but exchange properties can vary from particle to particle in the same resin batch (H11) and often the equilibrium data on one type of resin are conflicting (B2, M8), so it was decided to establish the equilibrium relations with the batch of resin used in this work. Other resin properties measured were the density of the resin in the H^+, Na^+ and K^+ forms and the size distribution, which were required for mass transfer calculations.

2. Theory

2.1. Ion exchange equilibria

2.1.1. Binary systems

When an ion exchanger containing counter ion B^b is placed in a solution containing counter ion A^a an equilibrium of the two counter ion species is set up between the two phases

$$a\,\bar{B}^{b} + b\,A^{a} \rightleftharpoons b\,\bar{A}^{a} + a\,B^{b}$$

where a, b are the valencies of the two ions.

Except in rare cases the exchange is reversible and the equilibrium is determined by the properties and amounts of the components present. Ion exchange is a stoichiometric reaction.

The concentrations of the two competing counter ion species in the ion exchanger are usually different from those in solution because the exchanger selects one ion in preference to the other. The selectivity of the exchanger is an important property and it has been utilised in this project to separate sodium and potassium ions.

The selectivity coefficient, K_{AB} is defined by the expression

$$K_{AB} = \frac{\left[\bar{c}_A\right]^b \left[c_B\right]^a}{\left[\bar{c}_B\right]^a \left[c_A\right]^b} \qquad (2.1)$$

The brackets represent ionic concentrations in the two phases and the selectivity coefficient is calculated from experimental concentration values.

This definition is of the same form as the equation obtained when the law of mass action is applied to ion exchange without activity corrections, but unlike the thermodynamic equilibrium constant, the selectivity coefficient is not constant, varying with experimental conditions and the ionic composition of the resin. In using this definition of the selectivity coefficient, the penetration of counter ions (which is associated with co-ion penetration) into the resin matrix in addition to those which are equivalent to the fixed ionic groups in the resin has been considered negligible. This is reasonable with a strongly acidic or basic resin*. In other words the ion exchange

*On the basis of a Donnan equilibrium, an approximate relation(G5) can be derived for the uptake of co-ions, $\bar{c}_{co}$, which will equal the additional counter ion penetration.

$$\bar{c}_{co} = \frac{c^2}{\bar{c}}$$

where all quantities are expressed in equivalent units.

$\therefore \bar{c}_{co} = \frac{0.1^2}{2} = 0.005$ meq/cm^3 resin in the present work or 0.25% of the exchange capacity of the resin. This value can be compared with the uptake of Na co-ions in a polystyrene D.V.B. anion exchanger of 5.2×10^{-3} meq/g. resin(G5). This corresponds to 0.4% of the exchange capacity of the resin.

capacity has been taken to be the content of fixed ionic groups.

The equivalent ionic fraction of an ion in solution is defined by

$$x_A = \frac{a\ c_A}{a\ c_A + b\ c_B} \qquad (2.2)$$

similarly in the resin

$$y_A = \frac{a\ \bar{c}_A}{a\ \bar{c}_A + b\bar{c}_B} \qquad (2.3)$$

Expressing the selectivity coefficient in terms of equivalent ionic fractions

$$K_{AB}\left[\frac{\bar{c}}{c}\right]^{b-a} = \frac{\left[\frac{\bar{c}_A}{\bar{c}}\right]^b \left[\frac{c_B}{c}\right]^a}{\left[\frac{\bar{c}_B}{\bar{c}}\right]^a \left[\frac{c_A}{c}\right]^b} = \frac{y_A^{\,b}\ x_B^{\,a}}{y_B^{\,a}\ x_A^{\,b}} \qquad (2.4)$$

In chromatographic applications of ion exchange where a trace ion A is being separated from an ion G in relatively gross concentration, the distribution coefficient λ_A can be conveniently used to describe the ion exchange equilibrium.

The distribution coefficient is defined by

$$\lambda_A = \frac{\bar{c}_A}{c_A} = \frac{y_A\ \bar{c}}{x_A\ c} \qquad (2.5)$$

Substituting from equation (2.4)

$$\lambda_A = K_{AG}^{\frac{1}{g}} \left[\frac{\bar{c}_G}{c_G}\right]^{\frac{a}{g}} \qquad (2.6)$$

G is present in large excess and although the concentration of A is varied over orders of magnitude (0.1% to 1% for example) the concentration of the gross ion G in the resin and solution phases is effectively constant. As K_{AG} can also be considered constant over the small concentration range, λ_A is constant, in other words the distribution coefficient for trace ion A is independent of its concentration and the uptake of the trace ion in the resin is directly proportional to its concentration in the external solution.

As $c_G \simeq c$ and $\bar{c}_G \simeq \bar{c}$, equation (2.6) can be written

$$\lambda_A \simeq K_{AG}^{\frac{1}{g}} \left[\frac{\bar{c}}{c}\right]^{\frac{a}{g}} \qquad (2.7)$$

Monovalent ion exchange

If the exchange of monovalent ions is considered, the above equations have the following form.

From equations (2.3) and (2.4)

$$x_A = \frac{c_A}{c} \text{ and } y_A = \frac{\bar{c}_A}{\bar{c}} \qquad (2.8)$$

From equations (2.1) and (2.4)

$$K_{AB} = \frac{\bar{c}_A \, c_B}{\bar{c}_B \, c_A} = \frac{y_A \, x_B}{y_B \, x_A} = \frac{y_A \, (1 - x_A)}{x_A \, (1 - y_A)} \qquad (2.9)$$

From equation (2.7)

$$\lambda_A = K_{AG} \left[\frac{\bar{c}}{c}\right] \qquad (2.10)$$

2.1.2. Ternary systems

Using the general definition of equation (2.1), the selectivity coefficient, K, can be calculated for any pair of ionic species in a ternary system. Similarly equations (2.5), (2.6) and (2.7) apply to ternary exchange systems and equation (2.10) to monovalent ternary systems.

General forms of equations (2.2) and (2.3)

$$x_A = \frac{a \, c_A}{\Sigma_i c_i} \qquad (2.11)$$

and $$y_A = \frac{a \, \bar{c}_A}{\Sigma_i \bar{c}_i} \qquad (2.12)$$

must be used. Equation (2.8) applies to monovalent ternary systems.

Trace and gross ionic fractions are discussed separately.

Trace ionic fractions.

It is generally assumed that interaction between the two trace components can be neglected so that the selectivity of the resin for each of the trace components in the mixture can be considered the same as in a system where there is only one trace component with the gross component.

There are few references to ternary or multi-component trace ionic fraction cation systems in the literature. Jasz and Lengyel[J1] investigated ternary and quaternary mixtures of the monovalent ions H^+, Na^+, Rb^+ and Cs^+ with the alkali metal ions in trace ionic fractions and the total cation concentration 0.001N. They found that the equilibrium relations between each of the trace cations and hydrogen were linear, so that each trace component behaved independently of the others in the ion exchange equilibria.

Hiester[H3] studied the $Li^+/K^+/H^+$ system in approximately 1N total concentration with the alkali metals in trace concentrations. Again the equilibrium distribution line for each of the trace components with hydrogen was linear. The resin used in both these investigations was of the sulphonated polystyrene type.

It can be concluded that the selectivity of the resin towards each of the trace ions in a mixture, with respect to the main component, is not affected by the presence of the

other trace ions. The general equations (2.1), (2.3), (2.5), (2.9) can all be used for ternary systems.

Gross ionic fractions

Little work has been published on ion exchange equilibria with gross ionic fractions.

Dranoff and Lapidus[D3] investigated the ternary systems $Na^+/H^+/Ag^+$ and $Cu^{++}/H^+/Ag^+$ (NO_3^- or SO_4^{--} anions) with Dowex 50, using a total concentration of 0.1N in solution. Results were represented on x - y diagrams, each ternary mixture being considered as three binary systems. Although their results showed much scatter, and it was known that the selectivity coefficient for each of the pairs varied considerably with resin loading, they found the single mean value of K which best fitted their results over the whole composition range. Because the mean value of K was usually within the range of K values given in the literature (their value of K_{NaH} of 2.8 can be compared with the range of 1.2 to 1.6 for K_{NaH} for Dowex 50 found by other workers [B2]) it was concluded that each pair of cations in a ternary mixture behaves as if the third cation is absent.

Hiester has studied the ternary $Li^+/K^+/H^+$ system [H4] with Chempro C-20 resin (a sulphonated polystyrene - DVB resin) with gross ionic fractions of the alkali metal ions. The total ion concentration was approximately 1N. Results for each

pair of cations were plotted as (for the K^+/H^+ pair for example) $y_K\, x_H$ against $x_K\, y_H$. A straight line could be drawn through the points on all diagrams, so that the selectivity coefficient for each pair of cations was constant over the whole concentration range.

It is known however that the selectivity coefficient varies in each of these binary systems. For example Ghate[G1] investigated K^+/H^+ exchange in Amberlite IR-120, a similar type of resin, with 1N concentrations of the cations. It was found that as y_K increased from 0, K_{KH} decreased from 11.8 to 1.26 at $y_K = 0.6$, and then increased to 3.2 as y_K rose to 1.0.

Although both Dranoff and Hiester concluded that the presence of the third cation species in a ternary gross ionic fraction system had no effect on the ion exchange equilibrium for each pair of cations, their conclusions must be regarded with scepticism.

2.2. The equilibrium stage concept.

Equilibrium stage theory has been used to interpret the Na^+/K^+ separation in the multistage countercurrent ion exchange runs.

A stage is a vessel in which the solution containing the ions to be separated and the resin are intimately mixed, allowed to approach equilibrium and then separated into two

phases which are then withdrawn. An ideal stage is one where contact between the liquid and the resin is sufficiently good and maintained for sufficient time that distribution equilibrium is established and the resin and liquid product streams leaving the stage are in equilibrium.

2.2.1. x - y diagrams.

In view of the complicated ion exchange equilibrium relations in ternary cation systems, especially when sodium and potassium are in gross ionic fractions, graphical methods are very useful in interpreting separation results.

Since the total ionic concentration in both phases is constant the material balance or operating line for each cation is linear and is defined by the general equation

$$y = \frac{Lc}{Sc} x + K_3 \qquad (2.13)$$

The equilibrium distribution line and the material balance line can be related by McCabe - Thiele methods (Case (a) Figure 9). The position of the operating line is fixed by the composition of both phases at either end of the system. For example in an extraction run the liquid product composition, x_n, is measured by analysis and the feed resin composition y_{n+1} is known so that the x - y coordinates of the operating line at the resin inlet end of the system are known. As the

FIGURE 9. EFFECT OF EXTRACTION FACTORS ON DISTRIBUTION IN A COUNTERCURRENT ION EXCHANGE PROCESS

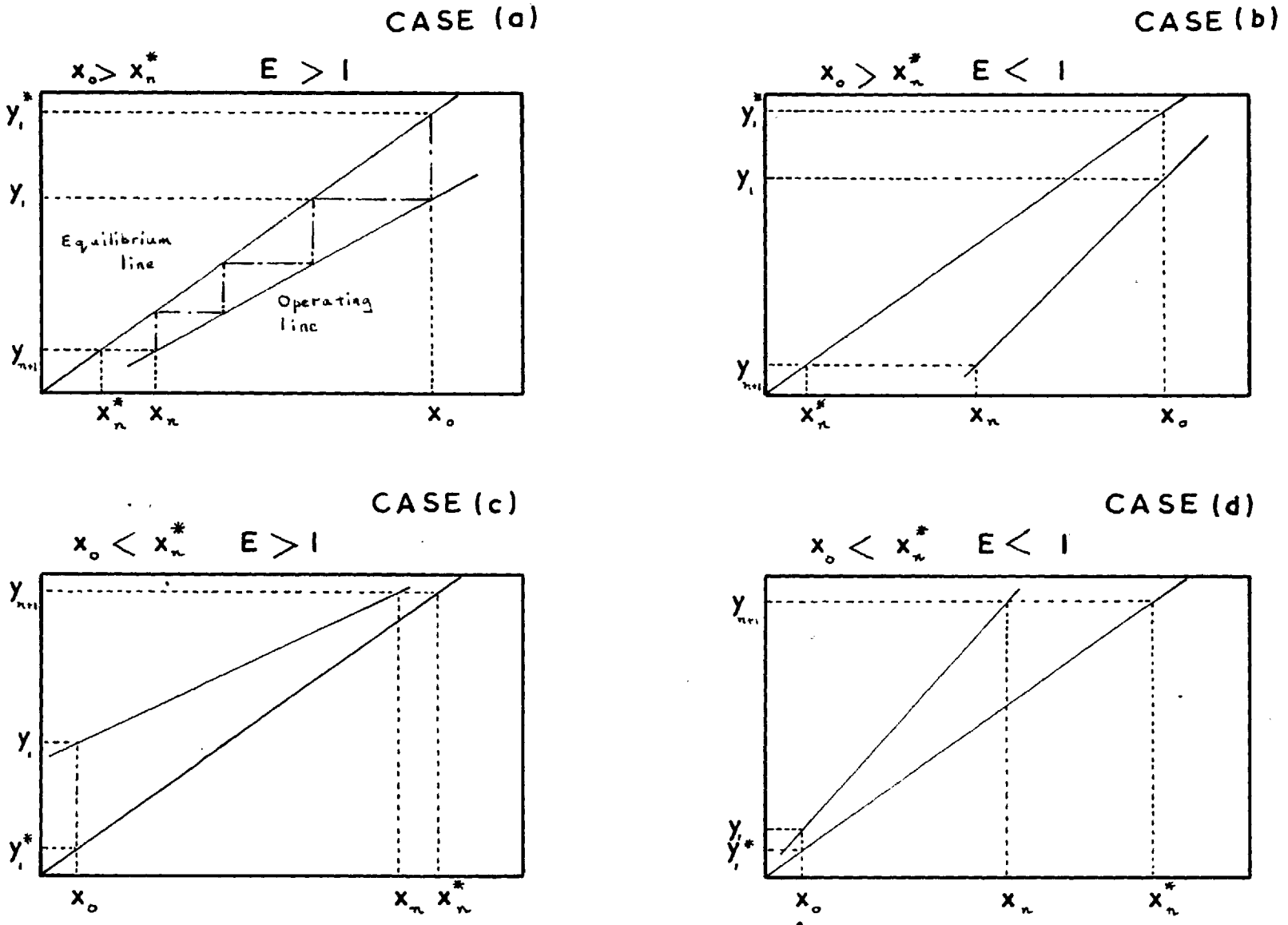

SYMBOLS REFER TO CATION A

composition of the liquid feed x_0 is known the number of equivalent ideal stages in the separation system can be stepped off. The number of full steps on the diagram gives the number of equivalent ideal stages.

The stepping-off process may not in practice yield a whole number of steps or ideal stages i.e. the terminal composition of the phases at the resin feed end of the system may be at the middle of a step. As a fraction of an ideal stage is not possible, the number of ideal stages on each side of the resin feed composition is noted in the results.

The number of equivalent ideal stages is dependent on the cation diffusivity, and the number of available equivalent ideal stages may be different for each of the cations being separated.

With gross ionic fractions in ternary systems the situation is complicated by the possibility that the equilibrium relations for each pair of cations are affected by the presence of the third cation.

2.2.2. Extraction factors.

An important feature of this work has been the use of extraction factors to influence the partition of sodium and potassium between the solution and resin phases in the countercurrent ion exchange separations. The utility of extraction

factors can be illustrated by the use of x - y diagrams. The direction of exchange of an ion species A between resin and solution is controlled by the concentration gradient i.e. by the difference between the concentration of A in one phase and the concentration of A in this phase which would be in equilibrium with the concentration of A in the other phase. Since ion exchange always takes place to reduce the gradient, it will vary continuously throughout a counter-current process. However the quantity of the species A which is transferred from one phase to the other in the dynamic conditions of a counter-current process can be influenced by the extraction factor.

1) System of component A in trace ionic fractions and component G in gross ionic fractions.

Species A is in trace ionic fractions, so that the selectivity coefficient K_{AG} and the distribution coefficient λ_A are both constant.

The extraction factor, E_A is defined by

$$E_A = \lambda_A \frac{S}{L} = \frac{y_A \bar{c} S}{x_A c L} = \frac{\text{slope of equilibrium line}}{\text{slope of operating line}} \qquad (2.14)$$

using equation (2.5)

$$\text{or} \quad E_A = K_{AG} \frac{\bar{c} . S}{c . L} \qquad (2.15)$$

using equation (2.10), which applies to monovalent ions.

Four different cases can be considered depending on the relative concentration of A in the two phases and whether E_A is greater or less than unity.

(a) $x_{A_o} > x^{*}_{A_n}$, $E_A > 1$

As the equivalent fraction of A in the feed liquid, x_{A_o}, is greater than the equivalent fraction of A in the liquid which would be in equilibrium with the quantity of A in the resin feed, $x^{*}_{A_n}$, A is transferred from the liquid to the resin phase in the process.

From Figure 9(a) it can be seen that if there are enough stages, x_{A_n} tends towards $x^{*}_{A_n}$, so that if the feed resin contains no A, complete removal of A from the liquid phase is possible. It is also apparent that in this case y_1 cannot equal y_1^{*} so that the equivalent fraction of A in the exit resin will be limited.

(b) $x_{A_o} > x^{*}_{A_n}$

$E_A < 1$

Again A is adsorbed into the resin, but in this case x_{A_n} cannot approach $x^{*}_{A_n}$ so that the extraction of A into the resin phase is limited even with an infinite number of stages. In this case y_1 can approach y_1^{*} so that the equivalent fraction of A in the resin can reach the value which would be in equilibrium with the liquid feed.

(c) $x_{A_o} < x_{A_n}$, $E_A > 1$

Because the equivalent fraction of A in the liquid feed, x_{A_o}, is less than that which would be in equilibrium with the quantity of A in the resin feed, $x_{A_n}^{*}$, A is transferred from the resin to the liquid phase in the process.

y_1 cannot approach y_1^{*} even when the liquid contains no A, and the resin cannot be completely eluted. x_{A_n} can approach $x_{A_n}^{*}$ with sufficient stages.

(d) $x_{A_o} < x_{A_n}^{*}$, $E_A < 1$

A is transferred from the resin into solution.

With sufficient stages, under these operating conditions, $y_1 \longrightarrow y_1^{*}$, so that the resin can be completely regenerated if the liquid feed contains no A.

x_{A_n} cannot approach $x_{A_n}^{*}$.

To summarise, if component A is to be adsorbed from solution into resin which initially contains no A:

$E_A > 1$ All A can be adsorbed from solution with sufficient stages.

$E_A < 1$ Removal of A from solution is limited.

If A is to be eluted from the resin using a liquid feed containing no A:

$E_A > 1$ Elution is limited.

$E_A < 1$ Full elution of A from the resin is possible with sufficient stages.

2) System of two components A and B in trace ionic fractions and component G in gross ionic fractions.

If the exchange system contains two trace components A and B, the system is more complicated but it is apparent that the following criteria can be put forward, assuming that the extraction factor for component B, E_B, is greater than that for component A, E_A:-

(i) A and B in the liquid feed, no A and B in the feed resin.

$E_A, E_B > 1$.

Both A and B can be fully adsorbed into the resin with sufficient stages. With insufficient stages to adsorb all A and B from solution, more B is adsorbed by the resin and the liquid is enriched in A. The recovery of A is probably low however.

$E_B > 1 > E_A$.

With sufficient stages, most of B can be adsorbed into the resin but the removal of A from solution is limited. In a separation process these are the optimum operating conditions for a good recovery and enrichment of A in the liquid phase.

$E_A, E_B < 1$

The removal of both components A and B is limited, with a tendency for "pinching" at the feed end of the process.

The operating conditions to give maximum separation of A and B are [F1] as follows.

$$\text{If } \frac{E_B}{E_A} = \alpha = \text{separation factor} \qquad (2.16)$$

$$E_B = \sqrt{\alpha} \text{ and } E_A = \frac{1}{\sqrt{\alpha}} \qquad (2.17)$$

(ii) A and B in the resin feed, no A and B in the liquid feed.

$E_A, E_B > 1.$

The removal of both species A and B from the resin into solution is limited.

$E_B > 1 > E_A.$

With sufficient stages all of A can be eluted from the resin but elution of B is limited. These operating conditions will enrich the resin in B with respect to A.

$E_A, E_B < 1.$

With sufficient stages, all of A and B can be eluted from the resin into solution.

2.2.3. Equilibrium stage separation theory.

The equations are only valid if the volumetric flowrate of both phases is constant throughout the process. Although ion exchange resins are known to swell or shrink according to their ionic form, the variation of volume is assumed to be less than the errors involved in volume measurement and hence the flowrates of both phases are taken to be constant. If the volumetric flowrates of the phases are constant, then another condition which applies to ion exchange separations, but not for example to solvent extraction, is that there is a constant total ion concentration in both phases at all points in the system as ion exchange is a stoichiometric process.

The equations are related to a ternary cation mixture of Na^+ and K^+ in the presence of H^+ (Cl^- anions) in which the alkali metals are being separated, but they are perfectly general providing the initial assumptions are fulfilled.

(1) Trace ionic fractions of sodium and potassium.

It can be assumed that the distribution coefficient, λ, and the extraction factor, E, are constant for Na and K. The performance of a separation process consisting of n ideal stages (Figure 10) can be expressed by the following equations which depend on the composition of the feed streams (C6, K2, S6).

FIGURE 10 STAGEWISE COUNTERCURRENT SEPARATION PROCESS

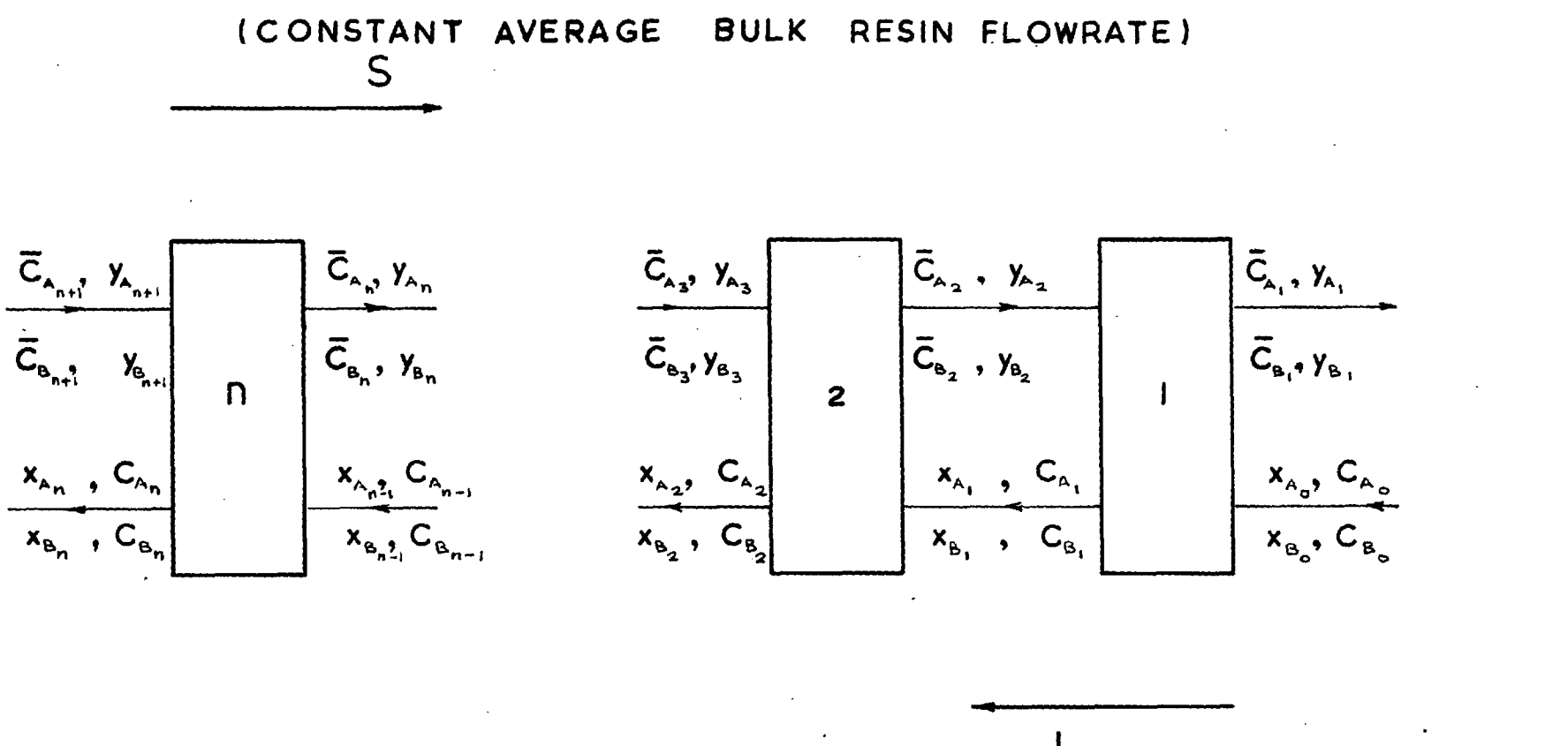

(a) Resin feed containing only H^+ ions, solution feed containing H^+, Na^+ and K^+ ions.

$$\frac{\text{Concentration of } Na^+ \text{ in solution leaving the } n^{th} \text{ stage}}{\text{Concentration of } Na^+ \text{ in solution feed}} =$$

$$\frac{c_{Na_n}}{c_{Na_o}} = \frac{x_{Na_n}}{x_{Na_o}} = \frac{E_{Na} - 1}{E^{n_{Na}+1} - 1} \qquad (2.18)$$

and similarly for the potassium ions.

(b) Resin feed containing H^+, Na^+ and K^+ ions, solution feed containing only H^+ ions.

The equation is analogous to the above equation i.e.

$$\frac{\text{Concentration of } Na^+ \text{ in the resin leaving the first stage}}{\text{Concentration of } Na^+ \text{ in the resin feed entering the } n^{th} \text{ stage}} =$$

$$\frac{\bar{c}_{Na_1}}{\bar{c}_{Na_{n+1}}} = \frac{y_{Na_1}}{y_{Na_{n+1}}} = \frac{\frac{1}{E_{Na}} - 1}{\left(\frac{1}{E_A}\right)^{n_{Na}+1} - 1} \qquad (2.19)$$

and similarly for the potassium ions

(c) Resin and solution feed streams containing H^+, Na^+ and K^+ ions.

Considering the solution phase, assuming $c_o < c_n^*$

Actual change in concentration of Na^+ in solution =
Maximum possible change in concentration of Na^+ in solution

$$\frac{c_{Na_n} - c_{Na_o}}{c^{*}_{Na_n} - c_{Na_o}} = \frac{x_{Na_n} - x_{Na_o}}{x^{*}_{Na_n} - x_{Na_o}} = \frac{E_{Na}^{n_{Na}+1} - E_{Na}}{E_{Na}^{n_{Na}+1} - 1} \qquad (2.20)$$

where $x^{*}_{Na_n} = \frac{y_{Na_{n+1}}}{m}$

(d) Resin and solution feed streams containing H^+, Na^+ and K^+ ions.

Considering the resin phase, assuming $\bar{c}_{n+1} > \bar{c}^{*}_{1}$

Actual change in Na^+ concentration in resin =
Maximum possible change in Na^+ concentration in resin

$$\frac{\bar{c}_{Na_{n+1}} - \bar{c}_{Na_1}}{\bar{c}_{Na_{n+1}} - \bar{c}^{*}_{Na_1}} = \frac{y_{Na_{n+1}} - y_{Na_1}}{y_{Na_{n+1}} - y^{*}_{Na_1}} = \frac{\left(\frac{1}{E}\right)^{n_{Na}+1} - \left(\frac{1}{E}\right)}{\left(\frac{1}{E}\right)^{n_{Na}+1} - 1} \qquad (2.21)$$

where $y^{*}_{Na_1} = m\, x_{Na_o}$

(2) Gross ionic fractions of sodium and potassium.

As pointed out in section 2.1.1. the selectivity coefficient and extraction factor can only be considered to be

constant with dilute solutions. With gross ionic fractions of the ions being separated, the distribution of sodium and potassium can be calculated either using equations analogous to those above or by graphical methods.

The equation for sodium concentration change in the liquid phase when the extraction factor varies from stage to stage and the incoming resin contains no sodium is(F1)

$$\frac{c_{Na_n}}{c_{Na_o}} = \frac{x_{Na_n}}{x_{Na_o}} = \frac{1}{1 + E_{Na_1} + E_{Na_1} \cdot E_{Na_2} + \ldots + E_{Na_1} \cdot E_{Na_2} \cdot \ldots \cdot E_{Na_{n-1}} \cdot E_{Na_n}} \quad (2.22)$$

where E_{Na_i} is the extraction factor for sodium in the i th stage. A similar equation applies to the potassium.

In all countercurrent ion exchange processes, a redistribution of Na^+, K^+ and H^+ will take place between the resin and solution. The enrichment of one of the ions being separated with respect to the other can be expressed by the enrichment factor, f. This is defined in general by the ratio of the concentrations of the two species in the product stream divided by the ratio of the two concentrations in the feed

stream. For example, the sodium enrichment factor for the solution phase, f_1, is expressed by

$$f_1 = \left(\frac{c_{Na}}{c_K}\right)_n \Big/ \left(\frac{c_{Na}}{c_K}\right)_o = \left(\frac{x_{Na}}{x_K}\right)_n \Big/ \left(\frac{x_{Na}}{x_K}\right)_o \qquad (2.23)$$

The purity of sodium with respect to potassium, P_{Na}, in the liquid product stream is defined by

$$P_{Na} = \frac{c_{Na}}{c_{Na}+c_K} = \frac{x_{Na}}{x_{Na}+x_K} \qquad (2.24)$$

Similar equations apply to the potassium.

2.2.4. Calculation of the number of equivalent ideal stages in the Na^+/K^+ separation processes.

In any countercurrent ion exchange process, the number of equivalent ideal stages for the change in trace concentration of a cation in the separation process can be calculated using equations (2.18), (2.19), 2.20) and (2.21).

For example consider the adsorption of trace sodium from solution by a H^+ form resin feed (Figure 10). From equation (2.18),

$$\frac{\text{Observed } Na^+ \text{ concentration in solution product}}{Na^+ \text{ concentration, feed solution}} =$$

$$\frac{c_{Na_n}}{c_{Na_o}} = \frac{E_{Na} - 1}{E_{Na}^{n_{Na}+1} - 1} \qquad (2.25)$$

This equation can be solved for n_{Na}, the number of equivalent ideal stages for Na^+ adsorption in the process.

In an analogous way equations (2.19), (2.20) and (2.21) can be used, when appropriate, to calculate the number of equivalent ideal stages in the process for the adsorption or elution of the trace species.

The overall stage efficiency in the process, β, is given by

$$\beta = \frac{\text{Number of equivalent ideal stages}}{\text{Number of actual stages.}} \qquad (2.26)$$

2.3. Mass transfer

2.3.1. Mass transfer coefficients

Many mass transfer correlations for ion exchange in fixed and fluidised beds have been put forward. They have various limitations depending on the simplifying assumptions made. In recent work Snowdon[S5] has calculated the Sherwood number for ion exchange in packed and fluidised beds using several published correlations and compared these values with experimental ones. As a result of his work Snowdon selected a correlation similar to that put forward by Carberry[C1, M6], i.e.

$$Sh = \frac{\phi}{e^{\frac{1}{2}}} \; Re^{\frac{1}{2}} \; Sc^{\frac{1}{3}} \qquad (2.27)$$

He calculated the constant ϕ for fixed and fluidised bed runs and found it to be greater for the fixed bed runs by about $\frac{1}{3}$. It was suggested that the mass transfer coefficients may vary with e in a way other than that simply due to variation in the interstitial fluid velocity and he suggested a new correlation.

$$Sh = \frac{\phi}{e} \; Re^{\frac{1}{2}} \; Sc^{\frac{1}{3}} \qquad (2.28)$$

giving greater dependence on the void fraction. Many published fixed and fluidised bed results were correlated to within 10% error with a value of $\phi = 0.8$. This correlation probably applies to the range $0.1 < Re < 1000$.

Snowdon has modified this correlation to allow for variation in the diffusivity of the exchanging ions with liquid composition,

$$D_{eff} = D_H \left[F_1 (x_A)\right]^{3/2} \qquad (2.29)$$

where $F_1 (x_A)$ is a complex factor depending on the equivalent fraction of ion species A at the liquid interface and in the bulk of the liquid.

For Na^+/H^+ exchange, with trace sodium ionic fractions, i.e. $x_H \rightarrow 1$, $F_1 (x_H) \rightarrow 0.274$, and

$$D_{eff} = D_H \times 0.274^{3/2} \qquad (2.30)$$

Substituting for D_{eff} in Sh and Sc in the mass transfer correlation

$$Sh_H = \frac{0.8 \times 0.274}{e} Re^{\frac{1}{2}} Sc_H^{\frac{1}{3}} \qquad (2.31)$$

$$Sh_H = \frac{k_L d}{D_H} \quad \text{and} \quad Sc_H = \frac{\mu}{\rho D_H}$$

$$\therefore k_L = \frac{0.22}{e} \frac{D_H}{d} Re^{\frac{1}{2}} Sc_H^{\frac{1}{3}} \qquad (2.32)$$

for Na^+/H^+ exchange with trace sodium. It is assumed that this correlation applies to the runs carried out in this project with trace concentrations of sodium and potassium with respect to hydrogen.

In the Na^+/K^+ separation runs the use of a strongly acidic medium cross-linked resin and dilute solutions should favour film diffusion control, however the ion exchange rate controlling step can be determined using a criterion given by Helfferich[H1].

$$\frac{2\,\bar{c}\,\bar{D}_{AB}}{c\,D_{AB}Sh}\,(5 + 2K_{AB}) \ll 1, \text{ particle diffusion control} \qquad (2.33a)$$

$$\frac{2\,\bar{c}\,\bar{D}_{AB}}{c\,D_{AB}Sh}\,(5 + 2K_{AB}) \gg 1, \text{ film diffusion control} \qquad (2.33b)$$

where D_{AB}, $\bar{D}_{AB}$ are the interdiffusion coefficients in the film and resin respectively. $\frac{D_{AB}}{\bar{D}_{AB}} \simeq 10$[H1], but the interdiffusion coefficient is the harmonic mean of the individual diffusion coefficients of the counter ions e.g. for monovalent ion exchange, $\bar{D}_{AB}$, the interdiffusion coefficient in the resin is given by

$$\bar{D}_{AB} = \frac{\bar{D}_A\,\bar{D}_B(\bar{C}_A + \bar{C}_B)}{\bar{c}_A\,\bar{D}_A + \bar{c}_B\,\bar{D}_B} \qquad (2.34)$$

and similarly for the liquid film.

2.3.2. Mass transfer model.

As described in section 1.3, the resin in the new contacting technique is fluidised in the forward flow period in which ion exchange occurs. There is some evidence[B1] from pilot

plant work with the new technique that both the liquid and resin phases are perfectly mixed in the forward flow cycle.

Under these conditions mass balance and mass transfer equations can be used to predict the composition of the liquid product from each stage.

A stage can be represented diagrammatically as follows:

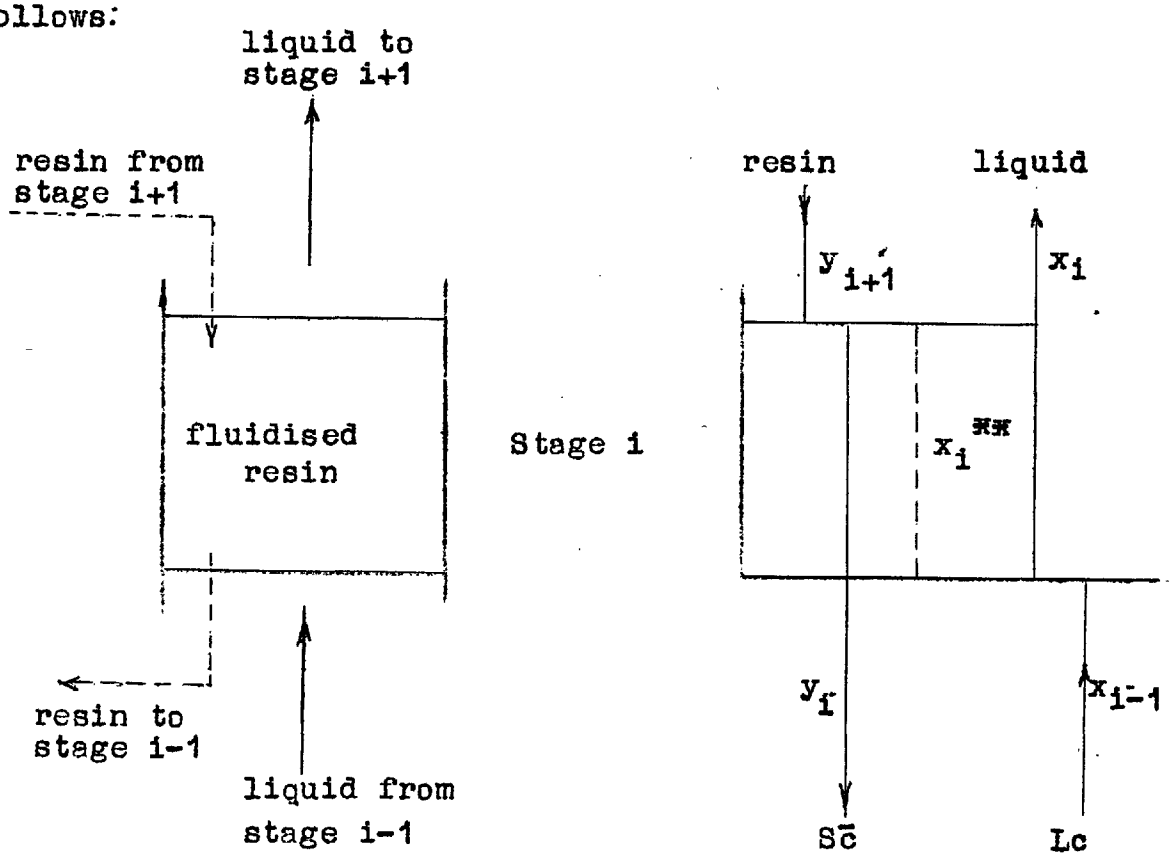

The two phases are perfectly mixed so that the composition of each is uniform over the stage. x_i^{**} is the liquid composition in equilibrium with the resin composition y_i and the concentration gradient for ion exchange is $(x_i - x_i^{**})$.

A mass balance over the stage gives

$$S\bar{c}\,(y_i - y_{i+1}) = Lc\,(x_{i-1} - x_i) = \Delta_i \qquad (2.35)$$

where Δ_i is the rate of ion exchange in the stage, expressed as equivalents per unit time.

If, as expected, liquid film diffusion controls ion exchange, then

$$\Delta_i = c\,K_L s'\,(x_i - x_i^{**}) \qquad (2.36)$$

where s' is the interfacial area between resin and solution in the stage.

Combining equations (2.35) and (2.36)

$$Lc\,(x_{i-1} - x_i) = cK_L\,s'(x_i - x_i^{**}) \qquad (2.37)$$

The composition of the liquid product x_n is known by analysis and the composition of the resin product y_1 can be calculated by a mass balance. x_1^{**} can be calculated from y_1 using the equilibrium relationship, and equation (2.37) solved for x_1, when K_L has been estimated. Δ_1 and y_2 can be calculated using equations (2.36) and (2.35) respectively. This procedure can be repeated for each stage to estimate the composition of the liquid product x_n.

3. Equilibrium data and other resin properties

3.1 Experimental

3.1.1 Volume exchange capacity.

The volume exchange capacity has been measured on a sample of conditioned resin in both the hydrogen and sodium forms. The directly measured volume exchange capacity has been compared with the value calculated from the weight capacity [H1,], using the relation

$$\bar{c}_{vol} = \bar{c}_{wt} \quad (1 - e)\, \rho_s \quad (1 - z) \qquad (3.1)$$

The resin initially in the hydrogen form was cycled twice through the sodium form and the physical properties in equation (3.1) measured for each resin form.

The volume exchange capacity of the resin depends on the degree of packing of the particles. To ensure consistent packing as far as possible in this work, all resin volumes were measured with tap settled resin. Tap settled resin volumes were measured by tapping the measuring cylinder repeatedly with a spatula until no further diminution of the resin volume occurred.

After measuring the tap settled volume the resin was washed into a filter tube to measure the exchange capacity of the resin. If the resin was in the hydrogen form, all H^+ ions were displaced from the resin by elution with 300 cm^3

$\frac{N}{10}$ Na Cl solution and the eluate titrated against $\frac{N}{10}$ Na OH using phenolphthalein indicator. If the resin was initially in the sodium form it was converted to the hydrogen form by elution with $\frac{N}{10}$ HCl until the eluate showed no trace of sodium when tested on the flame photometer. The resin sample was washed with distilled water to remove excess HCl from the resin particles (until there was no Cl^- reaction with Ag NO_3 solution) and then the exchange capacity determined as with resin in the hydrogen form.

To measure the weight capacity the resin was converted to its original cationic form by elution, washed thoroughly with distilled water and dried to constant weight at 105°C.

The values of properties required for equation (3.1) were determined as follows. Approximately 10 cm^3 of tap settled resin were measured out and washed into a weighed filter tube. The interstitial water was removed by centrifugation at 750g. A rubber cap was fitted to the top of the filter tube to prevent evaporation of water from the resin particles during this operation. To find the optimum centrifuging period a quantity of sodium form resin was centrifuged for 75 minutes, the resin being weighed after 30, 45, 60 and 75 minutes. The weight of moist sodium form resin decreased as the centrifuging period was increased to 75 minutes (Table 1). However as the change in the values of resin density and fractional void volume

TABLE 1 - Effect of centrifuging period on sodium form resin properties.

Centrifuging period (min.)	30	45	60	75
Wt. of resin (g.)	10.0641	10.0615	10.0419	10.0330
Resin density (g/cm^3)	1.2824	1.2825	1.2832	1.2835
Fractional void volume	0.3514	0.3516	0.3533	0.3540

was small after 30 minutes centrifuging, this was selected as the standard period.

The decrease in the weight of moist resin on centrifuging for periods longer than 30 minutes can be compared with the results of Pepper et al[P1], who worked with smaller (1g. wet weight) quantities of resin. They report that the weight of resin was constant to ± 2 mg. for centrifuging periods from 30 minutes to 6 hours at speeds corresponding to 225 to 530g.

After weighing, the resin was washed into a s.g. bottle and the density and fractional void volume measured by standard methods. The resin was washed into an evaporating dish and dried at 105°C to constant weight to determine its water content. The density and void fraction of K form resin were also measured.

In the course of continuous cation separation work the resin is normally in a free settled state. A number of experiments were made with hydrogen form resin quantities up to 360 cm^3 to find the relation between tap settled and free settled resin volumes. Free settled volumes were measured by initially inverting the measuring cylinder so that all resin particles settled freely when the cylinder was placed in its normal position. To determine the standard deviation, the free settled volumes of a quantity of resin were measured independently eight times.

3.1.2. Equilibrium measurements

Although equilibrium data have been reported for the K^+/H [G1,R3], Na^+/H [B2,R2,D4] and Na^+/K^+ [R3] systems with various types of strongly acidic polystyrene D.V.B. resins, the only references to Zeo-Karb 225 are with the Na^+/H^+ binary system [R1,T2]. Equilibrium measurements to obtain sufficient data to permit interpretation of the proposed Na^+/K^+ separation experiments were undertaken with the (-14 + 52) B.S.S. 8% D.V.B. Zeo-Karb 225 to be used.

Standard solutions of 0.1N. NaCl, 0.1N KCl and 1N hydrochloric acid were made up using A.R. grade chemicals. Finely powdered NaCl and KCl were dehydrated at 250 - 350°C [V2] before weighing and dissolution in demineralised water. The IN HCl was prepared by dilution of concentrated acid or from standard ampoules.

Hydrogen form Zeo-Karb 225 was prepared from the sodium form resin by conversion using 1N hydrochloric acid. Acid was passed through a column of the resin at a rate of approximately 1 $cm^3/(cm^2)(min)$ until the acidity of the column effluent equalled that of the influent. The resin was washed by running demineralised water through the column at the same rate until the effluent showed no chloride reaction with $AgNO_3$ solution. The same batch of hydrogen form resin was used in all batch equilibrium experiments.

Sodium and potassium resin forms were prepared from the hydrogen form resin by passing 0.1N chloride solution through the resin until the effluent showed no trace of acidity. Excess chloride was removed by washing with demineralised water.

The time required to reach equilibrium in the batch equilibrations was established by separate batch experiments. A carefully weighed quantity of H^+ form resin corresponding to approximately 0.5 cm^3 was added to 100 cm^3 of 0.001N NaCl or KCl solution well agitated by a magnetic stirrer. The attainment of equilibrium was followed by the change in the pH value of the solution which was measured at intervals up to 16 hours. Duplicate experiments were conducted for both NaCl and KCl solutions. The results for NaCl and KCl (Figure 11) showed that equilibrium was attained in about 1 hour, and a shaking time of $2\frac{1}{2}$ hours was therefore selected for the equilibrium experiments.

The measurement of resin quantities is difficult to carry out in a reproducible manner because of the varying amounts of water which a given quantity of resin will hold at different temperatures of drying, the dependence of its density on the swelling caused by different cations and on the degree of packing. In these equilibrations about 2 cm^3 of free settled resin were used in each experiment and the quantity of resin was defined by measuring the total exchange capacity of each aliquot

FIGURE 11. ATTAINMENT OF EQUILIBRIUM IN $\frac{N}{1000}$ KCl SOLUTION -(-14 + 52) BSS 8% D. V. B. H^+ FORM ZEO-KARB 225 SYSTEM

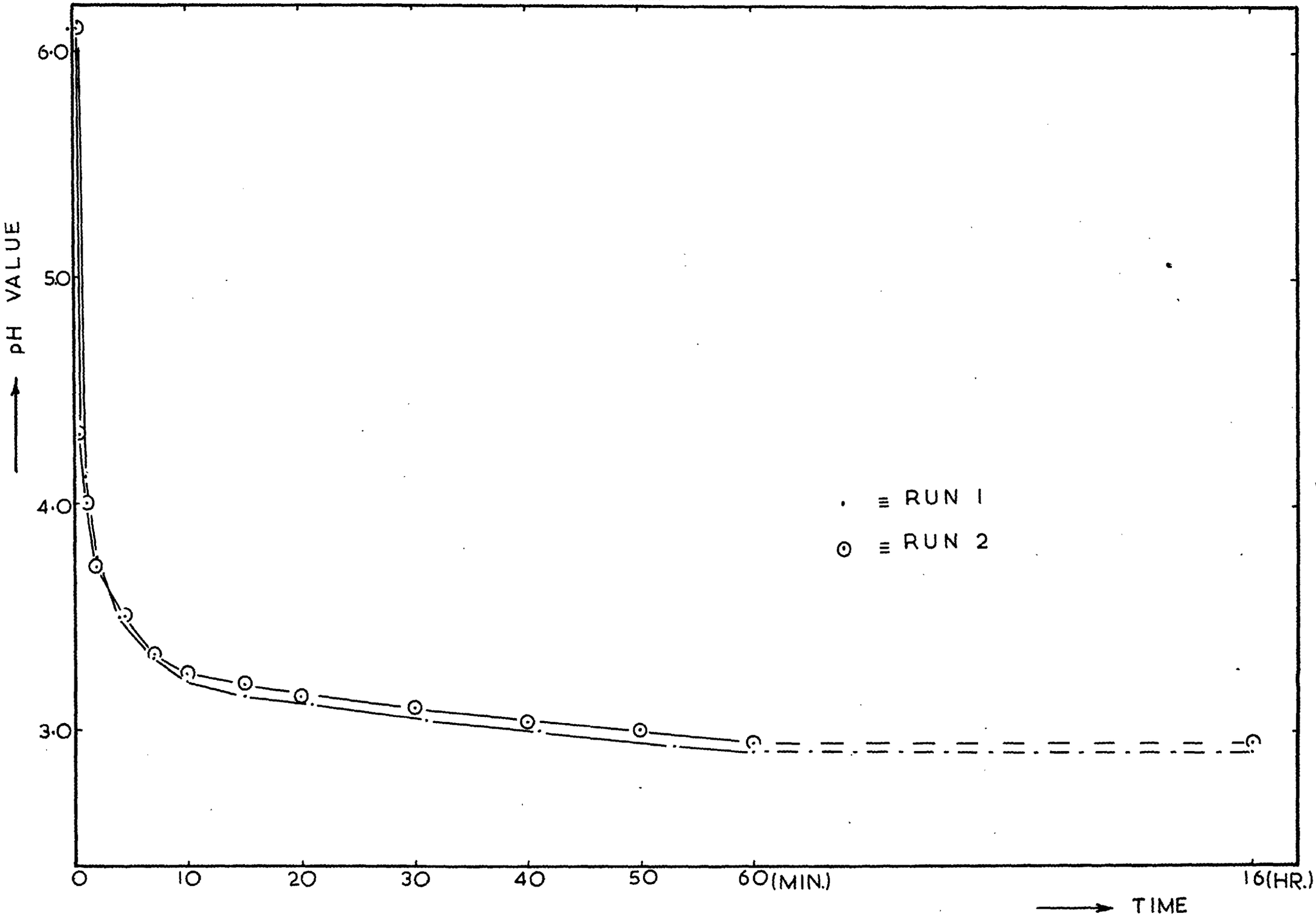

after equilibration.

After removal of interstitial water by centrifugation for 30 minutes the resin was added to the solution in a conical stoppered Pyrex flask. Pyrex was used in all work to avoid contaminating solutions by sodium leached from glassware. Conical flasks were used as some difficulty was experienced in washing all resin particles from the spherical flasks used in the original work. The mixture was agitated for $2\frac{1}{2}$ hours using a standard laboratory shaker. As the equilibrium is not affected by small temperature changes $(B4)$ all work was conducted in ambient conditions.

After equilibration the supernate was analysed for sodium and potassium using a flame photometer and in some experiments the hydrogen ion concentration was also measured by titration against $\frac{N}{10}$ NaOH (made from standard ampoules) using phendphthalein indicator. The amount of alkali metal ion adsorbed by the resin was calculated by difference. Each equilibration was carried out in duplicate.

The exchange capacity of each equilibrated resin aliquot was measured by washing the resin into a filter tube, reconverting to the hydrogen form with 0.1 N HCl and washing with demineralised water. In equilibrations where the resin was nearly saturated with Na or K about 250 cm^3 of 1N HCl were used for conversion followed by 0.1N HCl until the eluate showed no

trace of Na or K with the flame photometer. In early work the hydrogen ions were eluted from the resin by 1N NaCl and titrated with 0.1N NaOH to give the total exchange capacity of the resin. In later work the hydrogen form resin was washed from the filter tube into a conical flask, 25 cm^3 of 0.1N NaCl added and the resin titrated against $\frac{N}{10}$ NaOH. This procedure was simpler and reduced the experimental error.

3.1.3. Determination of sodium and potassium concentrations in solution.

Solutions were analysed for sodium and potassium using flame spectroscopy. The principle of this method of analysis is that the solution containing the alkali metal ions is atomised and sprayed into a non-luminous flame. At the high temperature existing in the flame much of the alkali metal salt is dissociated. A small proportion of the resulting alkali metal atoms is excited and the single outer s electron of these atoms is raised to a higher energy level. When the electron returns to a lower energy level or the ground state, light of a characteristic wavelength is emitted. The light from the flame passes through a monochromator or a system of filters to isolate the desired region of the spectrum. The intensity of the isolated radiation is measured by a photosensitive detector and some type of meter or electronic amplifier. After careful calibration of the flame photometer with solutions of known

composition it is possible readily to correlate the intensity in emission of the unknown sample with the amount of the same element present in a standard solution.

Two instruments have been used for this type of analysis

1) EEL flame photometer.*

A flame of towns gas and air is used, the air-flow at the entry to the mixing chamber being used to draw the sample solution into the chamber through a fine atomiser jet. The resulting mixture passes to the burner and is ignited. This instrument uses coloured glass cut-off filters to isolate the particular radiation. This method permits the use of simple selenium photocells followed by a mirror galvanometer to give a direct reading deflection proportional to the intensity of the radiation transmitted through the filter.

The maximum full scale reading with this instrument is given by 5 ppm Na^+ or 10 ppm K^+ concentrations. All solutions had to be diluted with demineralised water down to this concentration range for analysis.

Although the readings on the linear galvanometer scale are proportional to the current generated in the photocell, the flame intensity is not linearly proportional to the solution concentration. It was necessary to construct calibration

*Manufactured by Evans Electroselenium Ltd., St. Andrews Works, Halstead, Essex, U.K.

FIGURE 12. EEL FLAME PHOTOMETER CALIBRATION CURVES FOR NaCl AND KCl STANDARD SOLUTIONS

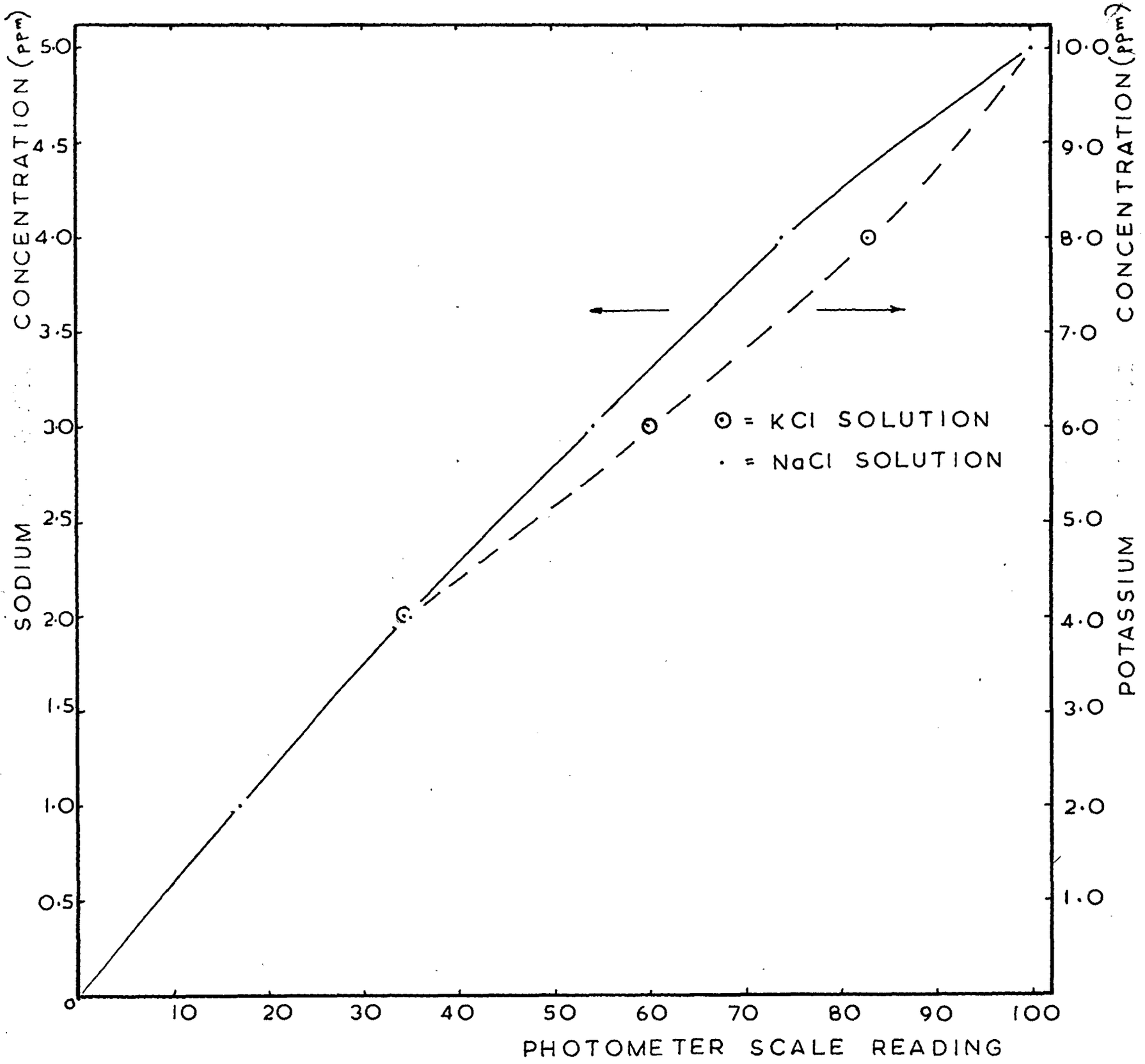

curves using standard solutions (Figure 12).

2) Unicam. SP 90 atomic absorption spectrophotometer*

This instrument later became available and was used to check some of the equilibrium data determined with the EEL flame photometer. This instrument, which uses an acetylene-air flame, employs a combination of slits and mirrors with a Littrow type monochromator to isolate the radiation being determined. The signal from the photomultiplier is amplified and rectified before passing to the output meter or an external potentiometric recorder. Owing to the unavoidable noise shown in the output signal more accurate estimates of the output reading can be made using a recorder.

As recommended in the Unicam method sheets, a maximum concentration of 20 ppm Na^+ was used in the analyses. Standard solutions of sodium and potassium with respectively 5 ppm, 7.5 ppm, 10 ppm, 12.5 ppm, 15 ppm and 20 ppm concentrations were prepared. Owing to the difficulty of exactly reproducing the operating conditions during analysis the operating procedure adopted was to run the 6 standard solutions through the instrument followed by the unknown solutions. This was done twice and then the standard solutions run through a third time.

*Manufactured by Unicam Instruments Ltd., York St., Cambridge, U.K.

The readings for each unknown solution were averaged and concentrations determined from a calibration curve plotted from the average standard solution readings.

Analytical errors

In general it can be assumed in this method of analysis that

(a) under defined conditions of flame excitation a sample emits light of wavelengths characteristic of the elements in the sample at a constant rate measured by the instrument, and

(b) the intensity of the characteristic emission as measured by the instrument is a function of the concentration of the element.

The accuracy of the result is thus limited by the errors made in determining the intensity of emission under supposedly standard conditions (errors of measurement) and those made in deducing the analytical result from the emission measured (errors of evaluation).

Measurement errors are produced by variation in the conditions of excitation, by errors made in the measurement of the emission and by the fact that flame emission, as a sum of individual processes subject to the laws of probability, is affected by a statistical distribution function. It is generally estimated that with careful work the measurement errors can be reduced to about 1%.

The errors of evaluation include errors of standardisation, interference due to the emission of other elements and interelement effects (suppression or enhancement). Evaluation errors in the analysis for alkali metals by flame spectroscopy can be significant. The sources of error and the measures taken to avert them will be discussed in some detail.

Effect of other alkali metals.

The dissociation of the alkali metal salt and excitation of the alkali metal atoms in the flame was briefly discussed above. In most cases the number of atoms in the lowest excited state is very small compared with the number of atoms in the ground state, and the ratio only becomes appreciable at very high temperatures and for states of low energy. Although the number of excited atoms increases exponentially with temperature, the number of unexcited atoms remains virtually constant. If the temperature is high enough a proportion of the atoms present will be ionised, removing atoms from the unionised ground state or low excited state. The alkali metals have a low ionisation potential and are significantly ionised in hot flames. The enhancement of the emission by alkali metals caused by the presence of other alkali metals is attributed to their effect on ionisation(E1). This is due to the absorption of energy involved in ionising the additional alkali metal with a consequent increase in the number of unionised

atoms of the element under analysis which are capable of giving emission. Because of the much smaller proportion of atoms which are ionised in the cooler flames used with the EEL flame photometer the enhancement effect is not observed.

There is another error in the analysis for potassium in the presence of sodium using the SP 90. Even in the absence of potassium there is some light of the characteristic K emission wavelength (7699A) detected by the SP 90. This is attributed to Na emission passing through the monochromator system, and is referred to as 'stray light'. As the sodium emission is very strong this can be a source of considerable error.

No enhancement by the presence of the other alkali metals was found with the EEL instrument, and no enhancement of 20 ppm Na^+ readings by 30ppm K concentrations was found with the SP 90. This is in indirect agreement with Dean (D2) who states that 100 ppm K gave a 2% enhancement of a 10 ppm Na reading.

The enhancement of K emission by the presence of sodium with the SP 90 was tested with a Rattin filter to prevent any sodium emission reaching the optical system. The reading of 53.5 given by a 5 ppm K^+ solution was enhanced by about 0.5%, 7.5%, 17.8% and 25% by the presence of 5, 10, 50 and 230 ppm Na^+ concentrations respectively. It is seen that the larger the sodium concentration the relatively smaller the enhancement effect. These results show a smaller enhancement than the 17%

and 56% enhancement of a 5 ppm K^+ emission by 20 ppm and 100 ppm Na^+ found by Poluektov[P5] with acetylene-air flames.

The additional effect caused by the strong sodium light was determined in tests without a Rattin filter. The 5 ppm K^+ reading was increased by 28% and 42% by the presence of 50 ppm and 230 ppm Na^+ concentrations respectively. The additional increase is more than 50% of the sodium enhancement of the K reading. Again it can be seen that high concentrations of Na cause a relatively smaller increase in the reading.

Owing to the errors in K analysis with the SP 90 caused by the presence of sodium, special precautions had to be taken.

(a) Solutions without sodium ions.

As chloride ions have no effect on K emission below 0.05 N concentrations, the K analyses were carried out in a similar way to the Na analyses. Standard solutions of 5 ppm, 7.5 ppm, 10 ppm, 12.5 ppm, 15 ppm and 20 ppm K^+ were made up and all K containing solutions diluted to a concentration below 20 ppm using demineralised water. Pipettes of 5 cm^3 volume or larger were used to reduce errors. For example a 0.1N KCl solution must be diluted 250 times to reduce the concentration to less than 20 ppm. The dilution procedure was to dilute in two stages. 10 cm^3 of the 0.1N solution were diluted down to 250 cm^3

and 10 cm^3 of this solution diluted down to 100 cm^3 using volumetric flasks.

(b) Solutions containing sodium ions.

As pointed out above the effect of the presence of sodium is relatively much smaller with higher concentrations of sodium ions. On dilution of the K containing solutions to a concentration less than 20 ppm, the highest sodium concentration would be $\simeq$ 40 ppm. To reduce to a minimum the effect of sodium concentrations up to 40 ppm, on dilution all solutions were made up to contain 0.01N NaCl concentrations in addition to the sodium already present in the diluted solution. A set of standard solutions of 5 ppm, 7.5 ppm, 10 ppm, 12.5 ppm, 15 ppm and 20 ppm K were also made up 0.01N in sodium chloride.

To prevent the spurious reading caused by stray sodium light a Rattin cut-off filter was placed between the burner and the optical system.

Potassium concentrations in the presence of sodium determined by the SP 90 using the above procedure were compared with values using the EEL flame photometer. The difference in K_{KH} (discussed more fully in section 3.2.3) calculated from the analytical results was within experimental error.

Chloride interference.

The presence of chlorine containing compounds in the gases in the flame leads to a reduction in the emission of the alkali metals (D2). Considering the case of sodium, the sodium will be present in the flame in the atomic form

$$2\ NaCl = Na + NaCl + Cl$$

Owing to the great excess of molecular hydrogen, the reaction

$$H_2 + Cl = HCl + H$$

gives rise to a very great excess of HCl over all other chlorine containing compounds. The HCl reacts with the atomic sodium

$$Na + HCl = NaCl + H$$

thus reducing the quantity of sodium atoms in the flame for excitation and emission. The effect on potassium is similar. Significant chloride suppression of Na and K emission has been found(C4) even with the cool coal gas-air flames used with the EEL flame photometer.

The effect of the presence of chloride ions on the emission from sodium and potassium was investigated with both the EEL and SP 90 instruments.

5 ppm Na^+ solutions with 0.1N and 0.01N HCl and 10 ppm K^+ solution with 0.1N HCl concentrations were prepared

and the emission from these solutions compared with that from 5 ppm Na^+ and 10 ppm K^+ solutions respectively. A 5 ppm K^+ solution with 0.05 N HCl was also compared with a 5 ppm K^+ solution. A Rattin filter was used in the K analyses using the SP 90 to obviate spurious readings caused by stray light from sodium impurities.

Sodium analysis.

EEl flame photometer.

There is no effect on the 5 ppm Na^+ emission caused by the presence of 0.01 N HCl but a 0.1N concentration causes a 2.5% decrease in the emission. Other workers(C4) showed graphically a 2.5% reduction in the emission of 10 ppm Na^+ by 0.1 N Cl^- and no change with 0.01N Cl^- concentrations.

SP 90 spectrophotometer.

0.01N HCl gave no interference but a 0.1N HCl concentration produced a 2.5% decrease in the emission (by 5 ppm Na).

It is apparent that solutions must be diluted at least 10 times to avoid Cl^- interference in the Na analyses.

Potassium analysis.

EEL flame photometer.

0.05 N HCl had no effect on 10 ppm K^+ emission but 0.1 N HCl reduced the emission by 7%. The graphical results of Colline and Polkinhorne(C4) show a 11% reduction in the emission

of 10 ppm K^+ by 0.1 N Cl^- concentrations, with an EEL instrument. SP 90 spectrophotometer.

0.05 N HCl concentrations caused no change in K emission but 0.1 N HCl caused a decrease of about 5%.

These results show that at least a two times dilution of the solutions (which all contain 0.1 N Cl^- concentrations) is required before accurate K analyses can be carried out.

Non-specificity of filters

Another possible source of error with the EEL flame photometer is that the Rattin filter does not give a sharp cut-off. Tests on 5 ppm Na^+ solutions containing 100 ppm K^+ and 10 ppm K^+ solutions containing 100 ppm Na^+ concentrations showed no differences from the emission with 5 ppm Na^+ and 10 ppm K^+ solutions respectively. Published values are in indirect agreement(M3).

On the determination of	Interference of	
	K	Na
K	-	10,000 µg/cm^3 Na → 10µg/cm^3 K
Na	10,000 µg/cm^3 K → 0µg/cm^3 Na	

3.1.4 Size distribution of resin.

A size distribution analysis on a sample of H^+ form (-14 + 52) B.S.S. Zeo-Karb 225 resin was carried out. A 200g quantity was successively mixed and quartered down to a 9g sample. The resin was wet sieved to determine the size distribution in the same state as it exists in experimental work. A bank of standard 8 in. diameter sieves was mounted in a mechanical shaker and after washing the resin into the top sieve, water was cascaded down the bank of shaking sieves. Each resin fraction was transferred to a sample bottle. Many resin particles adhered to the sieves but most could be dislodged by a high pressure jet of water directed at the upside-down sieve.

Each resin fraction was weighed so that a percentage weight distribution was obtained. By weighing a small number of particles from each fraction (40 of the larger particles, 150 of the smaller particles), the number of particles in each fraction could be estimated.

3.2 Results and discussion

3.2.1 Volume exchange capacity

Values of the volume exchange capacity and the physical properties required to calculate the volume exchange capacity from the weight exchange capacity are shown in Table 2. It can be seen that the density of the hydrogen form resin is

TABLE 2.

Properties of hydrogen sodium, and potassium forms of (-14 + 52) B.S.S.

Zeo-Karb 225 resin

Resin form	Expt. No.	Duplicate No.	Density (g/cm^3)	Voidage	Water content	Wt. capacity (meq/g)	Calc. volume capacity (meq/cm^3)	Measured volume capacity (meq/cm^3)	Packing
Hydrogen	H.1	1	1.2024	0.3570	0.5278	5.25	1.91	1.86	Tap
		2	1.2012	0.3545	0.5306	5.25	1.91	1.87	settled
Sodium	Na.1	1	1.2878	0.3636					Tap
		2	1.2880	0.3636					settled
Hydrogen	H.2	1	1.2111	0.3736		5.22			Tap
		2	1.2133	0.3860		5.28			settled
Sodium	Na.2	1	1.2810	0.3546	0.5466	4.90	1.837	1.85	Tap
		2	1.2824	0.3514	0.5494	4.92	1.844	1.83	settled
Hydrogen	F.3	1	1.2048	0.3637	0.5311	5.10	1.83	1.84	Tap
		2	1.2037	0.3597	0.5362	5.10	1.82	1.80	settled
Potassium	K.1	1	1.3002	0.3569					Free
		2	1.3023	0.3573					settled

appreciably less than that of the sodium form which in turn is slightly less than that of the K form resin. With this 8% cross linked resin, the swelling is dependent on the solvated size of the adsorbed cation. Since the volume of solvated ions increases in the order

$$H^+ > Na > K^+$$

the observed sequence of resin density is to be expected. Other factors which would influence the resin density to a lesser degree are (a) the atomic weight of the adsorbed cation - this would also cause the density to vary in the observed manner, and (b) when the larger solvated ions are adsorbed, the swelling pressure in the resin rises, and some free water molecules may be forced out of the resin matrix. This will tend to reduce the swelling.

There is reasonably good agreement between directly measured values of the volume exchange capacity and values calculated from the weight capacity for both Na^+ and H^+ resin forms. As the results from duplicate experiments show good agreement, variation of results from cycle to cyde of the hydrogen form is probably due to sample variation. Because the H^+ form resin has a lower density than the Na^+ form, there are less sulphonate groups per unit volume of resin in the H^+ form, so that the volume capacity of the H^+ form resin can be expected to be lower than that of the Na^+ form. This is the case for the H3 resin measure-

ments but not for the H.1 results. A value of 1.85 meq/cm^3 was taken for the tap settled volume capacity of both cationic forms. All measurements of the weight exchange capacity of the H^+ form resin gave values significantly higher than the values for the Na^+ form resin. In view of the much greater atomic weight of sodium this is to be expected.

The free settled and equivalent tap settled H^+ form resin volumes are shown in Table 3 and the values plotted in Figure 13. The standard deviation of the free settled resin volume is used[D1] to calculate the gradient of the line in Figure 13 and the standard deviation of the gradient and the tap settled resin volumes. The gradient is 1.015(5) with a standard deviation of 0.002. It is assumed that the results apply to the sodium form resin also. As the average exchange capacity for tap settled resin in either form is 1.85 meq/cm^3 the free settled volume capacity of both cationic resin forms is 1.82 meq/cm^3. The calculated standard deviation of the tap settled volumes is greater than the standard deviation of the free settled resin volumes. This is not unreasonable. In reaching the free settled state, the only process involved is a mutual rearrangement of the resin particles, whereas in reaching the tap settled state, the additional process of tapping is involved and as the degree of tapping will vary from experiment to experiment, an additional error is introduced.

TABLE 3

Relation between free settled and tap settled H^+ form resin volumes

Free settled volume (cm^3) y	Tap settled volume (cm^3) x
4.21	4.12
59.1	58.0
102.0	99.4
138.1	135.2
149.0	146.1
190.2	187.2
219.0	213.0
242.2	239.8
291.5	286.0
365.2	360.0
114.1	
114.1	
114.0	
114.2	
114.6	
114.5	
114.2	
114.6	

Mean free settled volume = 114.288 cm^3

Standard deviation = 0.242 cm^3

Standard deviation of tap settled volumes = 0.714 cm^3

FIGURE 13. RELATION BETWEEN FREE SETTLED AND TAP SETTLED RESIN VOLUMES

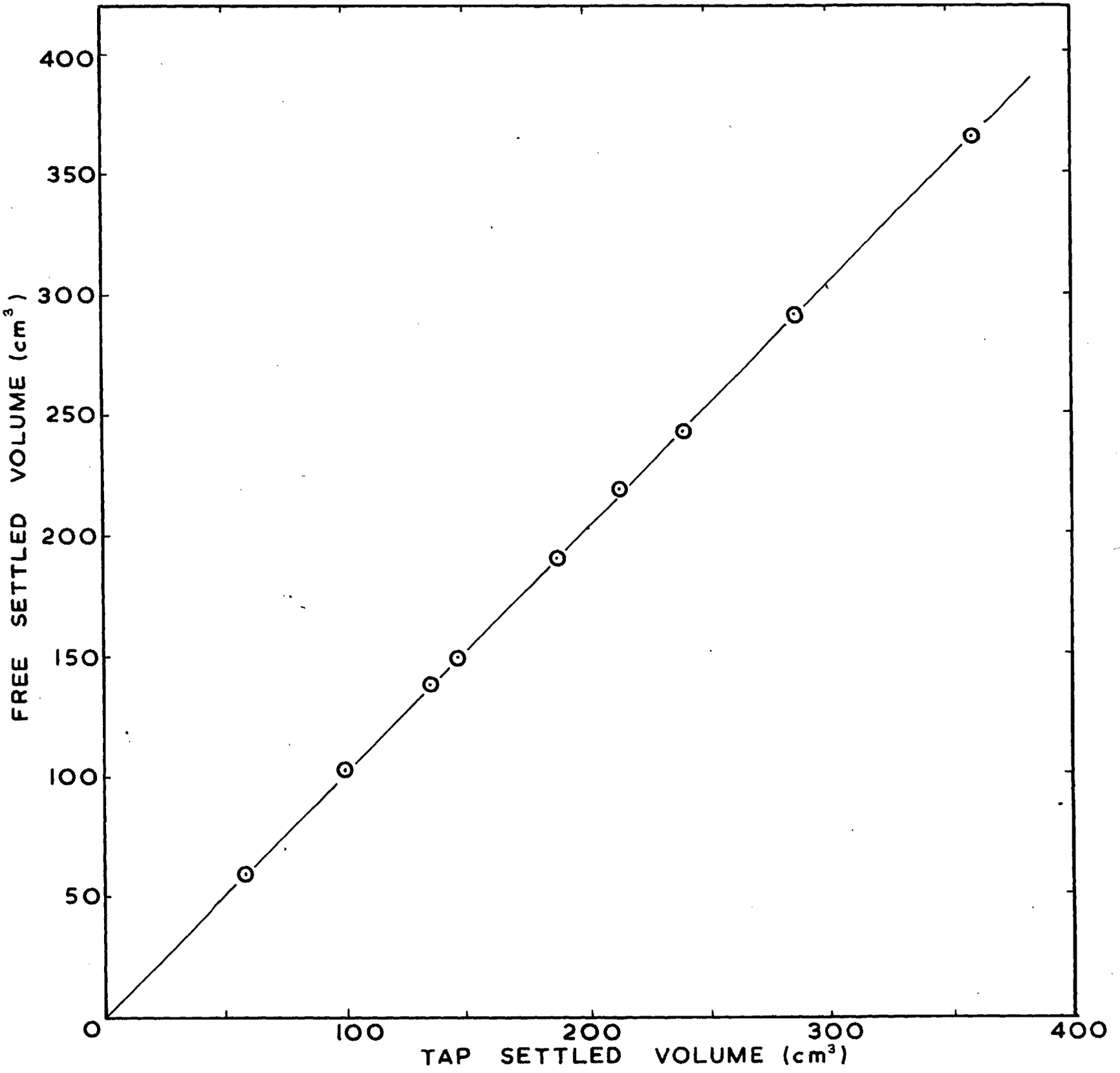

3.2.2. Equilibrium measurements with binary cation systems

$Na^+H^+ Cl^-$ system

Experimental conditions and results are shown in Table 4. When the results are plotted on an x - y diagram (Figure 14) a smooth equilibrium distribution curve can be drawn with the points showing little deviation from the line. The selectivity coefficient K_{NaH} has been calculated from values of x and y for Na and H using equation (2.9). It is not constant, and by plotting K_{NaH} against y_{Na} (Figure 15) it can be seen that there is a fairly consistent change in its value, with a maximum at $y \simeq 0.35$. The high value of K_{NaH} calculated for the A equilibrations is probably due to analytical errors. With the low concentration of sodium in the supernate, it was only diluted 2 times before analysis by the flame photometer, so that the Cl^- concentration in the solution analysed was 0.05 N. This concentration would have caused suppression of the sodium emission. After conversion of the emission reading to concentration, high values of y_{Na} and K_{NaH} would result.

Other workers have reported a maximum in the value of K_{NaH} for 8% D.V.B. Zeo-Karb 225. Redinha and Kitchener[R1] showed a flat maximum at a value of y_{Na} of 0.65. Turner et al[T2] fitted a polynomial of the form

TABLE 4 Results of equilibrium measurements on Na^+/H^+ exchange system.

Expt. No.	Volume of Solution (cm^3)	Initial Na^+ soln. Conc^n ($10^{-4}N$)	Final Na^+ soln. Conc.^{n} ($10^{-4}N$)	Calc. H^+ Conc^n (N)	Meas. H^+ Conc.^{n} (N)	Total Resin Capacity (meq)	x Na	y Na	K NaH	Av. x Na	Av y Na	Av K NaH
A1	20	25	6.44	0.0993		3.557	0.0064	0.0104	1.63	0.0063	0.0105	1.68
A2	20	25	6.17	0.0993		3.538	0.0062	0.0106	1.72			
L1	20	75	21.5	0.09785		3.458	0.0215	0.0309	1.45	0.022	0.0301	1.39
L2	20	75	22.4	0.0978		3.592	0.0224	0.0293	1.32			
B3	20	250	72.7	0.0927		3.325	0.0727	0.107	1.52	0.0719	0.109	1.58
B4	20	250	70.9	0.093		3.218	0.0709	0.111	1.64			
Na5	30	333	131.5	0.08685	0.0853	3.192	0.1315	0.19	1.55	0.1332	0.189	1.51
Na6	30	333	135.0	0.0865	0.0858	3.172	0.1350	0.188	1.48			
C3	20	750	219	0.0781		3.528	0.219	0.301	1.54			
C4	20	750	214	0.0786		3.52	0.214	0.301	1.58			
C5	20	750	205	0.0795		3.624	0.205	0.300	1.66	0.211	0.30	1.6
C6	20	750	205	0.0795		3.627	0.205	0.300	1.66			
C7	20	750	211	0.0789		3.563	0.211	0.307	1.66			
C8	20	750	211	0.0789		3.754	0.211	0.287	1.51			

/ Cont'd.....

TABLE 4. Continued.

Expt. No.	Volume of Solution (cm^3)	Initial Na^+ soln. Conc.^{n} ($10^{-4}N$)	Final Na^+ soln. Conc.^{n} ($10^{-4}N$)	Calc. H^+ Conc.^{n} (N)	Meas. H^+ Conc.^{n} (N)	Total Resin Capacity (meq)	x_{Na}	y_{Na}	K_{NaH}	Av x_{Na}	Av y_{Na}	Av K_{NaH}
Na51	20	1000	327.6	0.06724		3.068	0.328	0.438	1.603	0.334	0.446	1.56
Na52	20	1000	340.5	0.06595		2.99	0.341	0.441	1.529			
Na1	30	1000	432.9	0.05671	0.055	3.195	0.433	0.532	1.49	0.429	0.537	1.54
Na2	30	1000	425.0	0.0575	0.055	3.187	0.425	0.541	1.58			
Na71	40	1000	497.2	0.05028		3.364	0.497	0.5980	1.50	0.51	0.608	1.49
Na72	40	1000	522.9	0.04771		3.092	0.523	0.617	1.47			
Na3	50	1000	575.0	0.0425	0.0421	3.23	0.575	0.658	1.42	0.57	0.659	1.44
Na4	50	1000	565.0	0.0435	0.0426	3.296	0.565	0.66	1.46			
Na91	70	1000	657.2	0.03428		3.317	0.657	0.724	1.37	0.661	0.729	1.38
Na92	70	1000	664.3	0.03357		3.197	0.664	0.735	1.40			
Na7*	30	667	815.5	0.01845		3.149	0.816	0.858	1.37	0.816	0.858	1.36
Na8*	30	667	817.2	0.01828		3.172	0.817	0.858	1.35			
NH1*	30	822	910.9	0.00891		3.349	0.911	0.932	1.34	0.912	0.931	1.29
NH2*	30	822	913.9	0.00861		3.434	0.914	0.93	1.25			

* Sodium form resin used.

FIGURE 14. EQUILIBRIUM CURVES FOR Na^+/H^+ EXCHANGE IN 8% D.V.B. ZEO-KARB 225 RESIN

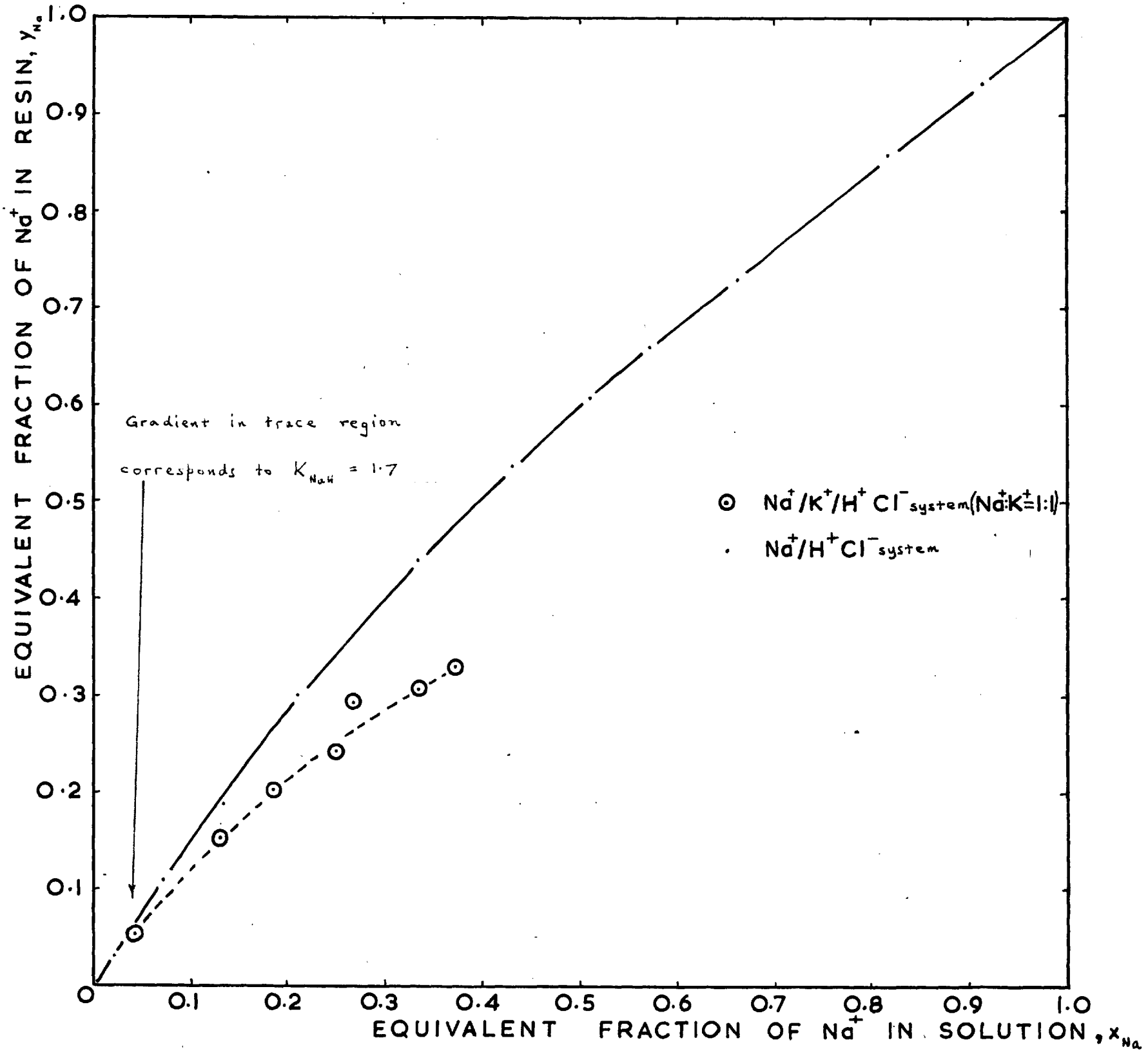

FIGURE 15. AFFINITY CURVES FOR Na^+/H^+ EXCHANGE IN (-14 + 52) BSS 8% D.V.B. ZEO-KARB 225 RESIN

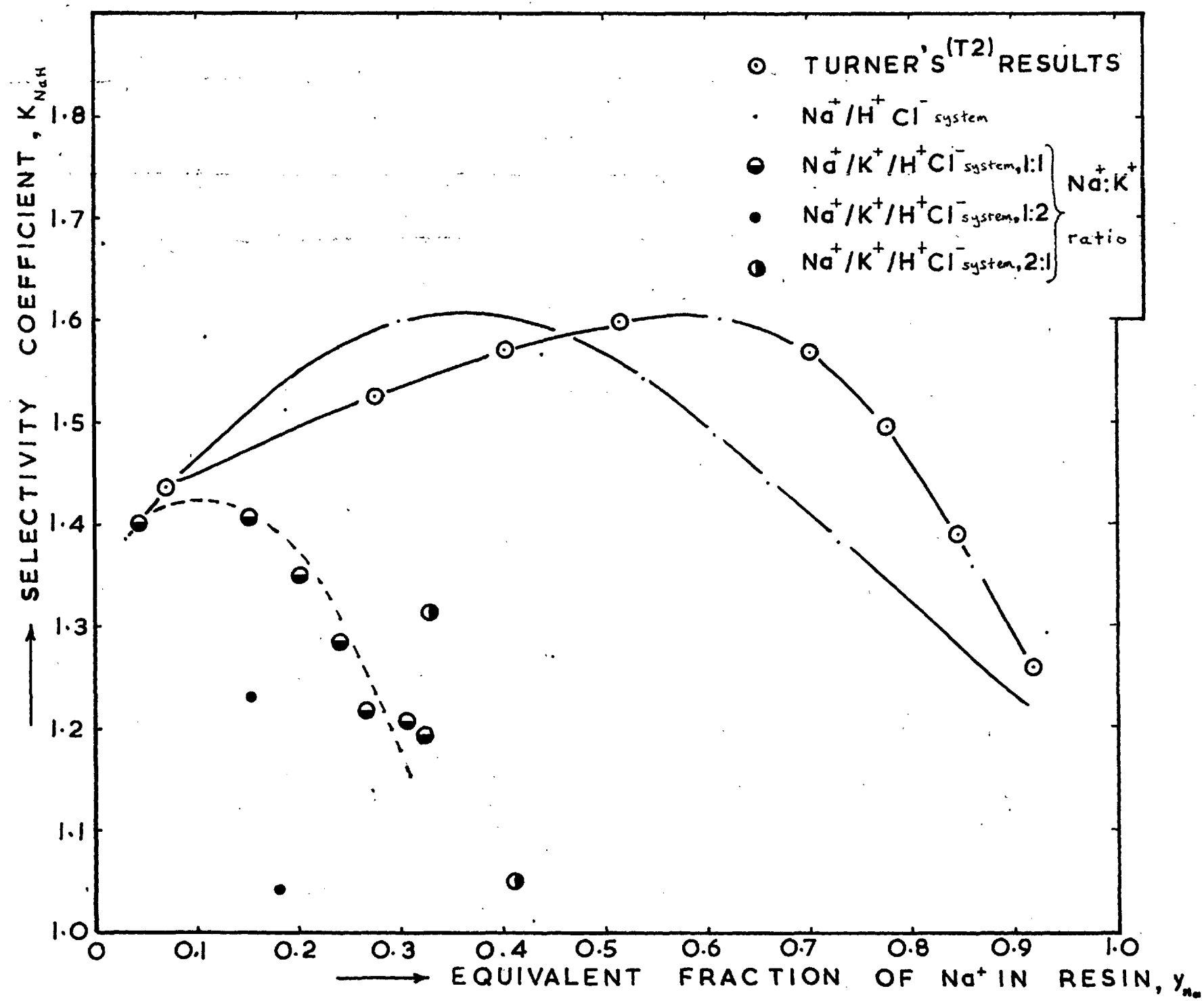

$$(1 - y_{Na}) = (1 - x_{Na}) + [A + B(1 - x_{Na}) + C(1 - x_{Na})^2]\, x_{Na}(1 - x_{Na}) \quad (3.2)$$

where A = -0.104, B = -1.132 and C = +0.834

to their equilibrium results. Values of the selectivity coefficient calculated from their results for various values of y_{Na} are plotted in Figure 15. It can be seen that this curve has a maximum at $y_{Na} = 0.55$. A maximum in the value of K_{NaH} has also been reported for 10% or less cross linked sulphonated polystyrene -D.V.B. resins by other workers (B1, D4, M8, R2,R3) with solutions of 0.2 N concentrations or less.

In the trace ionic fraction region the gradient of the equilibrium line corresponds to $K_{NaH} = 1.7$.

Some of the equilibrations have been repeated, and only recent results are included in Table 4.

K^+/H^+ Cl^- system.

Experimental conditions and results are shown in Table 5, and the equilibrium line is markedly curved (Figure 16) due to the variation in the value of K_{KH}. This can be seen better from the affinity curve in Figure 17. Although there is some scatter of the points there is a steady decrease in K_{KH} as y_K increases. When y_K, $y_H < 0.1$, the overall error in the value of K_{KH} can be higher than 10% (Appendix 1) which explains the

TABLE 5 Results of equilibrium measurements on K^+/H^+ exchange system

Expt. No.	Volume of Solution (cm^3)	Initial K^+ Conc (10^{-4}N)	Final K^+ Conc (10^{-4}N)	Calc H^+ Conc (N)	Meas. H^+ Conc. (N)	Total Resin Capacity (meq)	x_K	y_K	K_{KH}	Av. x_K	Av. y_K	Av. K_{KH}
D1	20	25	3.62	0.0996		3.466	0.00362	0.0123	3.43	0.00348	0.0121	3.52
D2	20	25	3.34	0.0997		3.638	0.00334	0.0119	3.60			
M1	20	75	9.8	0.099		3.575	0.0098	0.036	3.83	0.0098	0.0365	3.86
M2	20	75	9.8	0.099		3.528	0.0098	0.037	3.88			
E1	20	250	42.1	0.0958		3.569	0.042	0.116	3.0	0.0405	0.117	3.13
E2	20	250	39.4	0.0961		3.605	0.039	0.117	3.26			
F1	20	750	157.0	0.0843		3.308	0.157	0.358	3.0	0.156	0.357	3.02
F2	20	750	157.0	0.0846		3.346	0.154	0.356	3.04			
K53	20	1000	252.2	0.0748	0.074	3.145	0.252	0.476	2.69	0.249	0.47	2.67
K54	20	1000	246.5	0.0754	0.0758	3.242	0.247	0.465	2.655			
K61	25	1000	319.0	0.0681	0.0682	3.103	0.319	0.549	2.59	0.31	0.535	2.55
K62	25	1000	302.0	0.0698	0.0697	3.350	0.302	0.521	2.51			
K71	30	1000	378.0	0.0622	0.0621	3.148	0.378	0.593	2.395	0.372	0.587	2.40
K72	30	1000	366.0	0.0634	0.0635	3.275	0.366	0.581	2.40			

TABLE 5 Continued.

Expt No.	Volume of Solution (cm^3)	Initial K^+ Conc^n (10^{-4}N)	Final K^+ Conc^n (10^{-4}N)	Calc H^+ Conc (N)	Meas. H^+ Conc. (N)	Total Resin Capacity (meq)	x_K	y_K	K_{KH}	Av. x_K	Av. y_K	Av. K_{KH}
K81	40	1000	465.9	0.0534	0.0528	3.22	0.466	0.663	2.26	0.468	0.661	2.22
K82	40	1000	470.0	0.053	0.0527	3.22	0.47	0.659	2.17			
K91	50	1000	542.5	0.0458	0.0455	3.183	0.543	0.719	2.16	0.543	0.718	2.15
K92	50	1000	543.8	0.0456	0.0459	3.173	0.544	0.718	2.14			
KH3*	35	715	816.0	0.0184	0.0184	3.73	0.816	0.905	2.14	0.816	0.904	2.11
KH4*	35	715	816.0	0.0184	0.0184	3.637	0.816	0.902	2.08			

* Potassium form resin used.

FIGURE 16 EQUILIBRIUM CURVES FOR K^+/H^+ EXCHANGE IN 8% D.V.B.

ZEO-KARB 225 RESIN

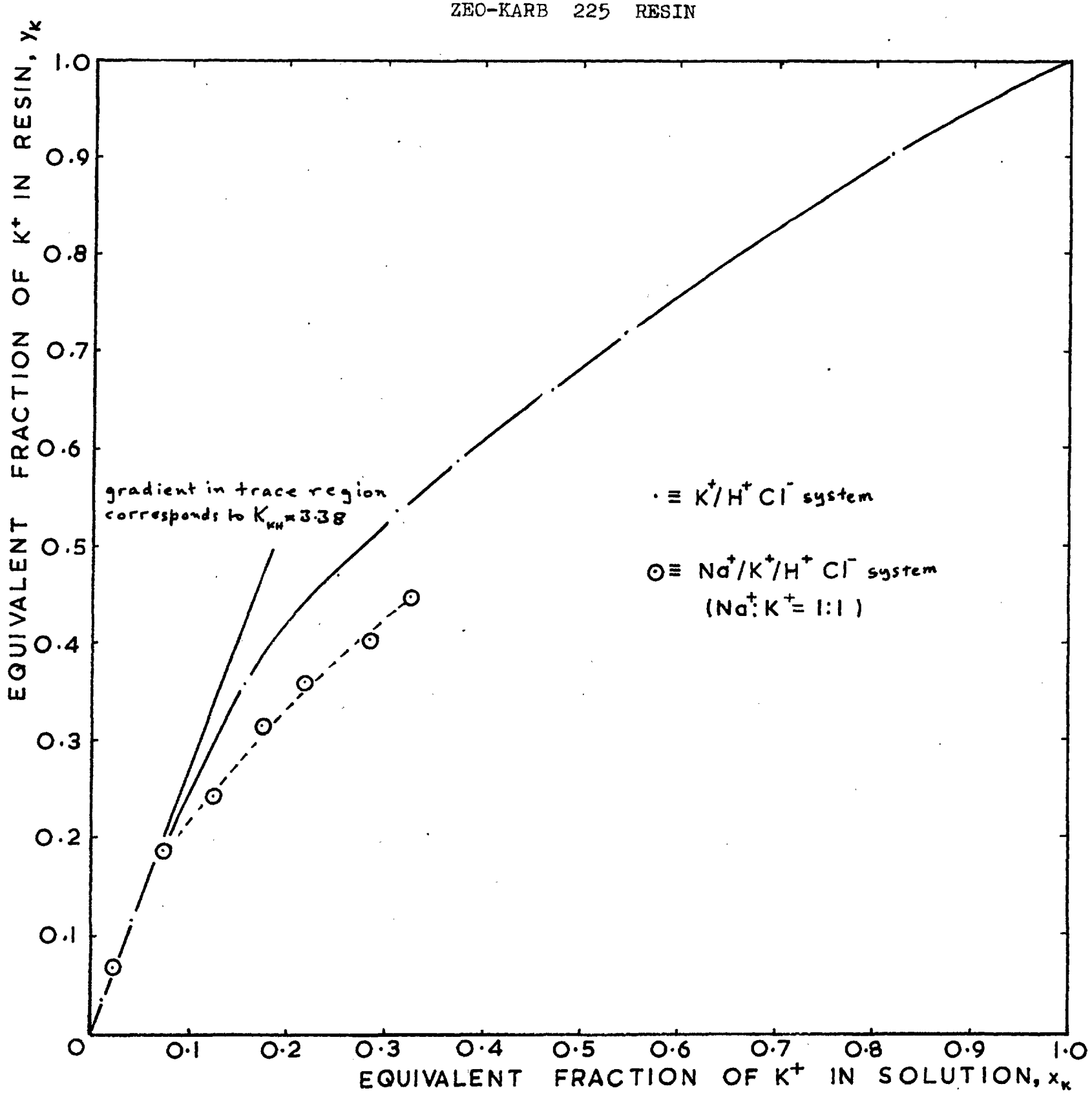

FIGURE 17. AFFINITY CURVES FOR K^+/H^+ EXCHANGE IN 8% D.V.B. ZEO-KARB 225 RESIN

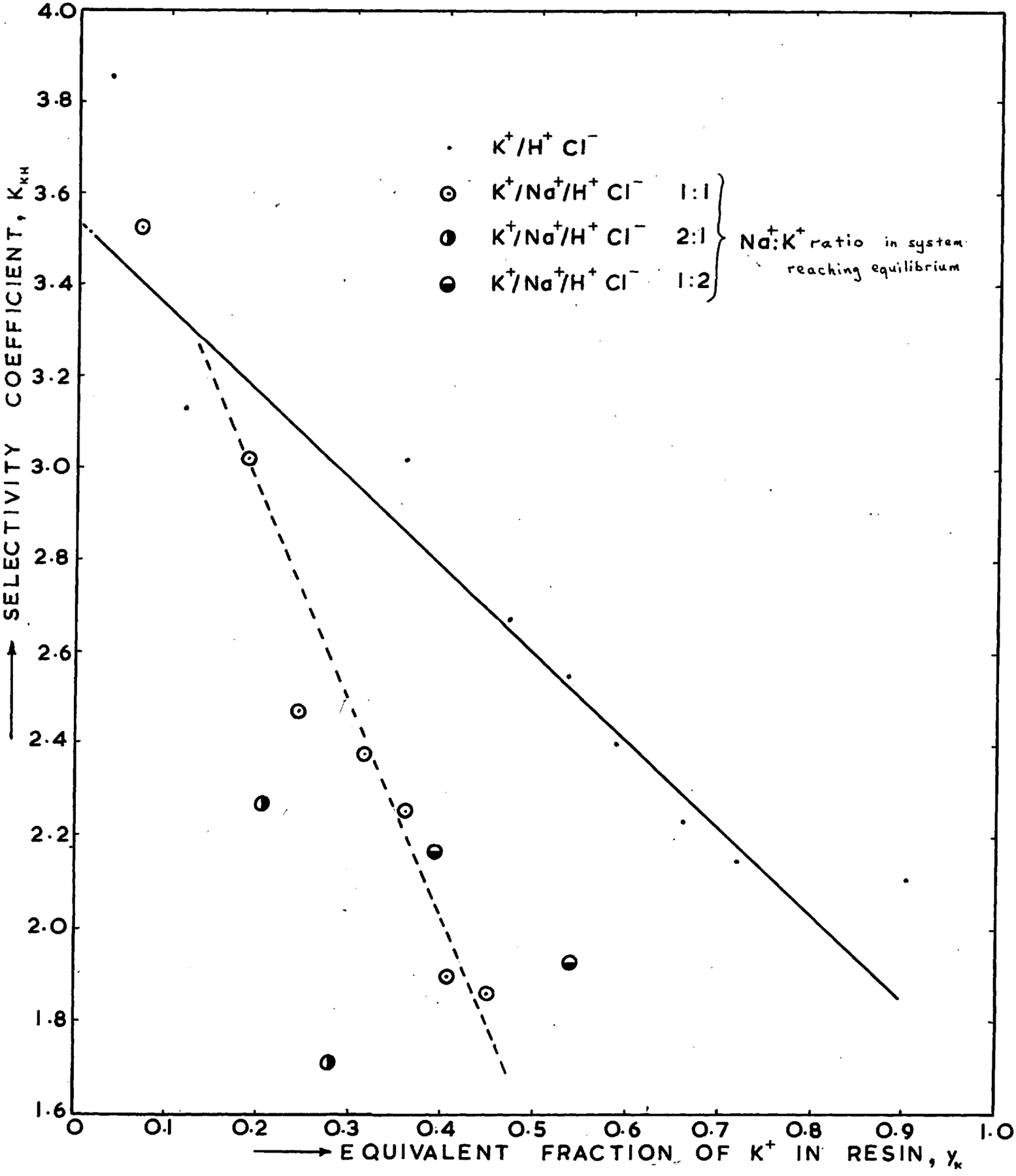

scatter of the points close to the ordinate axis.

K^+/Na^+ Cl^- system.

Experimental results and conditions are shown in Table 6 and are plotted on the x - y diagram (Figure 18). It can be seen from Table 6 that as the potassium loading on the resin, y_K, increases, the value of the selectivity coefficient K_{KNa} falls slightly. This is in agreement with the work of Reichenberg[R3] and Whitcombe[W1].

When ions of the same valency exchange, it is generally accepted that the selectivity of the resin depends primarily on the relative size of the hydrated ions. The larger hydrated ions cause greater swelling and the resin matrix is stretched. Because of its elasticity the matrix tends to contract and the resin prefers the ion with the smaller solvated volume. This tendency is highest when the resin matrix is highly strained, or when the swelling pressure is high. Thus the selectivity should increase with decreasing equivalent fraction of the smaller ion and with increasing degree of cross linking of the resin.

Although the classical swelling pressure theory above can explain many of the observed features of ion exchange, it does not explain others, for example, the maximum in the value of K_{NaH}, and the crossovers in the affinity curves for the Na - H

Table 6. Results of equilibrium measurements on K^+/Na^+ exchange system

Expt. No.	Resin form	Volume of Solution (cm^3)	Initial Na^+ Conc (N)	Final Na^+ Conc (N)	Initial K^+ Conc (N)	Final K^+ Conc (N)	Total Resin Capacity (meq)	x_{Na}	y_{Na}	x_K	y_K	K_{KNa}	Av. x_{Na}	Av. y_{Na}	Av. x_K	Av. y_K	Av. K_{KNa}
K1Na	K^+	20	0.05	0.0215(3)	0.05	0.0784(7)	3.596	0.215	0.158	0.785	0.842	1.457	0.214	0.158	0.786	0.842	1.45
K2Na	K^+	20	0.05	0.0213	0.05	0.0787	3.627	0.213	0.158	0.787	0.842	1.44					
K3Na	K^+	40	0.05	0.0426	0.05	0.0725	3.638	0.426	0.316	0.573	0.684	1.612	0.425	0.316	0.573	0.684	1.60
K4Na	K^+	40	0.05	0.0424	0.05	0.0574	3.641	0.424	0.316	0.574	0.684	1.594					
Na1K	Na^+	40	0.05	0.0689	0.05	0.0311	3.280	0.689	0.58	0.311	0.42	1.604	0.692	0.5815	0.308	0.419	1.62
Na2K	Na^+	40	0.05	0.0695	0.05	0.0305	3.336	0.695	0.583	0.305	0.417	1.63					
Na3K	Na^+	20	0.05	0.086	0.05	0.014	3.393	0.86	0.788	0.14	0.212	1.655	0.859	0.787	0.141	0.213	1.65
Na4K	Na^+	20	0.05	0.08585	0.05	0.01415	3.365	0.859	0.787	0.142	0.213	1.641					

FIGURE 18. EQUILIBRIUM CURVE FOR K^+/Na^+ EXCHANGE IN 8% D.V.B. ZEO-KARB 225 RESIN

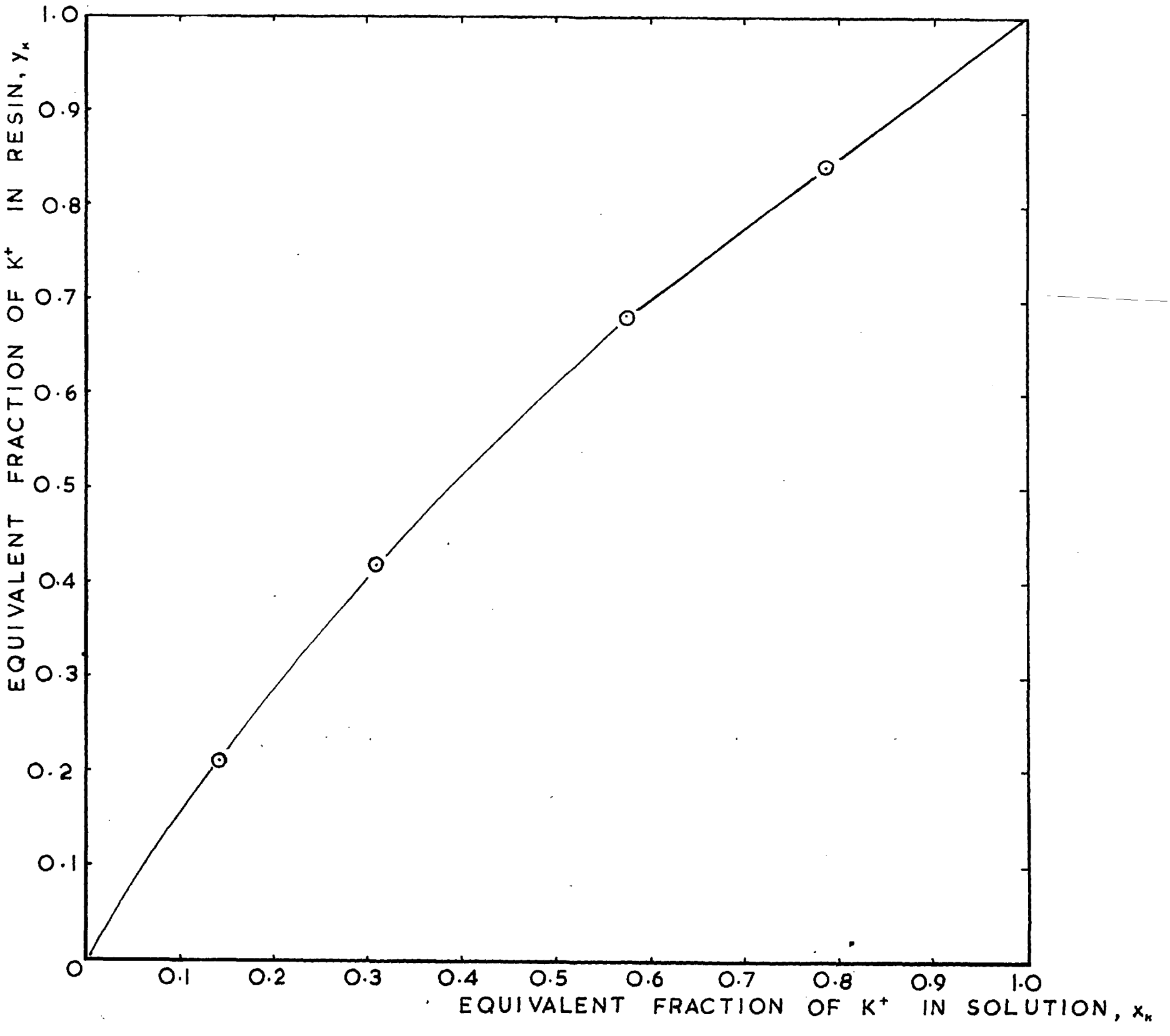

and K - H systems with resins of different cross linking at high values of y_{Na} and y_K[R3]. The role of electrostatic interactions, of ion hydration and water structure, of the non-polar resin matrix and its effect on the solvent and of specific interactions have not yet been clearly established.

Thermodynamic equations for the selectivity coefficient have been expressed[G3, G4] in terms of the swelling pressure and the ratio of the activity coefficients of the exchanging ions in the liquid and resin phases. For monovalent exchange,

$$\ln K_{AB} = \ln \frac{\gamma_A}{\gamma_B} + \ln \frac{\bar{\gamma}_B}{\bar{\gamma}_A} + \frac{\Pi}{RT} \left(\bar{V}_B - \bar{V}_A \right) \qquad (3.3)$$

where $\bar{V}$ is the partial molal volume of the respective ions, Π is the swelling pressure, and γ, the activity coefficient, refers to the respective ions.

With dilute solutions $\ln \frac{\bar{\gamma}_B}{\bar{\gamma}_A}$ is negligible so that K depends on the swelling pressure and the ratio of the activity coefficients in the resin.

In highly cross-linked resins where the swelling pressure is high, the swelling pressure should predominate. In low cross-linked resins where the swelling pressure is low, it can be expected that the ratio of the activity coefficients of the exchanging ions in the resin will predominate. With high

cross linking, the selectivity will be greatest when the matrix is highly strained, i.e. when the resin is saturated with the larger ion. As the smaller ion replaces the ions of larger volume, the matrix becomes less strained and the selectivity towards the smaller ions decreases. So in general with highly cross linked resins the selectivity of the resin towards the smaller of the solvated cations will decrease as the loading on the resin of this ion increases.

The situation in low cross-linked resins where the activity coefficient term is likely to predominate has been described by Glueckauf[G3]. The ratio of the activity coefficients of the two ions in the resin phase is dependent on the molal concentration of sulphonate groups in the resin. This increases as the smaller ions replace the larger ones and water is lost. Thus the selectivity coefficient should increase as the loading of the smaller solvated ion in the resin rises. In fact these changes in K_{AB} have been observed with the Na^+/H^+ exchange system[R2]. With 2% D.V.B. resin, K_{NaH} increased linearly as y_{Na} increased, and with 16% or higher D.V.B. resins, K_{NaH} decreased markedly as y_{Na} increased. It can be seen that the terms involving activity coefficients and swelling pressure respectively oppose each other. The maximum found experimentally in the value of K_{NaH} for 8% cross-linked Zeo-Karb 225 resin could be caused by the relative magnitude of the two opposing terms changing as y_{Na} varies.

With 8% cross-linked resin, K_{KH} decreased steadily (Figure 17) as y_K increased. In fact with resin of any cross-linking of 5% and above K_{KH} decreases as y_K rises[R3], so it seems that with the K^+/H^+ system, the term involving activity coefficients is very small compared with the swelling pressure term. The same reasoning applies to the change in K_{KNa} as y_K increases.

Although the observed changes in K_{KNa}, K_{NaH} and K_{KH} with resin loading have been explained, the situation is more complicated than it seems at first sight. Both the swelling pressure and activity coefficient terms in equation (3.3) depend on the relative size of the solvated ions. Evidence has been built up to show that the solvated size of a cation is not constant. In addition there is considerable variation in the degree of cross-linking in a resin bead of given nominal cross-linking, and perhaps also in the nature of the sulphonate groups. As these factors are of considerable importance for any explanation of changes in resin selectivity, the evidence will be briefly reviewed.

To explain changes in the selectivity coefficient for all binary exchange combinations of the ions H^+, Na^+, K^+ and Li^+, Reichenberg[R3] suggested that,

(a) there are physical differences in the exchange sites due to variation in cross-linking in the resin matrix.

(b) there is steric interference to the fully solvated cations reaching the sites in very highly cross-linked regions, and

(c) the cations lose some of the hydration water molecules to enable them to reach sites in highly cross-linked regions.

No proof was put forward to support these ideas.

Myers and Boyd[M8] tried to predict the selectivity of Dowex-50 for several exchange systems using thermodynamic equations. Differences with experimental values were attributed to the presence of sulphonate groups other than the p. benzyl sulphonic acid groups (i), for example the sulphonation of D.V.B. bridges (ii), the disulphonation of benzene rings (iii), or the sulphonation of ethyl styrene (iv) (which constitutes 45% to 60% of the D.V.B. isomeric mixture[H1]) could be caused by the drastic sulphonation conditions used in resin manufacture.

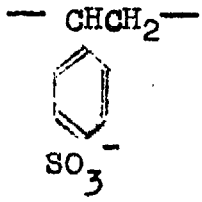

(i)

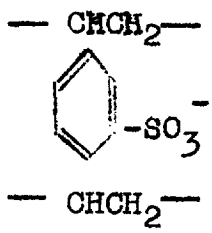

(ii)

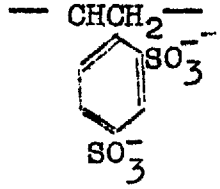

(iii)

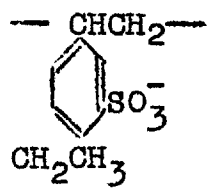

(iv)

Bonner's data[B3] also indicated at least two types of sulphonate group in Dowex 50.

Many workers have applied thermodynamic methods to ion exchange in an attempt to get qualitative information about the nature of the resin and the nature of the interactions between exchange sites, cations and water. The results of Cruickshank and Meares[C7] indicated a non-uniformity of exchange sites and they considered that a physical (i.e. in cross-linking) as opposed to a chemical non-uniformity explained their results satisfactorily.

Considerable differences in the selectivity coefficient K_{AgH}[H11] for different beads from the same batch of Dowex 50 indicated a large variation in the overall degree of cross-linking from bead to bead. The results could be explained theoretically on the basis of a two component system (i.e. two different types of sulphonate groups) or by considerable variation in the degree of cross-linking throughout the beads.

Glueckauf and Watts[G5] in very careful experiments found that the uptake of co-ions is not governed by a Donnan equation. As the Donnan law must apply to any two homogeneous phases, it was concluded that cross-linked ion exchange resins cannot be considered as homogeneous phases. Glueckauf[G4] calculated that there is a wide non-uniformity of cross-linking giving local counter-ion molalities at least 3 to 4 times the

average value of the resin molality, and also of course with regions with much lower fixed group concentrations than the mean. The resin matrix is permeated by a continuous network of aqueous fissures, some of which have the dimensions of the interchain distances in the matrix. From Glueckauf's conclusions it seems possible that some steric interference and cation desolvation is possible, as the mesh width of very highly cross-linked resin (H1) is of the order of a few angstrom units and the radius of solvated alkali metals is also a few angstrom units(M7).

Boyd and co-workers(B5,V1) regard the role of ion-solvent interactions as very important in resin selectivity. Heat and entropy changes caused by ion exchange in various systems are explained by the partial desolvation of a cation when it enters the resin and the more complete hydration of the other ion when it leaves the resin. Flett and Meares(F2) also consider that changes in ionic hydration during the exchange process are influential in deciding the relative selectivity of the resin.

The general qualitative picture which emerges is of considerable variation in the degree of cross-linking and of the concentration of sulphonate groups throughout the resin matrix. There is also the possibility of different types of sulphonate groups in the resin but no definite proof of this has been published. Cations are fully solvated by water

molecules in solution but when they enter the resin matrix they can lose some of the water molecules forming part of the solvation shell. In the more highly cross-linked regions of the resin, due to spatial limitations and the smaller number of water molecules available per ion, the cations are more completely desolvated with the sulphonate groups taking part in the cation solvation. The anion concentration is high in these regions so that cation-anion interactions will be very important. Such interactions will be promoted by the lower effective dielectric constant of the resin phase.

3.2.3. Equilibrium measurements with the ternary $Na^+/K^+/H^+$ Cl^- system.

Results are shown in Table 7.

The potassium concentrations measured by the SP 90 are generally fractionally higher than the values measured with the EEL flame photometer. There is no trend in the sodium concentrations measured by the two instruments. The difference in the values of the selectivity coefficient calculated on the basis of the concentrations measured with the two instruments is within experimental error (Appendix 1).

Equimolar quantities of K^+ and Na^+ ions in the exchange system reaching equilibrium

Results from the present work are plotted as

TABLE 7 Results of equilibrium measurements on $Na^+/K^+/H^+$ exchange system.

Expt. No.	Volume of Solution (cm^3)	Initial Na^+ Conc. ($10^{-4}N$)	Final Na^+ Conc. ($10^{-4}N$)	Initial K^+ Conc. ($10^{-4}N$)	Final K^+ Conc. ($10^{-4}N$)	Calc. H^+ Conc. (N)	Meas. H^+ Conc. (N)	Total Resin Capacity (meq)	x_{Na}	y_{Na}
G3	20	13.34	4.14	12.57	2.214	0.09936	0.0992	3.276	0.00414	0.00562
G4	20	13.34	4.14	12.57	2.117	0.09937	0.0992	3.327	0.00414	0.00553
H3	20	128	41.8	130	20.47	0.9377		3.182	0.0418	0.0542
H4	20	128	41.8	130	20.47	0.9377		3.164	0.0418	0.0542
H3*	20	128	41.0	130	21.33	0.9377		3.182	0.041	0.0547
H4*	20	128	41.2	130	21.25	0.9376		3.164	0.0412	0.0549
I3	20	383.5	130	384	75.2	0.08123		3.365	0.128	0.0151
I4	20	383.5	130.9	384	74.5	0.08121		3.272	0.129	0.154
I3*	20	383.5	132.7	384	74.6	0.08102		3.365	0.130	0.149
I4*	20	383.5	132.9	384	77.5	0.08072		3.272	0.131	0.153
NaK7	20	500	189.7	500	124.6	0.06847	0.0685	3.06	0.190	0.203
NaK8	20	500	184.5	500	121.2	0.06943	0.0694	3.122	0.185	0.202
NaK9	30	500	246.1	500	170.4	0.05835	0.0582	3.067	0.246	0.248

(Cont'd.)

TABLE 7 (Cont'd.)

x_K	y_K	K_{NaH}	K_{KH}	Av. x_{Na}	Av. x_K	Av. y_{Na}	Av. y_K	Av. K_{NaH}	Av. K_{KH}
0.00221	0.00623	1.36	2.87	0.0041	0.0217	0.00557	0.00625	1.35	2.93
0.00212	0.00628	1.34	2.98						
0.0205	0.0688	1.39	3.6	0.0418	0.0205	0.0542	0.0690	1.39	3.61
0.0205	0.0692	1.39	3.62						
0.0213	0.0683	1.43	3.42	0.0411	0.0213	0.0548	0.0685	1.43	3.44
0.0213	0.0687	1.42	3.46						
0.0739	0.184	1.41	2.98	0.128	0.0735	0.153	0.186	1.44	3.06
0.0733	0.189	1.46	3.14						
0.0733	0.184	1.37	3.0	0.131	0.0747	0.151	0.186	1.39	2.98
0.0762	0.187	1.41	2.9						
0.125	0.244	1.33	2.44	0.187	0.12	0.202	0.243	1.35	2.47
0.121	0.243	1.37	2.50						
0.170	0.322	1.37	2.57	0.248	0.173	0.243	0.315	1.29	2.38

(Cont'd.)

TABLE 7 (Cont'd.)

Expt. No.	Volume of Solution (cm^3)	Initial Na^+ Conc. (10^4N)	Final Na^+ Conc. (10^4N)	Initial K^+ Conc. (10^4N)	Final K^+ Conc. (10^4N)	Calc. H^+ Conc. (N)	Meas. H^+ Conc. (N)	Total Resin Capacity (meq)	x_{Na}	y_{Na}
NaK10	30	500	250.3	500	176.3	0.05734	0.0580	3.148	0.250	0.238
NaK11	40	500	292.7	500	216.4	0.0491	0.05	3.161	0.293	0.262
NaK12	40	500	292.7	500	216.4	0.0491	0.049	3.056	0.293	0.271
NaK13	60	500	333.0	500	280.7	0.03863	0.0383	3.28	0.333	0.306
NaK14	60	500	336.8	500	283.0	0.03802	0.0374	3.199	0.337	0.306
NaK15	80	500	375.2	500	325.6	0.02992	0.0296	3.095	0.375	0.323
NaK16	80	500	369.3	500	325.6	0.03051	0.0299	3.13	0.369	0.334
1KNa	30	667	310	333	111.9	0.05781	0.0585	3.253	0.31	0.329
2KNa	30	667	310	333	111	0.0579	0.0584	3.264	0.31	0.328
3KNa	60	667	450	333	187.6	0.03624	0.0372	3.174	0.45	0.41
4KNa	60	667	454	333	191	0.0355	0.0365	3.082	0.454	0.414
1NaK	30	333	165	667	240	0.0595	0.0583	3.246	0.165	0.155
2NaK	30	333	164.4	667	235.6	0.060	0.06	3.322	0.164	0.153
3NaK	30	333	237.0	667	379.5	0.03835	0.039	3.19	0.237	0.181
4NaK	30	333	237.5	667	382.5	0.0380	0.0391	3.163	0.238	0.182

* Analysis for K^+ and Na^+ concentrations by SP90 spectrophotometer. All other analyses by EEL flame photometer.

TABLE 7. (Cont'd)

x_K	y_K	K_{NaH}	K_{KH}	Av. x_{Na}	Av. x_K	Av. y_{Na}	Av. y_K	Av. K_{NaH}	Av. K_{KH}
0.176	0.308	1.20	2.21						
0.216	0.359	1.16	2.15	0.293	0.216	0.267	0.360	1.22	2.25
0.216	0.371	1.27	2.36						
0.281	0.401	1.21	1.88	0.335	0.282	0.306	0.404	1.21	1.89
0.283	0.4070	1.21	1.91						
0.326	0.451	1.13	1.83	0.372	0.326	0.328	0.448	1.19	1.86
0.326	0.446	1.25	1.90						
0.112	0.204	1.32	2.26	0.31	0.112	0.329	0.204	1.31	2.27
0.111	0.204	1.31	2.28						
0.188	0.276	1.05	1.70	0.452	0.189	0.412	0.276	1.05	1.71
0.191	0.277	1.05	1.73						
0.24	0.394	1.24	2.17	0.165	0.238	0.154	0.392	1.23	2.17
0.236	0.39	1.22	2.17						
0.38	0.54	1.05	1.96	0.237	0.381	0.182	0.538	1.04	1.93
0.383	0.537	1.03	1.90						

affinity curves as well as x - y diagrams (Figures 14, 15, 16, 17) to emphasise the changes caused by the presence of the third cation. When the sodium and potassium are in trace ionic fractions values of the selectivity coefficients, K_{NaH} and K_{KH} are virtually the same as in the respective binary systems. This is to be expected, the presence of another cation in trace ionic fractions will not affect the ion exchange system significantly. This is in agreement with the published work reviewed in section 2.1.2.

When the concentrations of sodium and potassium increase, the points on the x - y diagram differ more and more from the binary equilibrium curves. (Figures 14 and 16). This is reflected better in the affinity curves (Figures 15 and 17). It can be seen that as y_{Na} and y_K increase K_{NaH} and K_{KH} fall more rapidly in the ternary system than they do in the binary system. Thus in the ternary system, the resin is showing an increasingly smaller preference for each of the alkali metal species with respect to hydrogen. The marked decrease in resin selectivity observed is different from the results for gross ionic fraction studies published in the literature (section 2.1.2)

The effects observed in this work can be explained satisfactorily on the basis of swelling pressure or varying cross-linking in the resin.

On the classical swelling pressure theory, for a given value of y_{Na} in the ternary system there is a certain equivalent fraction of potassium in the resin in addition to hydrogen. Compared with the binary Na^+/H^+ system with the same value of y_{Na}, swelling of the resin in the ternary system is less, because the solvated volume of potassium ions is smaller than that of solvated hydrogen ions, so the resin will show a smaller selectivity towards the sodium, with respect to the hydrogen. The same reasoning applies to potassium. As the loading in the resin of each of the alkali metals increases, the selectivity of the resin towards each of them will decrease further from the selectivity in the respective binary systems.

If the variation of cross-linking causes different selectivity of the sulphonate groups for the alkali metal ions with respect to hydrogen, the observed effect can be explained by the competition of the sodium and potassium ions for the exchange sites. In the ternary system, for each of the alkali metal species, the sites showing greatest selectivity will be occupied at a faster rate than in the binary systems, and consequently the selectivity coefficient K_{KH} (or K_{NaH}) will decrease more quickly as y_K (or y_{Na}) increases.

Unequal quantities of K^+ and Na^+ ions in the exchange system reaching equilibrium

In the equilibrations where quantities of Na and K in the exchange system were respectively 1:2 and 2:1, the selectivity coefficient, for a given value of the alkali metal ion loading in the resin, was slightly different than for the equimolar system.

Considering the experiments where K:Na = 1:2, the value of K_{KH} tends to be lower and K_{NaH} higher than in the equimolar system, for the same value of y_K or y_{Na} respectively. This effect can be expected from swelling pressure considerations. When there is a higher proportion of sodium in the system, (compared with the equimolar case) for a given value of y_K there is a lower value of y_H. The swelling pressure is lower and the selectivity of the resin for potassium with respect to hydrogen is lower. For sodium there is an opposite tendency. For a given value of y_{Na}, compared with the equimolar case there is a higher value of y_H. The swelling pressure in the resin is greater and the selectivity of the resin for sodium, with respect to hydrogen, is higher.

To summarise this work, with the binary Na^+/H^+ and K^+/H^+ systems, it was found that the values of the selectivity coefficients, K_{NaH} and K_{KH}, of Zeo-Karb 225 changed markedly as the loading of the respective alkali metals in the resin

increased. K_{NaH} passed through a maximum K_{KH} decreased continuously.

When the alkali metals were in trace ionic fractions, the Na^+/H^+ and K^+/H^+ equilibria attained in the ternary system $Na^+/K^+/H^+$ were similar to those in the respective binary systems. These results are in general agreement with results published in the literature(H3, J1).

However as the ionic fraction of the alkali metals increased above the trace level in the ternary system the Na^+/H^+ and K^+/H^+ equilibrium distributions differed increasingly from the respective binary system values (Figures 15 and 17). This effect is contrary to the results reported by Hiester(H4) and Dranoff(D3) for ternary monovalent cation systems. Both these workers reported that the value of the selectivity coefficients in the ternary systems were the same as in the respective binary systems, and were constant. As it is known that even in the binary systems considered by these workers the selectivity coefficient varies considerably (section 2.1.2.) it seems unlikely that it will be constant in the ternary systems.

It was also found in the present work that the relative proportions of sodium and potassium in the ternary system reaching equilibrium affected the equilibrium distribution of sodium and potassium between the solution and resin phases. For example if the relative proportions of Na:K in the

system reaching equilibrium was 2:1, the equilibrium distribution of Na and K differed from that in which the relative proportions in the system were 1:1.

3.2.4. Size distribution of resin.

Results are tabulated in Table 8 and plotted in Figure 19 to show a weight % size distribution and a histogram of the fraction of particles in each size range. The size distribution is not normal but in the absence of knowledge about the pearl polymerisation process, it is not known why the distribution is skewed.

Miller[M5] performed a size distribution analysis on the same batch of resin. His results and the distribution quoted by Permutit[P2] are shown for comparison. The agreement between Miller's results and the present work is very close. Both show a rather higher proportion of the larger particles than the stated Permutit distribution.

An interesting feature of the present results was the small proportion of particles outside (-14 + 52) B.S.S. at both ends of the range.

TABLE 8 Size distribution analysis for (-14 + 52) BSS

8% DVB Zeo-Karb 225 resin.

Mesh number	Mesh size (mm)		Estimated wt % of sample passing sieve			Estimated number of particles held by sieve	Estimated % of total number held by sieve
	Tyler	B.S.S.	(P2) Permutit values	(M5) Miller's values	Present work		
14		1.204		100.0	99.66	48	0.052
14	1.169				99.49	24	0.026
16		1.003		90.1			
16	0.9906				92.88	1568	1.68
18		0.853	96.5	79.1			
20	0.8332				78.59	5102	5.48
24	0.7009				54.41	12980	13.95
22		0.699		60.6			
25		0.599	60.0	35.9			
28	0.5892				32.93	18140	19.79
30		0.50		19.0			
32	0.4952				7.55	36910	39.62
36		0.422	13.0	2.1			
35	0.4165				1.83	12990	13.95
44		0.353					
42	0.3505				0.534	2981	3.2
52		0.295	1.5	0			
48	0.2946				0.08	1612	1.73
60		0.251					
60	0.2463				0	500	0.54

FIGURE 19. SIZE DISTRIBUTION FOR (-14 + 52) B.S.S. 8% D.V.B. ZEO-KARB 225 RESIN.

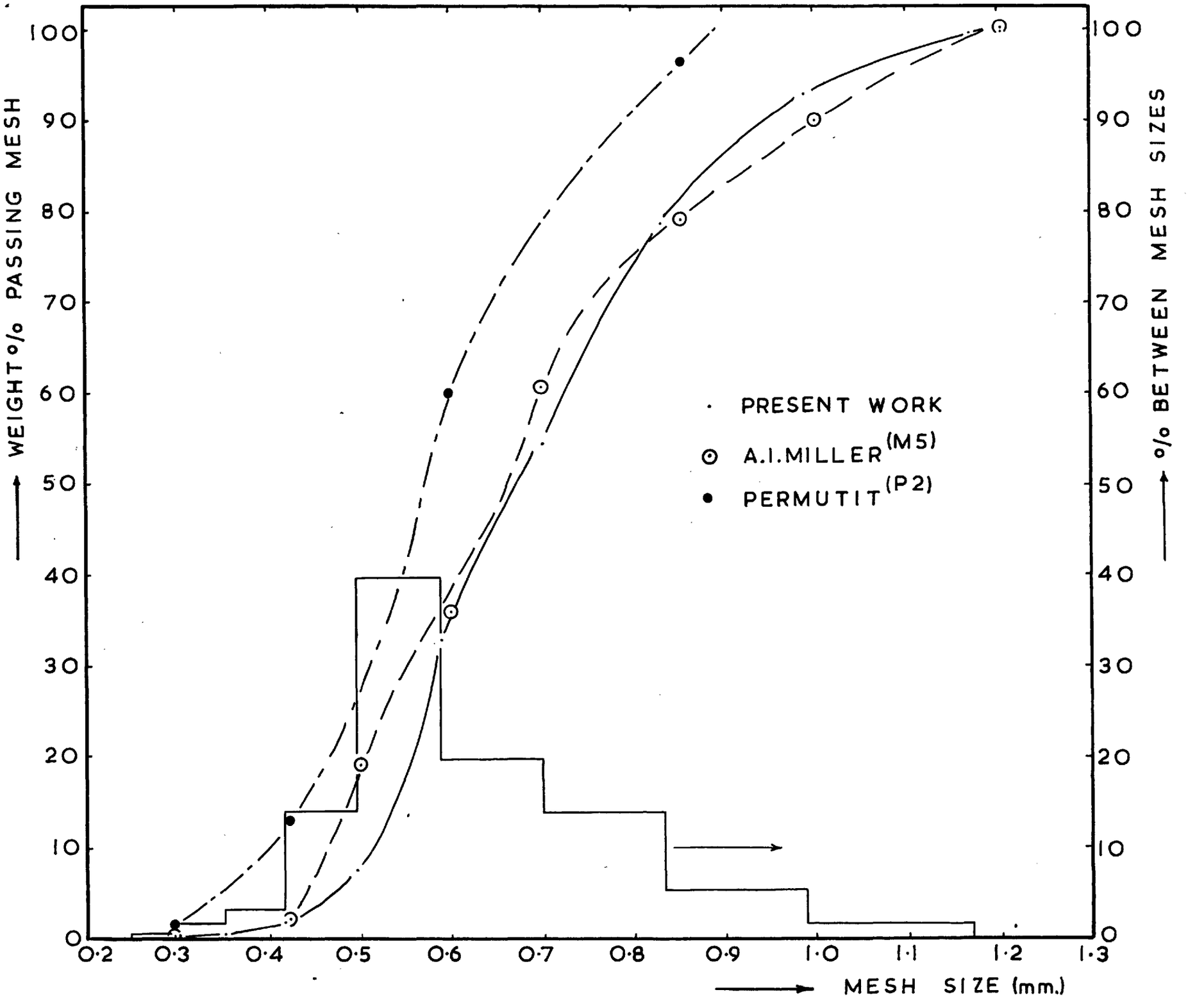

4. Hydrodynamics

4.1 Experimental

As outlined in section 1.3 a hydrodynamic operating diagram must be established to define the range of operating conditions. A single perspex contactor stage was filled with a small quantity of resin, run for one complete operating cycle (forward, settling and reverse periods) and the quantity of resin transferred from the stage in the reverse period, W, measured. This procedure was repeated with increasing quantities of resin for various values of the reverse period t_r. The flowrate of water which entrained resin from the stage in forward flow was also measured for various values of resin hold-up.

With the operation of a multistage contactor the pressure drop is an important consideration. The pressure drop when operating the contactor at the maximum liquid flowrate in forward flow was calculated using standard formulae (C5) for the pressure drop caused by sudden enlargements or contractions in the flow area.

Under normal operating conditions the greatest pressure drop occurs at the end of the reverse flow period when the direction of liquid flow is reversed to forward flow and the resin in each stage is packed in the retainer compartment. A very large resin hold-up, 4.7 cm^3/stage, (> twice the normal

operating value) was introduced into a thirty stage contactor and the pressure drop measured at the end of the reverse flow cycle by connecting a mercury manometer to the liquid inlet and a CCl_4 manometer to the liquid outlet.

4.2 Results and discussion

The hydrodynamic operating diagram is shown in Figure 20, where W, the volume of resin transferred, is plotted against $U_r\ t_r$, the volume of liquid displaced in the reverse flow period. The instantaneous liquid flowrate of 19.6 cm^3/min used in the experiments was approximately the value used in all countercurrent Na/K separations. It is seen that all experimental results lie to the right of the straight line $H > H_{critical}$. The intersection of this line with the abscissa, 2.95 cm^3, gives the minimum value of $U_r t_r$ to transfer resin from the stage. This is in fact very close to the volume of retainer and transfer lines (2.86 cm^3) measured experimentally.

With this flowrate entrainment of resin from the stage in forward flow does not occur until a hold-up of 4.85 cm^3. With the maximum pump output of 50 cm^3/min, entrainment occurs when the resin hold-up is greater than 3 cm^3.

It is generally considered [C3] that normal operation should give a hold-up in each stage less than $H_{critical}$ as

FIGURE 20. HYDRODYNAMIC OPERATING DIAGRAM

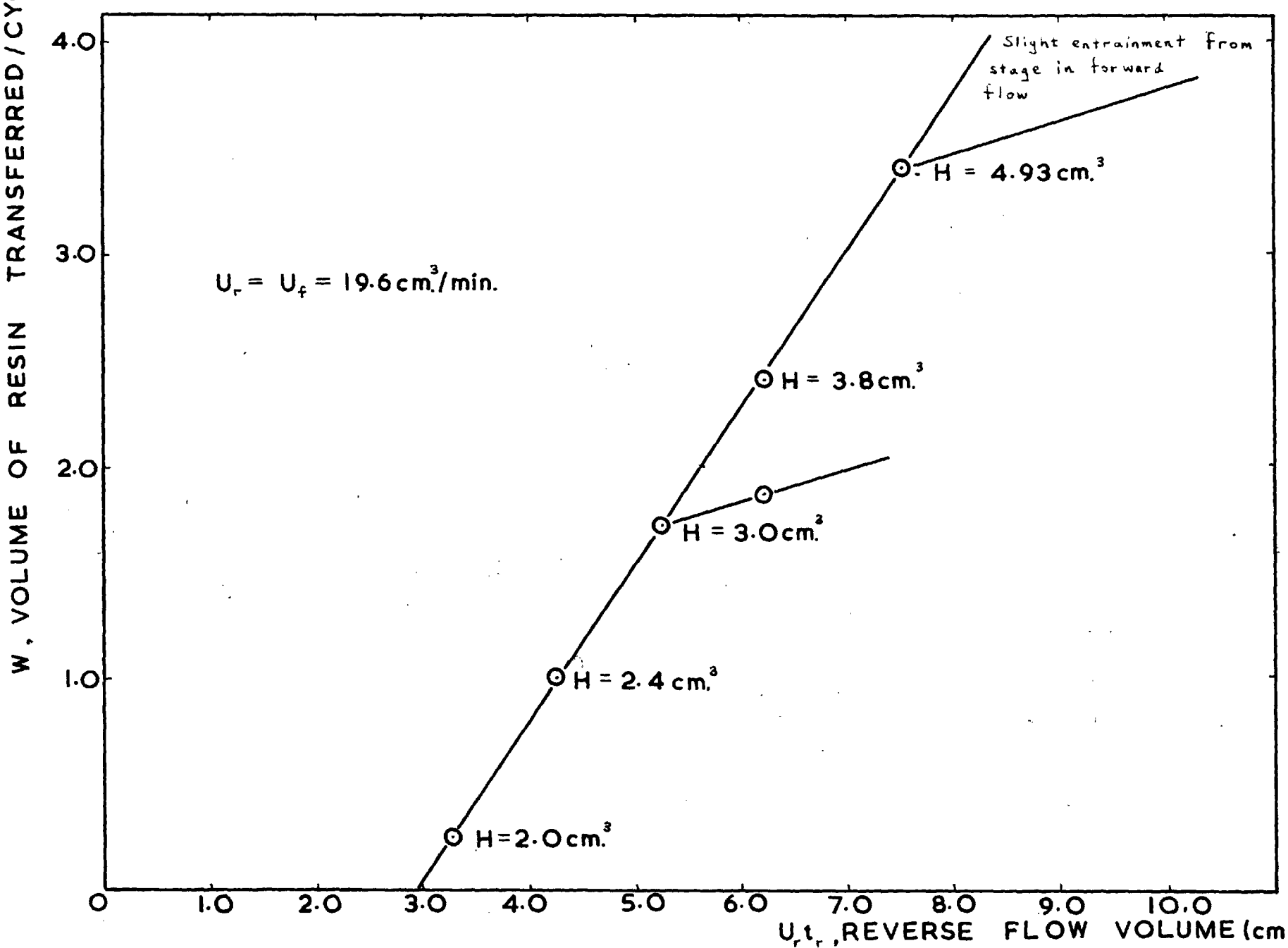

this ensures that the hold-up of resin in all stages remains stable (i.e. flooding does not occur) despite variations in the flow of the liquid or resin phases. Thus with the maximum liquid flowrate of 50 cm^3/min and a resin hold-up of 3 cm^3, Figure 20 shows that W can be as high as 1.6 cm^3/cycle.

The loss of head in forward flow at the maximum flowrate was calculated to be 0.115 cm water/stage, so that the pressure drop through the contactor is not a limitation on operation.

With an excessively large resin hold-up of 4.7 cm^3/stage, the loss in head when the liquid flow reverses at the end of the reverse period was only 3.4 cm water/stage.

A liquid flowrate of about 18 cm^3/min was chosen for the Na/K separation work with the new stage design. At this flowrate it was observed that the resin is gently fluidised and channelling of liquid in forward flow at the sides of the contactor compartment is negligible so that the mass transfer performance should be reproducible from stage to stage and from run to run. This is essential in an investigation of the complex multistage ion exchange separations anticipated in this work.

The nett volumetric flow of liquid depends on the proportion of the operating cycle used for forward and reverse flow. The resin flowrate depends on the nett liquid flowrate

and the $\frac{L}{S}$ ratio required. The reverse flow period in all runs was 2 seconds larger than required in normal operation to ensure that sufficient resin transfer from all stages occurred each cycle. With such a reverse flow period, operation could be conducted over a very wide range of resin flowrates without altering other operating conditions because the value of W was controlled by the volume of resin fed into the contactor.

5. Countercurrent ion exchange of sodium and potassium.

5.1 Experimental

5.1.1 Single section runs.

A flowsheet of the equipment used in the single section runs, with trace or gross concentrations of alkali metal ions, is shown in Figure 21. The liquid storage tanks were either Q.V.F or standard laboratory glassware.

As described in section 1.3 the contactor used in this work operated in three cycles, forward flow, no flow and reverse flow, with a cycle timer controlling the three way Dewrance solenoid valves V1 and V2 to give the desired operation. The feed liquid used in the trace concentration runs contained 0.075 N hydrochloric acid. To prevent corrosion of the liquid feed pump P1 and valves V1 and V2 and metallic contamination of feed liquid, odourless kerosene was used as a buffer between the feed liquid and the pump. Teflon sleeved $\frac{1}{16}$ in. asbestos gaskets were used between the Q.V.F. components of the liquid feed tank T1 to prevent deterioration of the gaskets under prolonged contact with the kerosene. For the same reason the pipelines between the kerosene storage tank T4, P1 and the top of T1 were made from $\frac{3}{16}$ in. I.D. copper tubing with a flange connection at the top of T1. Other liquid pipelines were plasticised P.V.C. tubing.

FIGURE 21. FLOWSHEET FOR SINGLE SECTION ION EXCHANGE SEPARATION WORK

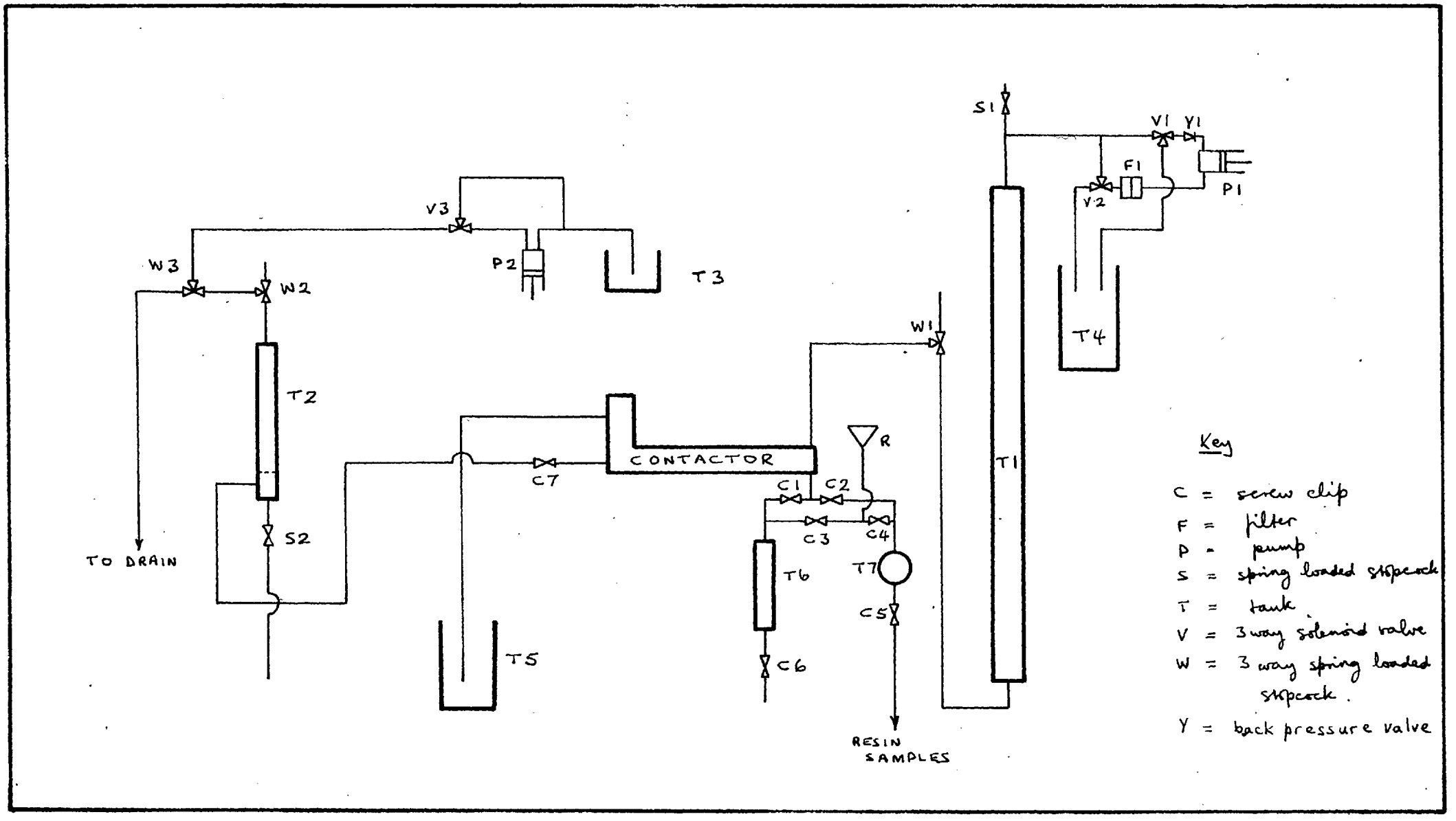

P.V.C. tubing was used initially to connect the T2 resin column outlet to the contactor,but the pressure in the line forced resin particles into the tubing to cause frictional drag and a very variable flowrate. Nylon tubing did not have this disadvantage and narrow gauge ($\frac{3}{16}$ in. I.D.) tubing was used as the resin flowrates were small.

The timer was a standard five channel timer using photocells and a masked disc rotated by a synchronous motor. In some runs an alternative mains pulse timer with decade counting tubes was used.

The pumps used in this work had to deliver a constant reproducible output under prolonged operation and it was necessary to have the facility of controlling the output to fine limits to obtain the desired flowrate. D.C.L. pumps gave satisfactory trouble-free operation. In initial runs with the glass contactor stages, with flowrates up to 70 cm^3/min., a D.C.L. 'M' pump was used, with a D.C.L. micropump for the resin column T2. In runs with the perspex contactor where liquid flowrates up to 20 cm^3/min. were required, D.C.L. Series II micropumps were used.

A back pressure valve was placed in the outlet line of all pumps to prevent any siphoning of liquid through the pump from the 9 feet high feed tanks. Sintered glass filters of 0 porosity were placed in the inlet lines to all pumps or pump heads to prevent particles of dirt from impairing the operation

of the pump ball valves and the solenoid valves.

The glass contactors used in initial work are shown in Figure 4. They were constructed for convenience in banks of 3 with ball and socket Quickfit joints to give flexible links between banks. Before assembly each bank was filled with water by gravity. The ball and socket joints were lightly greased to give water-tight connections.

The design of the components of the perspex contactor is shown in Figure 5.

To avoid the necessity of handling many components when assembling the multistage contactor it was decided to assemble the components in banks of ten stages. This was done by screwing a 6 B.A. threaded rod through the $\frac{1}{8}$ in. diameter holes of each component after counterboring the end sections to prevent the projection of the rod cheesehead and nut.

Although the finish of the perspex is accurate to a small tolerance, adjacent faces of all components were lightly greased with Apiezon M stopcock grease to make joints watertight. When banks of ten stages were connected together resin and liquid inlet components and associated baffles were required to complete the contactor. A $\frac{1}{4}$ in. thick stainless steel plate was placed at each end of the contactor to distribute evenly the pressure from the carpenter's cramp used to keep the contactor components in

position. A 6 feet cramp was required for 100 stages. Figure 22 shows the 100 stage contactor and associated equipment and a bank of ten stages is shown in Figure 7.

The liquid outlet of the contactor must be open to the atmosphere as liquid is pumped into the contactor in the forward flow period and out of the contactor in the reverse flow period. A small reservoir of liquid was situated at the liquid outlet to prevent air being sucked into the contactor in the reverse flow period. The liquid product overflowed from the reservoir into a 5 l. beaker T5.

The liquid feed composition in the various runs was as follows:

(a) trace concentration extraction runs: 0.0125 N.NaCl, 0.0125 N KCl, 0.075 N HCl.

(b) trace concentration rectification and elution runs: 0.1 N HCl.

(c) gross concentration runs: 0.05 N NaCl, 0.05 N KCl.

The solutions were made up from standard 1 N stock solutions by dilution, and the composition checked by analysis.

In the trace concentration single section extraction and three section runs, and the gross concentration runs, a hydrogen form resin feed was used. For the trace single section

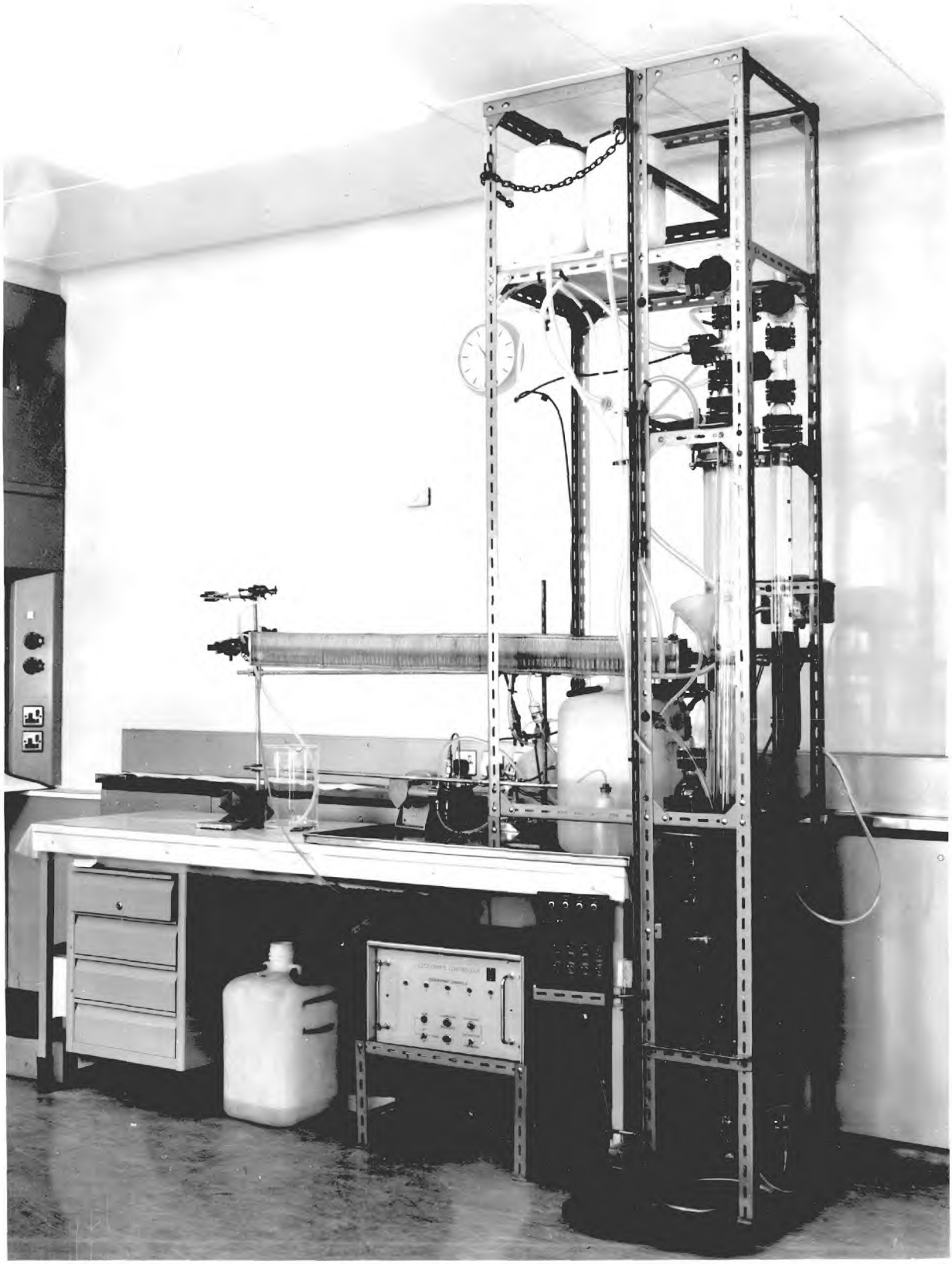

FIGURE 22 EQUIPMENT USED IN ION EXCHANGE SEPARATION WORK

rectification and elution runs, resin of composition similar to the product from extraction run 3 was prepared. The run 3 resin product composition was calculated to be $y_{Na} = 0.1$, $y_K = 0.103$, $y_H = 0.797$. Using the equilibrium distribution curves for the Na^+/H^+ and K^+/H^+ systems it was calculated that 1650 cm^3 of 0.125 N NaCl, 0.125 N KCl solution would give the desired resin composition after equilibration with 1000 cm^3 hydrogen form resin. Water in the interstices of the resin was removed by filtration in a Büchner funnel before the resin was added to the 1650 cm^3 solution. After vigorously stirring the mixture in a 5 l. beaker for 5 hours the resin was again filtered dry in a Büchner funnel. It was then washed in a column with distilled water at a flowrate of 1 $cm^3/(cm^2)(min)$ until the eluate showed no chloride reaction with $AgNO_3$ solution. The composition of the resin was checked in duplicate by eluting 2 cm^3 aliquots of resin with an accurately measured 350 cm^3 volume of $\frac{N}{10}$ HCl. The concentrations of sodium and potassium in the eluate were measured by flame photometer analysis. The actual resin composition was $y_{Na} = 0.092$, $y_K = 0.0955$, $y_H = 0.813$.

The resin flowrates used in this project were small, the highest value was 1.5 cm^3/min in runs 1 and 3. The most satisfactory way of feeding resin was to pump water (using a D.C.L. pump) into the top of a vertical column of settled resin and water, the resin being displaced from the bottom of the

column in dense phase flow. However it was found that the quantity of resin displaced from the column varied during most of the runs. As a constant volume of water + resin was displaced from the column each cycle, the void fraction of the resin + water mixture leaving the column varied.

The diameter and depth of the resin column seemed to affect the variability of the resin flowrate. A modified 100 cm^3 burette, 1.4 cm. I.D. and a $\frac{5}{8}$ in. dia. Q.V.F. column gave especially variable flowrates. The outlet from the base of the burette had an internal diameter of $\frac{1}{4}$ in. The resin was observed to move jerkily through the outlet. Columns of 1 in. and 2 in. diameter gave steadier flowrates but with shallow resin beds (about 2 ft. deep) the flowrate became more variable.

With the small diameter vessels, the jerking of the resin was probably caused by bridging of the particles in the column outlet. With shallow beds in the larger diameter columns the variation in flowrate is believed to be due to increased slip of water through the interstices of the resin. The variation in resin flowrate in most runs is presumed to be caused by a combination of particle bridging and variable slip.

Methods in the literature(G10) for constant solids flowrates would be of no use with the low resin flowrates used in this work. The development of a suitable flow control method is

a major development project. As time did not permit such a venture, variations in the resin flowrate had to be tolerated.

The resin product passes from the contactor into the product vessels T6 or T7, thereby avoiding any exchange between the resin product and the liquid feed. T7 was only used in the trace concentration elution and rectification runs in which resin product samples were required. To remove resin from the product vessel T6, the outlet from the contactor was closed by a screw clip C1 and the line to the reservoir R unclipped at C3. When C6 was opened water could flow from R and resin was displaced from T6. Resin entering the resin product vessel displaced its volume of water back into the contactor to dilute the feed liquid. During steady state runs the resin product was drained off every half hour, so that the resin product vessel contained distilled water and the composition of the liquid displaced back into the contactor was known.

The progress of a run could be followed from the change in composition of the liquid product. Periodic titration of liquid product samples against $\frac{N}{10}$ NaOH indicated whether steady state had been attained. As a further check the concentration of Na and K in the product samples could be measured using the EEL flame photometer.

When steady state had apparently been attained and maintained for an hour or two a steady state run was commenced

without stopping the equipment, so that the dynamic steady state in the contactor was not affected. Bulk and half hourly samples of product streams were taken for analysis. A volume check was made on all feed and product liquid and resin streams at the beginning and end of the steady state run to permit volume balances to be made.

5.1.2 Three section runs.

A modification of the arrangement in the three section process (Figure 8b) was made for these runs. Instead of removing all the liquid used in the elution section as potassium rich product and introducing fresh $\frac{N}{10}$ HCl into the rectification section, some of the liquid leaving the elution section was used as the influent to the rectification section. This simplified the pipework and reduced the number of pumps required. It was thought that this would not affect the performance of the rectification and extraction sections markedly as the alkali metal ion concentration in the elution section was expected to be low. With the $\frac{L}{S}$ ratio in the elution section about twice that in the rest of the contactor this modification resulted in an almost equal volume of Na rich and K rich products respectively.

A liquid feed containing equimolar (0.075N) concentrations of sodium and potassium was used.

To obtain the greatest amount of information from these runs the resin leaving the elution section was not recirculated as the feed to the extraction section. Thus the composition of the feed resin was constant and known, and the composition of the resin product was known after analysis. In addition fluctuation of the composition of the resin product, if this resin were used as the feed resin, would impose an additional variable on the process delaying the attainment of steady state operation.

In runs 10, 11 and 12 with the perspex contactor an instantaneous liquid flowrate of about 16 cm^3/min. from P1 gave satisfactory operation in the reverse flow period and it was decided to use the same flowrate and time period for reverse flow in the three section runs.

As the equipment (Figure 23) was built up from that used in the single section work, only one of Series II pump heads, P1, had the system of two Dewrance three way valves and associated pipework required for forward flow, reverse flow and feed recirculation, so that the choice of a flowrate of 16 cm^3/min. for reverse flow in the contactor established the output from P1. The resin flowrate must be maintained constant in all sections of the contactor and the control system was designed so that only P1 operated on the contactor during the reverse flow period. In this period the other pumps recirculated liquid back to the pump inlet.

FIGURE 23 FLOWSHEET FOR THREE SECTION ION EXCHANGE SEPARATION WORK

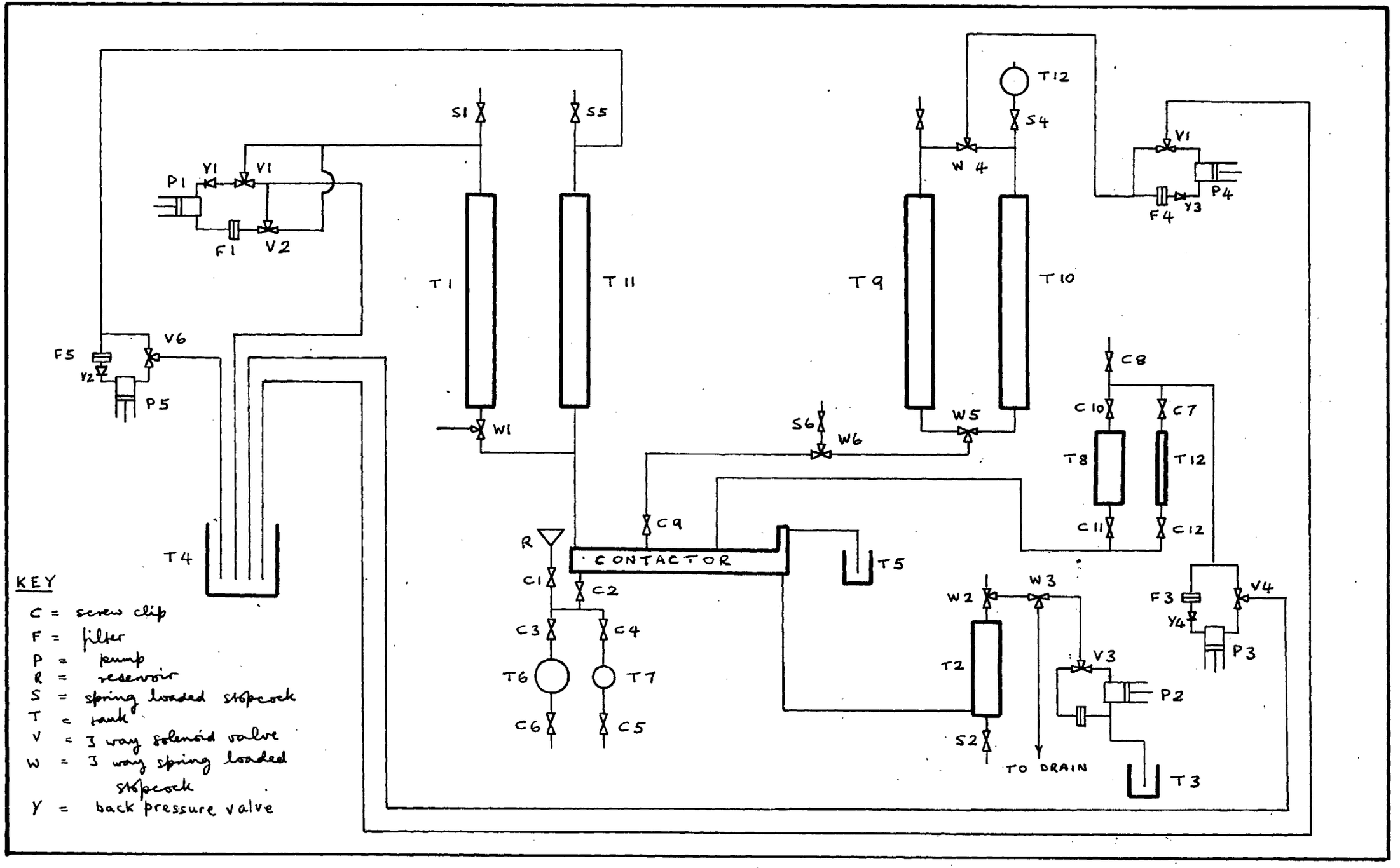

P1 also operated on the contactor in the forward flow period. The resin flowrate was adjusted to give the lowest $\frac{L}{S}$ ratio required in the contactor (i.e. in the rectification section) based on the net forward flow of liquid produced by P1. Higher values of $\frac{L}{S}$ were achieved by the use of additional pump heads which only operated on the contactor in the forward flow period. To get a $\frac{L}{S}$ ratio of about 70 in the elution section, where the liquid influent is $\frac{N}{10}$ HCl, an additional pump head, P5, and $\frac{N}{10}$ HCl storage tank, T 11, were connected to the elution section liquid inlet. Potassium rich liquid product was withdrawn by P4 to give the $\frac{L}{S}$ ratio desired in the rectification section.

The equimolar Na/K feed liquid was introduced from T8 by P3 to give the required flowrate ratio and alkali metal concentration in the extraction section. The sodium rich liquid product overflowed from the extraction section as in previous runs.

Pumps P3, P4 and P5 only operate on the contactor in the forward flow period. For the rest of the cycle they recirculate liquid back to the pump inlet. This was achieved using the Dewrance 3-way solenoid valves actuated by the timer. As the forward flow period was more than half the total operating period, the valves were set up so that they were in the de-energised position in the forward flow period. To simplify the timer control the no flow period was abolished.

Q.V.F. and standard laboratory glassware were used for the extra liquid storage vessels needed for the three section separation runs. Kerosene was used to displace the various liquid feed and product streams to avoid corrosion of pumps.

Only P1 had the system of two Dewrance three way valves and pipework required for pumping liquid into and out of the liquid storage tank as well as recirculating kerosene back to T4. Thus P1 had to be extensively used in filling and emptying all the other storage vessels (T8, T9, T10 and T11). This was readily done by temporarily connecting the top outlet from T1 to the top outlet of the other tanks by P.V.C. tubing.

Resin was introduced into the contactor in a similar way. T8 was filled with distilled water and connected to P1 via T1. P1 was operated using the same time cycle and setting as during a run. The resin introduced into each section was as follows,

(a) extraction section: the resin hold-up from a 10 stage extraction run was used,

(b) rectification section: the resin product from an extraction run was used, and

(c) elution section: the extraction section resin product was mixed with two parts of H^+ resin.

It was hoped that the attainment of steady state conditions was hastened by this procedure.

Two liquid feed tanks T8 and T12 were used. T8 was a 1 l. separating flask graduated in 20 cm^3 divisions. This did not give accurate volume measurement and for the steady state runs, the feed liquid was pumped from T12, a modified 100 cm^3 burette graduated to 0.2 cm^3.

Two potassium rich liquid product storage vessels were required, a large one, T10, to collect the liquid withdrawn before the steady state run, and a smaller one, T9, to collect the steady state K rich product.

To check the approach to steady state the Na rich and K rich product streams were sampled periodically. The potassium rich product stream was sampled by closing C9 to prevent siphoning of liquid through the contactor, and opening S4 and S6. If the K rich product was being pumped into T9, the 3 way (W4) stopcock had to be turned to connect T12 to T9. Kerosene siphoned from T12 into T9 or T10 to displace the K rich product through S6. Liquid in the line from W6 to S6 was rejected to avoid collecting an unrepresentative sample. To avoid disturbing the run the sampling operation had to be completed in the reverse flow period when there was no suction on T9 or T10. The overflowing Na rich product stream could be sampled at any time without difficulty.

These samples were titrated with $\frac{N}{10}$ NaOH and analysed by the EEL flame photometer to check the approach to steady state.

When analyses showed that steady state had been maintained for several hours a steady state run was commenced. As with other separation runs a volume check was made on all feed and produce streams at the beginning and end of the steady state run. This was more complicated with the 3 section runs. More vessels had to be checked and the three way stopcocks W4 and W5 had to be altered so that the K rich liquid product was pumped into T9 which contained only kerosene, to avoid contamination of the liquid product. Also the feed liquid vessel was changed from T8 to T12.

After the first run a sampling point was installed in the rectification section so that samples of liquid leaving this section could be taken. The sampling point was located at the top of the penultimate contactor compartment to avoid contamination by the liquid feed, which was introduced into an enlarged section between the rectification and extraction sections. A $\frac{3}{32}$ in. dia. hole was drilled from the outside to the apex of the contactor compartment and the rubber disc from a standard serum cap was fixed over the hole with Araldite. A 1 cm^3 liquid sample could be withdrawn using a syringe. In the reverse flow period liquid from the extraction section with a higher alkali metal ion content was pumped into the rectification section, so

it was necessary to take the sample just before the end of the forward flow cycle.

During the steady state run half hourly samples of the Na rich and K rich product streams and the rectification section effluent were taken, and the resin product was drained off every half hour.

At the end of the run the resin hold-up in each section was measured.

5.1.3. Design of Na^+/K^+ separation experiments.

From section 3.2.2, $K_{KH} = 3.38$ and $K_{NaH} = 1.7$
From section 3.2.1, $\bar{c} = 1.82$ meq/cm^3. and $c = 0.1$ meq/cm^3

From equation (2.15),

$$E_K = K_{KH} \frac{\bar{c}}{c} \frac{S}{L} = 61.5 \frac{S}{L} \qquad (5.1)$$

$$E_{Na} = K_{NaH} \frac{\bar{c}}{c} \frac{S}{L} = 31.0 \frac{S}{L} \qquad (5.2)$$

The optimum operating conditions to get a Na^+/K^+ separation can be calculated using criteria 2 (i) and 2 (ii) in section 2.2.2.

(i) Na^+ and K^+ in either the solution or resin feed streams.

The optimum operating conditions are

$$E_K > 1 > E_{Na} \text{ or } 61.5 > \frac{L}{S} > 31.0 \qquad (5.3)$$

From equation (2.17), maximum separation of Na and K results when

$$E_K = \sqrt{\alpha} \quad \text{and} \quad E_{Na} = \frac{1}{\sqrt{\alpha}}$$

where the separation factor, α , $= \frac{E_K}{E_{Na}} = \frac{K_{KH}}{K_{NaH}} = \frac{3.38}{1.7} \simeq 2.0$

$\therefore$ $E_K = 1.414$ and $E_{Na} = 0.707$.

Introducing these values into equations (5.1) and (5.2), the flowrate ratio $\frac{L}{S}$ should be 43.5.

(ii) Na^+ and K^+ in the resin feed.

The optimum operating conditions for eluting both species from the resin are

$$E_{Na}, E_K < 1 \quad \text{or} \quad \frac{L}{S} > 61.5 \qquad (5.4)$$

5.2 Trace ionic fraction results and discussion

With the limited number of glass stages available before the perspex contactor components were fabricated, it was not possible to have an effective two or three section separation system using the glass stages and therefore a number of extraction, rectification and elution runs were carried out separately to establish the feasibility of a three section Na^+/K^+ separation using the new contacting technique. Some extraction runs were also carried out with the perspex contactor before it was used in a three section separation.

5.2.1. Single section extraction runs with glass contactor.

Results for these runs are shown in Tables 9, 10 and 11. The extraction factors were calculated using values of K_{NaH} of 1.7 and K_{KH} of 3.38 which were the average values in the trace ionic fraction range (section 3.2.2). The number of equivalent ideal stages and stage efficiency for each run were calculated using equations in section 2.2.4.

The six stage runs 1 and 2 were carried out under similar operating conditions. It can be seen that the sodium enrichment fluctuated during both runs. As the concentration of sodium and potassium in the liquid product fluctuated, the variations are attributed to variation in the resin flowrate. In run 2 the sodium enrichment generally decreased during the run,

TABLE 9. Operating conditions and results of trace continuous countercurrent ion exchange Na^+/K^+ separation runs using the glass contactor

Type	Extraction					Elution		Rectification	
Run Number	1	2	3	4	5	6	7	8	9
Number of stages	6	6	15	15	15	15	15	15	15
Forward flow period t_f (s)	40	40.33	40	38	38	38	38	38	38
No flow period t_s(s)	5	6	5	6	6	6	6	6	6
Reverse flow period t_r (s)	15	13.67	15	16	16	16	16	16	16
Liquid flowrate $U_f = U_r$ (cm^3/min)	65.5	66.7	65.5	66.7	66.7	66.7	66.7	66.7	66.7
Average liquid flowrate L(cm^3/min)	27.25	29.75	27.25	24.45	24.45	24.45	24.45	24.45	24.45
Average resin flowrate S(cm^3/min)	1.48	1.27	1.48	0.63	0.45	0.29	0.1	0.66	0.46
Ratio $\frac{L}{S}$	18.4	23.5	18.4	38.8	54.1	85	24.0	37.1	53.2

(cont,d...)

TABLE 9 Continued.

Type	Extraction					Elution		Rectification	
Run Number	1	2	3	4	5	6	7	8	9
Extraction factor E_{Na}	1.68	1.32	1.68	0.8	0.57	0.365	0.129	0.833	0.581
Extraction factor E_K	3.34	2.63	3.34	1.59	1.14	0.725	0.256	1.67	1.15
Number of cycles	189	150	-	170	177	149	147	153	151
Total liquid feed (cm^3)	5151	4475	-	4150	4325	3650	3590	3750	3700
Total resin feed (cm^3)	280	190	-	107	80	43	15	101	69.5
Liquid feed concentration c_{Na} (10^4N)	125	125	125	125	125	0	0	0	0
Liquid feed concentration c_K (10^4N)	125	125	125	125	125	0	0	0	0
Liquid feed concentration c_H (10^4N)	750	750	750	750	750	1000	1000	1000	1000

(cont.d...)

TABLE 9 Continued.

Type	Extraction					Elution		Rectification	
Run Number	1	2	3	4	5	6	7	8	9
Resin feed concentration $\bar{c}_{Na}$ (meq/cm^3)	0	0	0	0	0	0.167	0.167	0.167	0.167
Resin feed concentration $\bar{c}_K$ (meq/cm^3)	0	0	0	0	0	0.174	0.174	0.174	0.174
Resin feed concentration $\bar{c}_H$ (meq/cm^3)	1.82	1.82	1.82	1.82	1.82	1.479	1.479	1.479	1.479
Resin hold-up per stage (cm3)		6.27		6.12	6.17	5.37	3.88	6.12	6.17
Liquid product concentration c_{Na} (10^4N)	8.73	13.6	2.77	47.9	55.2	18.8	6.39	43.1	27.24
Liquid product concentration c_K (10^4N)	1.64	1.42	0.0434	4.96	5.99	22.4	6.63	31.15	29.4
Liquid product concentration c_H (N)	0.099	0.0985	0.1	0.0947	0.0939	0.0959	0.0987	0.0926	0.0943

(cont.d...)

TABLE 9. Continued.

Type	Extraction					Elution		Rectification	
Run Number	1	2	3	4	5	6	7	8	9
Recovery of Na^+ in liquid product (%)	7.43	10.6	2.4	40.0	46.0				
Enrichment of Na in liquid product (f_1)	5.33	9.65	63.0	9.65	9.21				
Resin product $\bar{c}_{Na}$ concentration (10^4 meq/cm^3)						8.6	2.36	16.7	7.77
Resin product $\bar{c}_K$ concentration (10^4 meq/cm^3)						23.8	2.24	189	74.5
Resin product $\bar{c}_H$ concentration (meq/cm^3)						1.83	1.83	1.81	1.82
Enrichment of K in resin product (f_2)								10.9	9.23

(cont.d...)

TABLE 9. Continued.

Type		Extraction					Elution		Rectification	
Run Number		1	2	3	4	5	6	7	8	9
Number of equivalent ideal stages	n_{Na}	3 to 4	3 to 4	5 to 6	1 to 2*	4 to 5*	4 to 5	3 to 4	15	8 to 9
	n_K	3 to 4	4 to 5	6 to 7	5 to 6	9 to 10	9 to 10	4 to 5		
Stage efficiency(%) based on	n_{Na}	59.5	66.0	38	10.0	30.0	32.0	21.0	100	55.0
	n_K	55.0	69.0	42	35.0	63.0	63.0	31.0		

*Limited adsorption of Na^+ ions into the resin.

TABLE 10 Liquid product concentrations during trace extraction runs using the glass contactor. Samples taken every 30 minutes. Bulk product mixed and analysed for each run.

	Run 1				Run 2			
Sample Number	Na^+ Conc (10^6N)	K^+ Conc (10^6N)	H^+ Conc (N)	Na Enrich-ment	Na^+ Conc (10^6N)	K^+ Conc (10^6N)	H^+ Conc (N)	Na Enrich-ment
1	725	130	0.0905	5.6	1280	124	0.0926	10.3
2	745	150	0.0876	4.96	1450	137	0.0924	10.6
3	816	150	0.0891	5.45	1470	162	0.0924	9.1
4	899	150	0.0904	6.0	1540	164	0.0920	9.4
5	920	161	0.0907	5.7	1620	189	0.0922	8.6
6	925	166	0.0908	5.57				
7	905	150	0.0925	6.04				
8	881	156	0.0931	5.65				
Bulk	873	164	0.0907	5.33	1360	141	0.0925	9.65

(cont.d...)

TABLE 10

(Continued)

Sample Number	Run 3				Run 4				Run 5			
	Na^+ Conc (10^6N)	K^+ Conc (10^6N)	H^+ Conc (N)	Na Enrich-ment	Na^+ Conc (10^6N)	K^+ Conc (10^6N)	H^+ Conc (N)	Na Enrich-ment	Na^+ Conc (10^6N)	K^+ Conc (10^6N)	H^+ Conc (N)	Na Enrich-ment
1	240	6.05	0.0971	39.6	4960	572	0.0905	8.7	4350	369	0.0914	11.8
2	290	2.69	0.0975	108.0	4880	525	0.0906	9.3	5130	451	0.0905	11.4
3	275	6.05	0.0971	45.5	4660	497	0.0908	9.4	5710	588	0.0898	9.7
4	302	2.69	0.0971	112.0	4575	467	0.0910	9.8	5960	685	0.0895	8.7
5	128	1.34			4575	445	0.0910	10.3	6140	806	0.0892	7.6
6	73	5.38			4530	423	0.0910	10.7	6400	938	0.0888	6.83
7												
8												
Bulk	277	4.37	0.0972	63.5	4790	496	0.0907	9.65	5520	599	0.0900	9.21

indicating an overall decrease in the resin flowrate. The sodium enrichment in the bulk liquid product sample was much greater in run 2 than run 1 but the stage efficiency was of the same order, 59.5% and 55% for Na and K in run 1 and 66% and 69% for Na and K respectively in run 2. These values are close enough, considering the variation in the resin flowrate, to indicate that an ion exchange separation using this type of contactor is reproducible. Further evidence on the reproducibility will arise in the separations reported later.

The operating conditions in run 3, when fifteen stages were used, were similar to those in runs 1 and 2. The electronic timer performed erratically after 2 hours steady state operation so the bulk liquid concentrations were not used in calculating the number of equivalent ideal stages. The analyses of the first four samples were averaged to give the process performance and the flowrates were known from the feed volumes during the 2 hours steady operation.

The concentration of potassium in the liquid product samples was extremely low, a fraction of 1 ppm. The significant variation in the K concentration of the liquid product samples is assumed to be due to K contamination. This similarly affected the Na enrichment values, which were probably of the order of the values in the liquid product samples where there was no contamination, i.e. ca. 110.

The use of fifteen stages gave an average Na enrichment of 63.5 in the liquid product, a considerable improvement on the value obtained with six stages. The number of equivalent ideal stages for this run was between 6 and 7 for Na and between 7 and 8 for K, with an average stage efficiency of 40%. In view of the assumptions made to calculate the average liquid product composition and the suggested K contamination of the product samples, some doubt can be attached to this value.

In runs 1, 2 and 3, although the overall stage efficency varied from run to run, the stage efficiency for Na^+ and K^+ adsorption respectively in each run was similar. Because the diffusivity of K^+ ions is greater than that of sodium ions, a higher stage efficiency can be expected for K^+ adsorption or elution. This was the case in runs 2 and 3. Unrepresentative samples or analytical errors were probably the reason for the higher stage efficiency for sodium in run 1.

In a practical separation process, high purity of the required component in the liquid product stream is not the only aim. A good recovery of this component is required, otherwise much of the component may be discharged in the waste streams The extraction factors for sodium and potassium, E_{Na} and E_K respectively, in the first three runs were greater than unity, so that both components were extracted into the resin phase giving a low recovery of sodium in the liquid product (Table 9),

especially in the fifteen stage run where the recovery was only 2.4%.

As discussed in section 2.2.2., to obtain a good recovery of sodium in the liquid product and a good separation of Na and K, E_{Na} must be less than unity and E_K greater than unity, so that

$$31.0 < \frac{L}{S} < 61.5 \qquad (5.3)$$

In runs 4 and 5 these operating conditions were used with 15 stages. In run 4 there was a slight increase in the Na enrichment (Table 10) and a decrease in the sodium and potassium concentrations in the liquid product samples, indicating a small continuous increase in the resin flowrate.

The effect of operating with $E_{Na} < 1$, which gave limited adsorption of sodium is shown by the low value of n_{Na} of between 1 and 2 equivalent theoretical stages, with a stage efficiency of about 10%, for run 4. The number of equivalent ideal stages for K^+ adsorption was between 5 and 6, with a stage efficiency of 36%. (Table 9). The low stage efficiency was probably caused by the resin flowrate increasing during the run. Owing to the delay in the response of the contactor caused by the resin hold-up, if the resin flowrate rises, the contactor at any time is operating with a lower resin flowrate than the average flowrate to that time, and the stage efficiency based on the liquid product analyses is low. The Na enrichment with

respect to potassium in solution of 9.65 in this run was satisfactory.

The reduction in Na enrichment and increase of Na^+ and K^+ concentrations in the liquid phase in run 5 (Table 10) indicate a steady fall in the resin flowrate. The number of equivalent ideal stages for sodium adsorption was again much lower than the value for K adsorption in this run (Table 9). The stage efficiency for K adsorption of 63% is more in line with the value in runs 1 and 2.

The stage efficiency for both Na^+ and K^+ adsorption, except when Na adsorption was limited by operating with $E_{Na} < 1$, has varied from 36% to 70%. The variation of stage efficiency over this range was probably caused by the unavoidable variation in the resin flowrate.

The effect of operating the contactor with $E_{Na} < 1 < E_K$ has brought about a remarkable increase in the sodium recovery. Between $\frac{1}{2}$ and $\frac{1}{3}$ of the sodium in the feed was obtained in the liquid product in runs 4 and 5, but the Na enrichment was lower than in run 3. A lower Na enrichment would be expected with higher $\frac{L}{S}$ ratios, as the total resin exchange capacity in the contactor relative to the quantity of cations in the liquid phase has been reduced. The resin capacity is the means of effecting the separation of Na and K, so that reduced capacity will give a poorer enrichment in the liquid product. The

TABLE 11 Volume balance for trace extraction runs using the glass contactor.

Run No.	Phase	IN		OUT	
		Description	Volume (cm^3)	Description	Volume (cm^3)
1	Liquid	Feed	5151		
		Water feed to resin column	325	Product	5533
		Total	5476		
	Resin	Feed	275	Product	280
2	Liquid	Feed	4475		
		Water feed to resin column	295	Product	4770
		Total	4770		
	Resin	Feed	190	Product	200
3	Liquid	Feed	4947		
		Water feed to resin column	405	Product	5358
		Total	5352		
	Resin	Feed	330	Product	327
4	Liquid	Feed	4150		
		Water feed to resin column	192	Product	4353
		Total	4342		
	Resin	Feed	107	Product	111
5	Liquid	Feed	4325		
		Water feed to resin column	178	Product	4508
		Total	4503		
	Resin	Feed	80	Product	85

performance of the 15 stage contactor in run 5 giving a sodium enrichment of 9.2 and Na recovery of 46% is very satisfactory. To get a better enrichment of sodium under these operating conditions, a greater number of stages must be used in the contactor. Volume balances (Table 11) were generally good in these runs.

5.2.2. Single section elution runs with the glass contactor. The composition of the feed resin was $\bar{c}_{Na} = 0.167$ meq/cm^3, $\bar{c}_K = 0.174$ meq/cm^3, $\bar{c}_H = 1.479$ meq/cm^3. Operating conditions and results are shown in Table 9.

The $\frac{L}{S}$ ratio in run 6 gave extraction factors for sodium and potassium of 0.365 and 0.725 respectively (Table 9). Bulk resin analyses (Table 12) show that the sodium concentration was reduced 170 times to 0.00093 meq/cm^3 and the potassium concentration about 70 times to 0.0024 meq/cm^3 so that complete regeneration of the resin was achieved for practical purposes. Using equation (2.19) for this run, the sodium elution corresponded to between 4 and 5 equivalent ideal stages and potassium elution corresponded to between 9 and 10 ideal stages.

The liquid product samples (Table 12) showed little variation in composition during the run. Despite this there was much variation in the composition of the half hourly resin samples. Considering the variation in the composition, the mass balance (Table 13) was good.

TABLE 12 Liquid and resin product concentrations during trace elution and rectification runs using glass contactor
Samples taken every 30 mins.
Total product mixed and analysed for each run.

Sample No.	ELUTION											
	Run 6: average resin flowrate = 0.29 cm^3/min						Run 7: average resin flowrate = 0.1 cm^3/min					
	Liquid			Resin			Liquid			Resin		
	Na^+ Conc (10^6N)	K^+ Conc (10^6N)	H^+ Conc (N)	Na^+ Conc 10^6meq/cm^3	K^+ Conc 10^6meq/cm^3	H^+ Conc meq/cm^3	Na^+ Conc (10^6N)	K^+ Conc (10^6N)	H^+ Conc (N)	Na^+ Conc 10^6meq/cm^3	K^+ Conc 10^6meq/cm^3	H^+ Conc meq/cm^3
1	1790	2220	0.0940	710	198	1.82	630	733	0.0966	302	332	1.82
2	1910	2355	0.0917	540	254	1.82	486	621	0.0967	252	197	1.82
3	1910	2280	0.0918	535	168	1.82	695	650	0.0967	192	205	1.82
4	1980	2215	0.0918	870	273	1.82	782	690	0.0966	145	160	1.82
5	1880	2215	0.0919	380	131	1.82	760	650	0.0966	292	238	1.82
Bulk	1880	2240	0.0919	860	238	1.82	639	663	0.0967	236	224	1.82

	RECTIFICATION											
	Run 8: average resin flowrate = 0.66 cm^3/min						Run 9: average resin flowrate = 0.46 cm^3/min					
	Liquid			Resin			Liquid			Resin		
	Na^+ Conc (10^6N)	K^+ Conc (10^6N)	H^+ Conc (N)	Na^+ Conc 10^6meq/cm^3	K^+ Conc 10^6meq/cm^3	H^+ Conc meq/cm^3	Na^+ Conc (10^6N)	K^+ Conc (10^6N)	H^+ Conc (N)	Na^+ Conc 10^6meq/cm^3	K^+ Conc 10^6meq/cm^3	H^+ Conc meq/cm^3
1	4060	3000	0.0885	1640	16460	1.802	2580	2940	0.0911	770	690	1.81
2	4160	3035	0.0883	1320	17800	1.801	2600	2940	0.0911	760	643	1.81
3	4310	3115	0.0881	1780	20400	1.798	2700	2940	0.0910	735	735	1.81
4	4160	3060	0.0883	1870	21700	1.796	2745	2940	0.0909	624	700	1.81
5	4310	3035	0.0882	1840	21400	1.797	2780	2940	0.0909	616	671	1.81
Bulk	4310	3115	0.0881	1670	18900	1.800	2724	2940	0.0909	777	745	1.81

TABLE 13 Mass balances for trace elution and rectification runs using the glass contactor

Run Number	Phase	IN					OUT				
		Volume (cm^3)	Na Conc (meq/cm^3)	K Conc (meq/cm^3)	Na Quantity (meq)	K Quantity (meq)	Volume (cm^3)	Na Conc (meq/cm^3)	K Conc (meq/cm^3)	Na Quantity (meq)	K Quantity (meq)
6	Liquid Resin Total	4.3	0.167	0.174	7.19 7.19	7.5 7.5	3773 40.6	1.88×10^{-3} 8.6×10^{-4}	2.15×10^{-3} 2.38×10^{-3}	7.1 0.035 7.135	8.1 0.1 8.2
7	Liquid Resin Total	15	0.167	0.174	2.5 2.5	2.61 2.61	3700 15	6.39×10^{-4}	6.63×10^{-4}	2.36 0.04 2.40	2.45 0.03 2.48
8	Liquid Resin Total	101	0.167	0.174	16.9 16.9	17.6 17.6	3960 112	4.31×10^{-3} 1.67×10^{-3}	3.12×10^{-3} 1.89×10^{-2}	17.1 0.19 17.29	12.33 2.12 14.45
9	Liquid* Resin Total	69.5	0.167	0.174	11.6 11.6	12.1 12.1	3856 69.5	2.72×10^{-3} 7.77×10^{-4}	2.94×10^{-3} 7.45×10^{-3}	10.5 0.05 10.55	11.32 0.52 11.84

* NOTE Influent resin volume not measured and taken to be equal to effluent resin volume

In run 7 the concentrations of sodium and potassium were reduced to 0.00066 and 0.00063 meq/cm^3, a reduction of approximately 250 times in each case. Sodium elution corresponded to between 3 and 4 ideal stages and K elution to between 4 and 5 ideal stages in this run. Owing to the relatively large liquid flowrate, the concentration of K and Na in the liquid product was very low.

Discussion

It is thought that variation in the resin flowrate, unavoidable at the low feed rates used in the elution runs, caused the fluctuation in composition shown by the half hourly resin samples.

Virtually complete regeneration of the resin was achieved in these runs so that the resin could be used as the feed for extraction runs.

The much higher stage efficiency for potassium elution in run 6 can be explained by reference to an x - y diagram (Figure 24). The equilibrium curve for the K - H system has a gradient approximately twice that for the Na - H system, and the operating line gradient is greater than that for both equilibrium lines (E_{Na}, $E_K < 1$). If the number of ideal stages is stepped off it is readily seen that the bulk of the sodium elution is achieved in the first few stages. Subsequent stages

FIGURE 24 x - y DIAGRAM FOR ELUTION RUN 6.

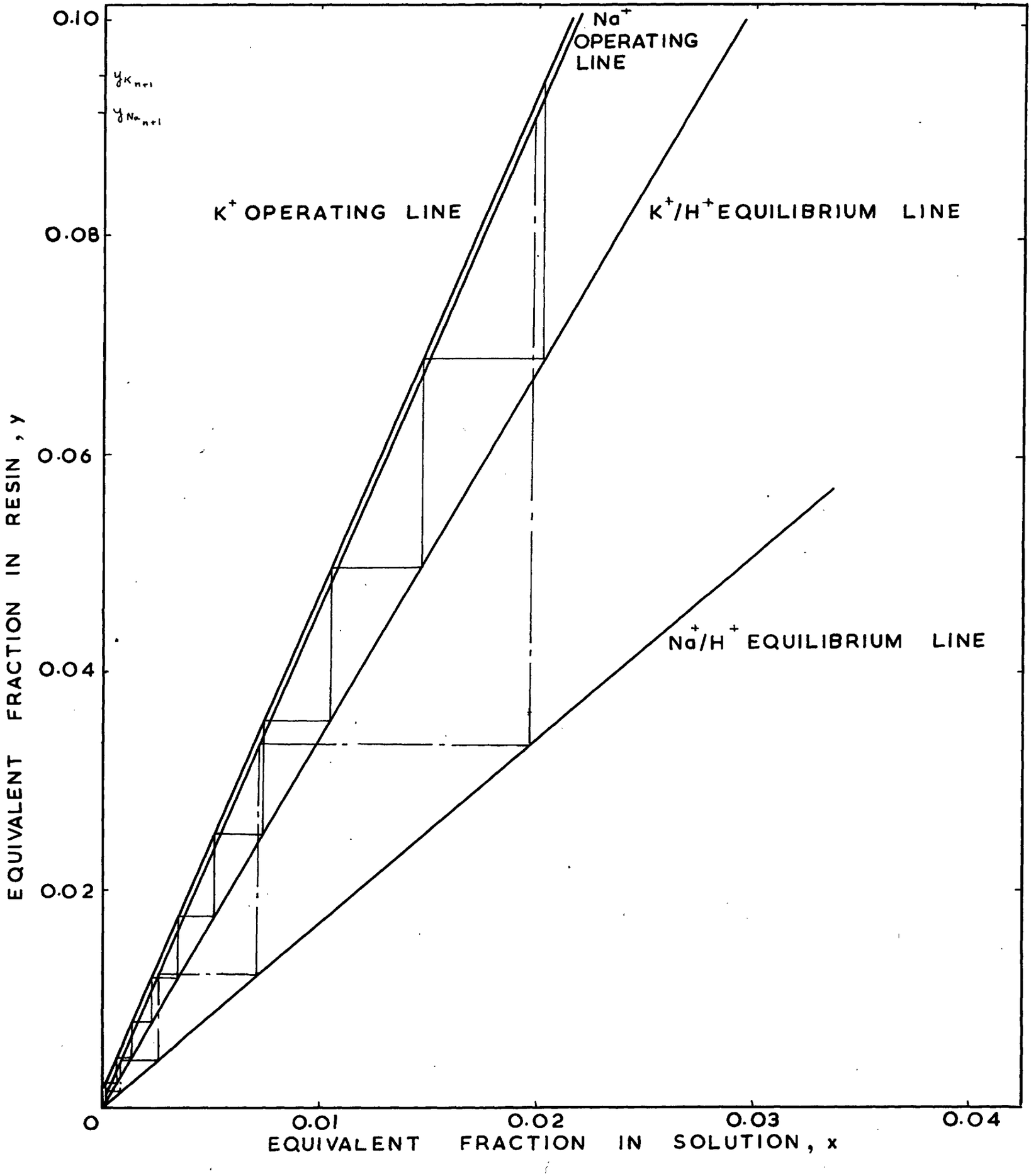

FIGURE 25. x - y DIAGRAM FOR ELUTION RUN 7

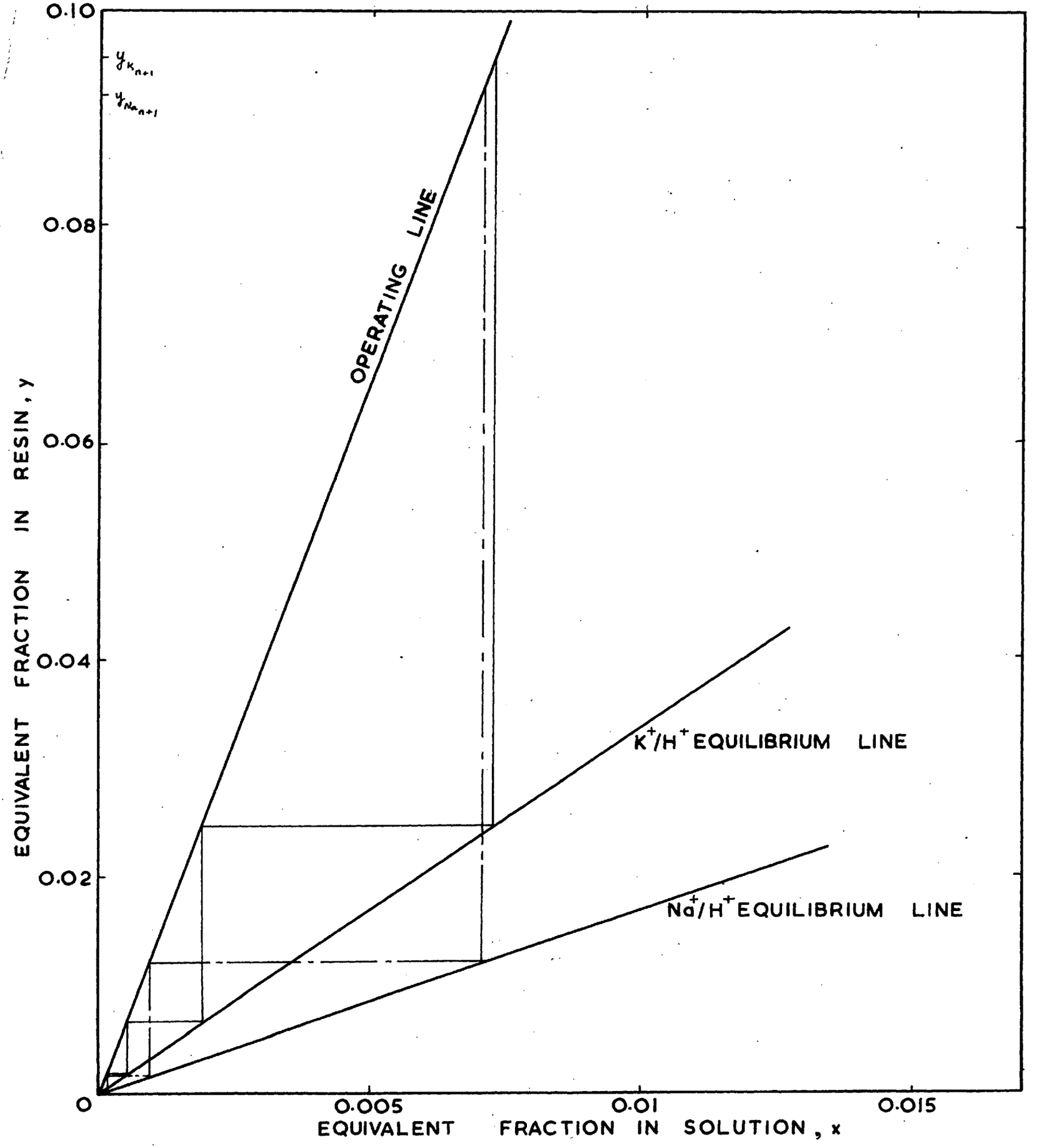

are eluting extremely small quantities of sodium from the resin so that the overall stage efficiency for sodium is low.

With the K-H system it can be seen that the reduction in y in each stage is small, each stage elutes a reasonable fraction of the potassium from the resin and the overall stage efficiency is much higher.

In run 7, the operating line is much steeper than both the equilibrium lines, most of the sodium and potassium is eluted in the first few stages (Figure 25) and the stage efficiency for both cations is low.

5.2.3. Single section rectification runs with the glass contactor.

Operating conditions are shown in Table 9, half hourly liquid and resin product analyses in Table 12 and mass balances in Table 13.

The liquid product samples from both runs showed little variation in composition.

In run 8 values of E_K and E_{Na} were 1.67 and 0.83 respectively, so that elution of potassium from the resin was limited. The ratio $\frac{\bar{c}_K}{\bar{c}_{Na}}$ was increased from a value of 1.05 for the feed resin to 11.5 in the resin product, corresponding to an enrichment of K^+ with respect to Na^+ in the resin of 10.8. The number of equivalent ideal stages for Na^+ elution was 15

corresponding to a stage efficiency of 100%. This is much higher than any of the previous values and it was presumably the result of analysis of an unrepresentative resin sample, despite the good mass balance for sodium. The total potassium in the product streams was 18% too low, (Table 13).

Run 9 was also operated to get limited elution of K^+ ions. The ratio $\frac{\bar{c}_K}{\bar{c}_{Na}}$ increased from 1.05 in the feed to 9.6 in the bulk resin product, corresponding to a potassium enrichment of 9.15. The sodium elution from the resin corresponded to between 8 and 9 equivalent ideal stages, or a stage efficiency of 55%.

The mass balance for this run was good, the discrepancy for both sodium and potassium being within 10%.

Discussion

The rectification runs gave a good separation of sodium from potassium in the resin. Considering a possible three section separation system on the basis of experimental results, extraction run 4, rectification run 8 and elution run 6 have been combined into a composite system (Figure 26). All calculations are based on 1 litre of resin, volume change of the resin with composition being ignored.

The liquid product from run 4 contained 90.5% pure sodium with respect to potassium. The resin product from the run with composition $y_{Na} = 0.164$, $y_K = 0.256$, contained a

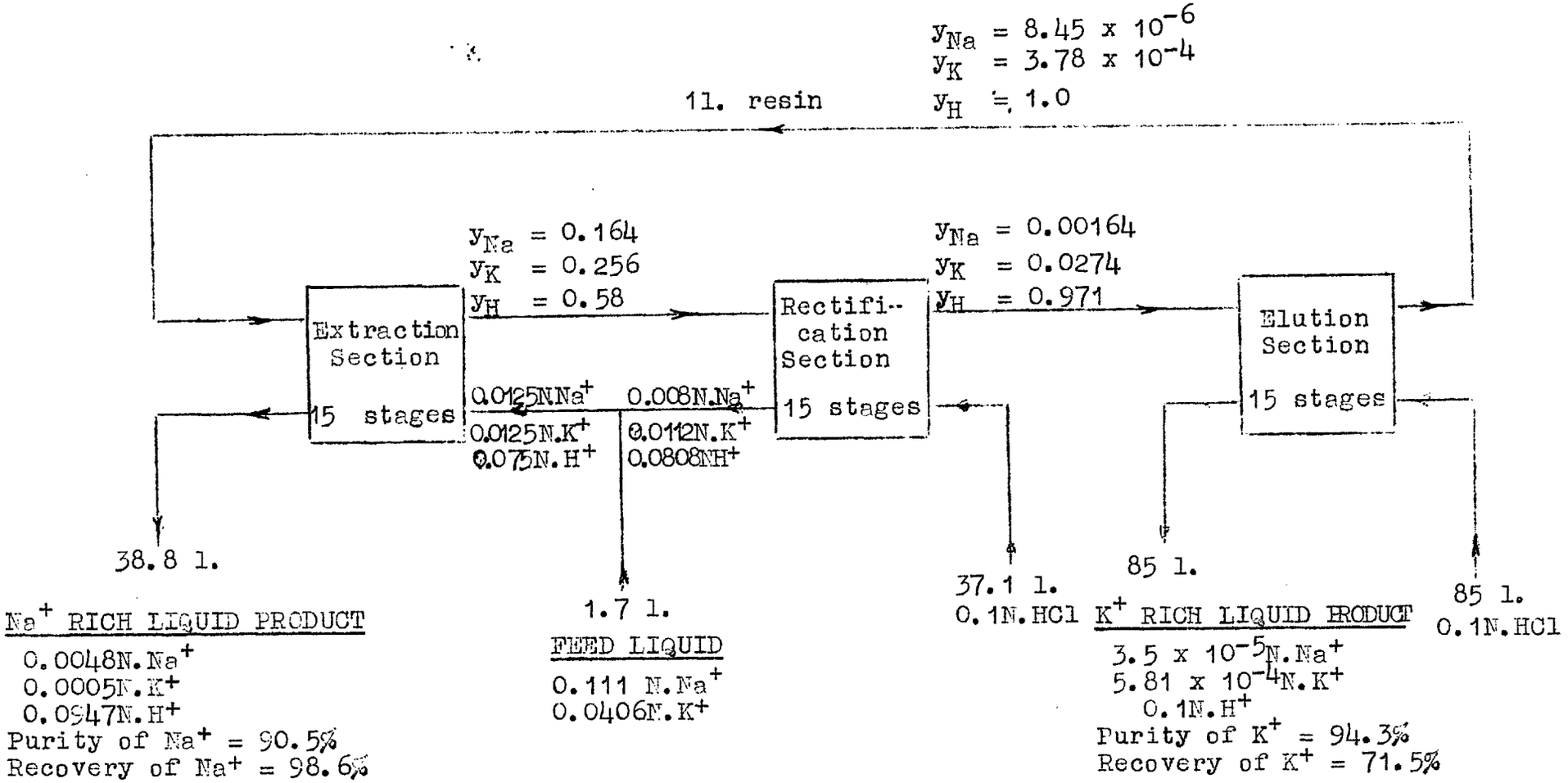

FIGURE 26 COMPOSITE THREE SECTION Na^+/K^+ SEPARATION PROCESS

higher proportion of alkali metal ions than the resin feed used in rectification run 8. Assuming the same performance in the composite rectification system i.e. $\left[\frac{y_1}{y_{n+1}}\right]_{Na} = 0.01$ and $\left[\frac{y_1}{y_{n+1}}\right]_{K} = 0.107$, the rectified resin has the composition $y_{Na} = 0.00164$, $y_K = 0.0274$. The corresponding rectification section liquid product has concentrations of Na and K of 0.008N and 0.0112N respectively. The 1.7l liquid feed must have a composition of 0.111 N.Na^+ and 0.0406 N.K^+ to give an extraction section feed concentration of 0.0125 N.Na^+, 0.0125 N.K^+ and 0.075 N.H^+ (In fact due to mass balance approximations the H^+ concentration is 0.0774 N).

Applying the elution performance in run 6 to the composite rectification section resin product i.e. $\left[\frac{y_1}{y_{n+1}}\right]_{Na} = 0.00515$ and $\left[\frac{y_1}{y_{n+1}}\right]_{K} = 0.0138$, the eluted resin has the composition $y_{Na} = 8.45 \times 10^{-6}$, $y_K = 0.000378$ $y_H = 0.9996$, which is suitable for recirculation to the extraction section.

The liquid product from the elution section has a composition of $c_{Na} = 3.5 \times 10^{-5}$N, $c_K = 5.81 \times 10^{-4}$N, $c_H =$ 0.0994 N, i.e. the K is 94.3% pure with respect to sodium.

Hiester has applied equilibrium stage theory to trace ion exchange separations using a mixer settler(H2) and a continuous countercurrent dense phase contactor(H3). The

mixer-settler was a special modified batch laboratory device in which the phases were not separated and moved countercurrent until equilibrium had been attained. The separations achieved experimentally corresponded to theoretical predictions. The number of equivalent ideal stages in the dense phase contactor was also calculated using the equilibrium stage theory but as the number varied with operating conditions and all but one of the runs were simple extraction runs, the work cannot be regarded as a rigorous proof of the general applicability of this theory to continuous countercurrent ion exchange.

Within the range of $\frac{L}{S}$ ratios of 18.5 to 54 investigated in the present work, the stage efficiency of the glass contactor varied between 36% and 70%, apart from Na^+ elution in run 9. Considering the wide range of operating conditions, the comparatively short operating period of the runs and the unavoidable variation in the resin flowrate and the size of the glass stages, the stage efficiency was reasonably constant. It can be concluded that the equilibrium stage theory can be used to predict the trace ion exchange separations achieved and also that with this type of countercurrent contactor, as the number of stages is changed, the ion exchange separation will be changed in a predictable manner.

5.2.4. Single section extraction runs with the perspex contactor

Results for the three runs are shown in Tables 14, 15 and 16.

It was difficult to get a constant resin flowrate with the small value required in run 10 (Table 14). Approximate checks on the flowrate using the drop in level in the resin column showed that despite corrective action, the flowrate dropped throughout the run. This caused the increase in Na and K concentrations and the fall in the sodium enrichment in the liquid product samples (Table 15).

In this run the effect on Na^+/K^+ separation of operating with E_{Na} and E_K less than unity was investigated.

The sodium enrichment and recovery were 3.65 and 53.4% respectively. This performance was very satisfactory as it was achieved with a very small resin flowrate relative to the liquid flowrate (the average $\frac{L}{S}$ ratio was 72.6).

With E_{Na}, E_K less than unity, adsorption of Na^+ and K^+ ions into the resin was limited. There were probably more equivalent ideal stages for K^+ adsorption as the gradient of the K^+ operating line was little greater than that of the K^+/H^+ equilibrium line. Assuming a constant stage efficiency, the number of ideal stages for K^+ adsorption and $\frac{L}{S}$ ratio have

TABLE 14: Operating conditions and results of trace continuous countercurrent ion exchange extraction runs using the perspex contactor

Run number	10	11	12
Number of stages	10	40	10
Forward flow period t_f (s)	40	37	39
No flow period t_s (s)	3	1	1
Reverse flow period t_r (s)	17	22	20
Liquid flowrate $U_f = U_r$ (cm^3/min)	15.72	16.8	15.5
Average liquid flowrate L (cm^3/min)	6.04	4.2	4.9
*Average resin flowrate S (cm^3/min)	0.083	0.1368	0.127
*Ratio L/S	72.6	31.2	38.9
*Extraction factor E_{Na}	0.427	0.995	0.800
*Extraction factor E_K	0.846	1.975	1.58
Number of cycles	150	155	153
Total liquid feed (cm^3)	905	650	750
Total resin feed (cm^3)	12.46	18.9	18.9
Liquid feed concentration c_{Na} (10^4N)	125	125	125
Liquid feed concentration c_K (10^4N)	125	125	125
Liquid feed concentration c_H (10^4N)	750	750	750
Liquid product concentration c_{Na} (10^4N)	66.7	0.0915	25.7
Liquid product concentration c_K (10^4N)	18.3	0.0261	1.15
Liquid product concentration c_H (N)	0.0822	0.1	0.0856
Enrichment of Na in liquid product (f_1)	3.65	3.5	22.3
Recovery of Na in liquid product (%)	53.5	0	20.6
Number of equivalent ideal stages n_K	10		8
Stage efficiency based on n_K (%)	100		80

* As resin volumes are very small these values are based on the average of the feed and product resin volumes.

TABLE 15: Liquid product concentrations during trace extraction runs in the perspex contactor.

(Samples taken every 30 minutes. Bulk product mixed and analysed for each run).

	RUN 10					RUN 11				RUN 12			
Sample number	Na^+ conc (10^6N)	K^+ conc (10^6N)	H^+ conc (N)	Na enrich-ment	Calc $\frac{L}{S}$	Na^+ conc (10^6N)	K^+ conc (10^6N)	H^+ conc (N)	Na enrich-ment	Na^+ conc (10^6N)	K^+ conc (10^6N)	H^+ conc (N)	Na enrich-ment
1	5800	1390	0.0845	4.17	64.0	9.15	3.07	0.079	3	2080	76.2	0.0861	27.3
2	5900	1590	0.0832	3.71		9.15	4.1	0.079	2.23	2560	112	0.0856	22.8
3	6200	1960	0.0825	3.16		9.15	3.07	0.079	3	2900	148	0.0852	19.6
4	6670	2530	0.0815	2.64		9.15	3.07	0.079	3	3140	179	0.0849	17.6
5	6870	2655	0.0812	2.59	76.5	9.15	3.07	0.079	3	2860	171	0.0852	16.7
Bulk	6670	1830	0.0822	3.65		9.15	2.61	0.079	4.5	2570	115	0.0856	22.3

TABLE 16: Volume balance for trace extraction runs in the perspex contactor.

Run no.	Phase	IN		OUT	
		Description	Volume (cm^3)	Description	Volume (cm^3)
10	Liquid	Feed	905		
		Water feed to resin column	93		
		Total	998	Product	1022
	Resin	Feed	12.46	Product	12.8
11	Liquid	Feed	650		
		Water feed to resin column	173		
		Total	823	Product	829
	Resin	Feed	18.9	Product	23.5
12	Liquid	Feed	750		
		Water feed to resin column	100		
		Total	850	Product	866
	Resin	Feed	18.9	Product	20.1

been calculated for samples 1 and 5 using equation (2.18) and the experimental Na^+ enrichment values, with the condition that the average $\frac{L}{S}$ ratio for these samples approximated the average during the whole run.

The $\frac{L}{S}$ ratio thus calculated increased from 64.0 to 76.5 during the run (the average value of 70.3 is less than the measured average ratio of 72.6 but the difference is within experimental errors). The stage efficiency for K adsorption of 100% is very satisfactory considering that this run was the first attempted with the perspex contactor.

Analysis of the liquid product samples in run 11 (Table 15) showed that virtually all the sodium and potassium was adsorbed by the resin. There was an enrichment of sodium in the bulk liquid product of about 3.5 (analyses at these low concentrations are subject to uncertainty) corresponding to between 1 and 2 ideal stages.

The results are explained by an enrichment of sodium in the liquid phase occurring initially as potassium is preferentially adsorbed in the resin. However after about 20 stages, all potassium was probably adsorbed, and, as K_{NaH} is greater than unity, the sodium displaced the H^+ on the resin. The result was that the sodium concentration in the liquid product was also reduced to an extremely low value.

No problems were experienced with the hydrodynamic behaviour of the new design when used as a multi-stage unit.

The volume balance for both phases (Table 16) was good.

Only ten stages were used in run 12 to avoid adsorbing all alkali metal ions into the resin.

As in run 10 the resin flowrate fell so that the liquid product samples show an increase in the Na and K concentrations and a decrease in the sodium enrichment during the run (Table 15). The sodium enrichment of 22.3 coupled with the sodium recovery of 20.6% shown in the bulk liquid product is very satisfactory considering that only ten stages were used.

To avoid the tedious trial and error calculations for $\frac{L}{S}$ and number of stages used in run 10, the number of equivalent ideal stages for K^+ adsorption ($E_{Na} < 1$ ensured limited adsorption of sodium ions into the resin) has been calculated using the average $\frac{L}{S}$ ratio for the run. n_K was 8 corresponding to a stage efficiency of 80%. This is in fair agreement with the value of 100% calculated for K^+ adsorption in run 10.

The volume balance (Table 16) for both phases was again good.

5.2.5. Three section runs.

Operating conditions and results for the three runs are shown in Tables 17, 18, 19, 20, 21 and 22.

Run 13

The three section separation is a complicated process and this run was carried out at a relatively higher resin flowrate (lower $\frac{L}{S}$ ratio) than proposed in the composite three section process (Figure 26) to reduce the time required to attain steady state.

The aim of this run was to establish that steady state operation is feasible using the rigorous test of mass balances.

The sodium purity and recovery were 90% and 50% respectively in the sodium rich product stream. With the K rich product stream the potassium purity and recovery were 66% and 70% respectively (Table 17). This separation performance was highly encouraging considering that the optimum operating conditions of the composite separation were not used.

In this run only the sodium rich product stream was sampled every half hour. The sodium enrichment in the sodium rich stream increased during the run owing to a slight increase in the Na concentration and a 30% decrease in the K concentration (Table 18). These changes were presumably caused by a change in

TABLE 17 Operating conditions and results of continuous countercurrent trace ion exchange Na^+/K^+ separations using a three section perspex contactor.

Run number	13	14	15
Number of stages extraction section	10	5	5
Number of stages rectification section	10	5	5
Number of stages elution section	10	5	5
Forward flow period t_f (s)	37	37	37
No flow period t_s (s)	0	0	0
Reverse flow period t_r (s)	23	23	23
Control $\frac{N}{10}$ HCl flowrate $u_f = u_r$ (cm^3/min)	6.0	6.33	6.3
Average control $\frac{N}{10}$ HCl flowrate (cm^3/min)	3.7	3.9	3.88
Average elution $\frac{N}{10}$ HCl flowrate (cm^3/min)	5.11	7.11	6.52
Average K rich product flowrate (cm^3/min)	5.62	6.35	5.67
Average centre feed flowrate (cm^3/min)	0.28	0.31	0.313
Average sodium rich product flowrate (cm^3/min)	4.25	5.71	5.82
Average resin flowrate (cm^3/min)	0.124	0.176	0.132
$\frac{L_S}{L_L}$ ratio in extraction section	28.6	28.31	38.8
$\frac{L_S}{L_L}$ ratio in rectification section	26.3	26.8	36.6
$\frac{L_S}{L_L}$ ratio in elution section	71.6	63.1	79.75
Extraction factors in extraction section E_{Na}	1.08	1.07	0.78
Extraction factors in extraction section E_K	2.15	2.13	1.55
Extraction factors in rectification section E_{Na}	1.18	1.17	0.85
Extraction factors in rectification section E_K	2.34	2.32	1.7
Extraction factors in elution section E_{Na}	0.43	0.49	0.39
Extraction factors in elution section E_K	0.86	0.975	0.78
Number of cycles	150	210	273
Centre liquid feed concentration c_{Na} (N)	0.075	0.075	0.075
Centre liquid feed concentration c_K(N)	0.075	0.075	0.075
Centre liquid feed concentration c_H(N)	0	0	0
Resin feed concentration $\bar{c}_{Na}$ (meq/cm^3)	0	0	0
Resin feed concentration $\bar{c}_K$ (meq/cm^3)	0	0	0
Resin feed concentration $\bar{c}_H$ (meq/cm^3)	1.82	1.82	1.82
Rectification section effluent concentration c_{Na} (10^4N)		54.7	31.23
Rectification section effluent concentration c_K (10^4N)		40.02	64.2
Rectification section effluent concentration c_H (N)		0.090	0.090
K rich product concentration c_{Na} (10^4N)	13.31	9.87	4.26
K rich product concentration c_K (10^4N)	25.42	24.0	23.8
K rich product concentration c_H (N)	0.095	0.095	0.0964
Na rich product concentration c_{Na} (10^4N)	25.2	25.2	36.7
Na rich product concentration c_K (10^4N)	3.205	2.65	12.53
Na rich product concentration c_H (N)	0.084	0.085	0.085
Resin product concentration $\bar{c}_{Na}$(10^4meq/cm^3)	232	24.2	8.28
Resin product concentration $\bar{c}$– (10^4meq/cm^3)	416	240	148

TABLE 17 (CONTD.)

Run number	13	14	15
Resin product concentration $\bar{c}_H$ (meq/cm^3)	1.755	1.794	1.805
Na recovery in Na rich product (%)	51.0	62.6	91
Na purity in Na. rich product (%)	88.6	90.5	74.5
K recovery in K rich product (%)	68.2	65.9	57.4
K purity in K rich product (%)	65.7	71.0	85.0
Loss of Na in resin product (%)	13.7	1.84	0.46
Loss of K in resin product (%)	24.6	18.2	8.3
Number of equivalent ideal stages in extraction section n_{Na}		2 to 3	
Number of equivalent ideal stages in extraction section n_K		3 to 4	3
Number of equivalent ideal stages in rectification section n_{Na}			3 to 4
Number of equivalent ideal stages in rectification section n_K			
Number of equivalent ideal stages in elution section n_{Na}		3 to 4	3 to 4
Number of equivalent ideal stages in elution section n_K		5 to 6	5 to 6
Stage efficiency in extraction section (%)			
based on n_{Na}		42	
based on n_K		72	60
Stage efficiency in rectification section (%)			
based on n_{Na}			65
based on n_K			
Stage efficiency in elution section (%)			
based on n_{Na}		75	69
based on n_K		110	105
Resin hold-up, extraction section (cm^3/stage)	2.13	2.5	2.2
Resin hold-up in rectification section (cm^3/stage)	2.05	2.25	2.58
Resin hold-up in elution section (cm^3/stage)	1.61	2.1	2.06

TABLE 18 Liquid product concentrations during three section run 13

Description	Sample Number	Na^+ concentration (10^4N)	K^+ concentration (10^4N)	H^+ concentration (N)	Na^+ enrichment	K^+ enrichment
Na^+ rich product	1	24.0	3.63	0.0840	6.61	
	2	26.47	3.205	0.0838	8.26	
	3	26.47	2.865	0.0838	9.25	
	4	26.47	2.73	0.0838	9.7	
	5	26.62	2.49	0.0838	10.7	
	Bulk	25.2	3.205	0.0839	7.85	
K^+ rich product	Bulk	13.31	25.42	0.0952		1.91

the operation of the rectification and/or elution sections, but in the absence of periodic samples of the K rich product or resin streams, no definite explanation can be made at present. Further discussion may be possible after repeating the run.

The loss of sodium and potassium in the resin product stream was 13.7% and 24.6% respectively. This is a poor performance considering that 10 stages were used in the elution section and the $\frac{L}{S}$ ratio of 71.6 produced values of E_{Na} and E_K less than unity (Table 17).

It is noticeable that the K rich product stream contained a comparatively high concentration of sodium. This was caused by the extraction factors for Na and K being greater than unity in the rectification and extraction sections. Both cation species would tend to be extracted into the resin in both sections. This resulted in a comparatively high alkali metal concentration in the resin entering the elution section, giving the observed high Na^+ concentration in the K rich product and the undesirably high proportion of alkali metals not eluted from the resin.

Calculation of the number of equivalent ideal stages in each section in this run was not possible because samples of the liquid effluent from the rectification section, which was mixed with the feed liquid, were not taken for analysis.

The volume balance (Table 21) and the mass balances for sodium and potassium (Table 22) were good.

The overall mass balance is an indication of the accuracy of the analyses in this run. An additional check can be made as the operating lines of the rectification and extraction sections should intersect at the composition of the feed liquid (i.e. $x_{Na} = x_K = 0.5$) on the x - y diagrams for both the Na - H and K - H systems, from material balance considerations. This can be tested graphically, but as the slopes of the operating lines are very similar, more accuracy can be achieved by calculation.

The slope of the operating lines is known from the flowrate ($\frac{L}{S}$) ratios in each section. By a mass balance over the elution section, the composition of the resin entering this section from the rectification section can be calculated. The mean composition of the liquid phase at this point is known from the analysis of the potassium rich liquid product and so the equations of the sodium and potassium rectification section operating lines are known.

The composition of the liquid leaving the extraction section can be calculated from the concentrations in the Na rich product after making allowance for dilution by interstitial water introduced with the resin feed, and so the equations for the Na and K operating lines in the extraction section are also

known. The equations can be solved to give the intersection points as $x_{Na} = 0.50$ and $x_K = 0.492$. These values are remarkably close to the actual liquid feed composition.

Run 14

Five stages per section were used in this run and operating conditions were similar to those in run 13 (Table 17). Half hourly samples of the potassium rich product and the rectification section effluent were taken in addition to samples of the sodium rich product (Table 19). Volume and mass balances are shown in Tables 21 and 22 respectively.

Operating conditions and results of analyses are shown diagrammatically in Figure 27 for ease of reference.

The composition of the various liquid streams was fairly constant showing that the resin flowrate did not vary greatly during this run. However certain trends are apparent. The concentrations of Na and K in the sodium rich liquid samples decreased steadily during the first half of the run and then increased again, and there was a corresponding increase followed by a decrease in the sodium enrichment. The rectification section effluent samples show a similar trend. The K rich product samples on the other hand show an opposite trend. There was an initial steady increase and then a decrease in the Na and K concentrations and the K enrichment fell and then rose again.

TABLE 19 Liquid product concentrations during three section run 14

Description	Sample Number	Na^+ concentration (10^4N)	K^+ concentration (10^4N)	H^+ concentration (N)	Na^+ enrichment	K^+ enrichment
Na^+ rich product	1	25.2	2.755	0.085	9.15	
	2	23.75	2.535	0.085	9.37	
	3	22.2	2.31	0.086	9.61	
	4	22.7	2.27	0.085	10.0	
	5	23.2	2.4	0.085	9.67	
	6	24.2	2.62	0.085	9.23	
	7	26.2	2.66	0.085	9.85	
	Bulk	25.2	2.648	0.085	9.52	
K^+ rich product	1	8.22	21.55	0.096		2.62
	2	9.76	23.85	0.096		2.45
	3	9.76	23.55	0.096		2.42
	4	11.6	25.3	0.095		2.18
	5	11.4	24.8	0.095		2.18
	6	10.63	24.5	0.095		2.30
	7	9.675	23.15	0.096		2.39
	Bulk	9.87	24.0	0.096		2.43
Rectification section effluent	1	49.5	41.1	0.090	1.205	
	2	56.5	42.3	0.089	1.337	
	3	58.1	41.7	0.089	1.393	
	4	57.6	40.0	0.089	1.44	
	5	52.1	36.15	0.090	1.44	
	6	52.9	38.9	0.09	1.36	
	7	56.0	40.0	0.089	1.4	
	Average	54.7	40.0	0.090	1.36	

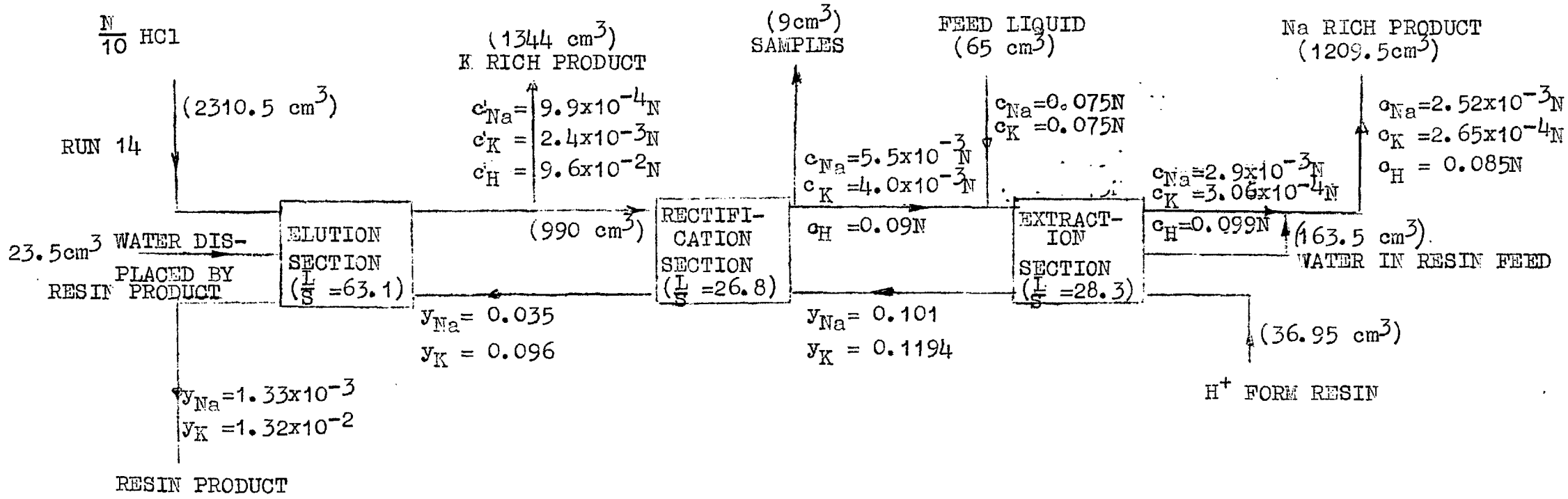

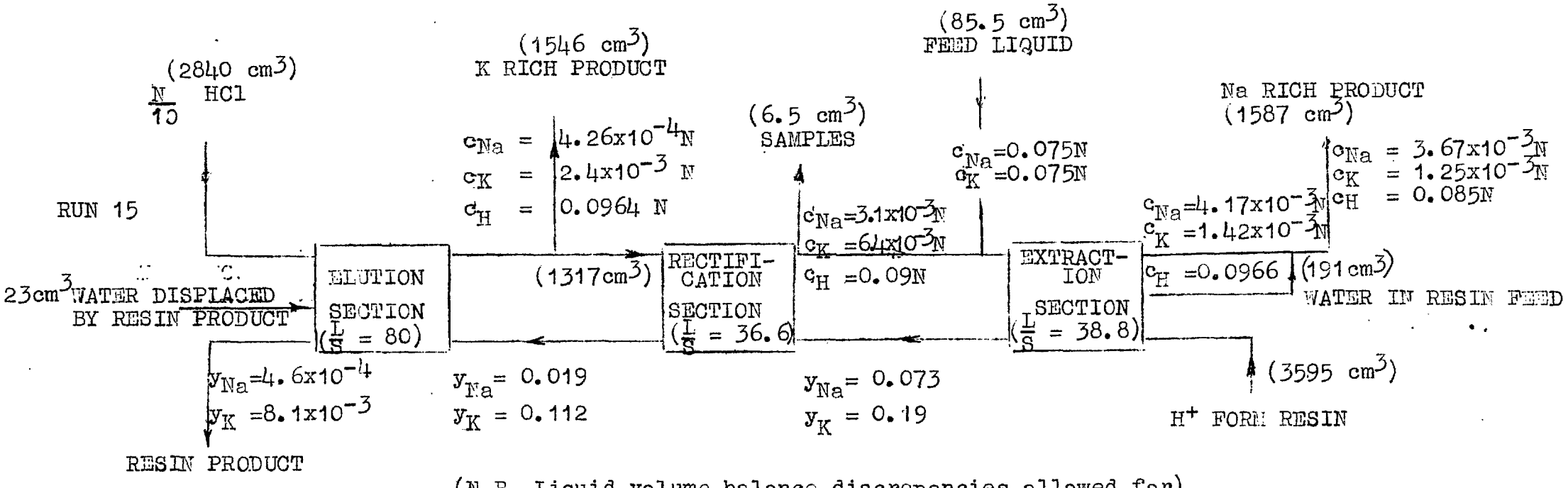

(N.B. Liquid volume balance discrepancies allowed for).

FIGURE 27. BLOCK DIAGRAMS FOR THREE SECTION RUNS 14 AND 15

These trends seem to indicate a gradual increase in the resin flowrate during the first half of the run and a gradual decrease during the second half.

With a rise in the resin flowrate, the concentrations of sodium and potassium in solution decreased in the extraction and rectification sections as the alkali metal ions were present in trace ionic fractions. Thus with an increasing resin flowrate an increasing quantity of alkali metal ions entered the elution section in the resin. With the extraction factors for Na and K less than unity, the alkali metal ions tended to be extracted back into the liquid phase. After a time interval caused by the slow replacement of the resin hold-up an increased concentration of sodium and potassium in the potassium rich product would be expected. The reverse of these trends would occur with a decreasing resin flowrate. The fact that the concentration of Na^+ and K^+ in the K rich product increased right from the start of the steady state run indicates that the resin flowrate had been increasing for some time before the steady state run.

The suggestion that the resin flowrate decreased in the second half of the run is supported by the fact that the volume of resin collected as product was greater than that fed into the contactor. The decrease over the second half of the run would affect the feed volume but owing to the resin hold-up it

would affect the resin product volume to a much smaller degree.

The Na^+/K^+ separation performance in this 15 stage run was of the same order but rather better than that in run 13 when 30 stages were used. Also the quantity of sodium and potassium not eluted from the resin in the elution section was much less in run 14. As already noted the sodium enrichment in the Na rich product samples increased during run 13 (Table 18), the enrichment of 10.7 for the last sample being greater than that in any of the samples in run 14. The sodium concentration increased and the potassium concentration decreased in the Na rich product during run 13. So the explanation for the poorer performance of the 30 stage contactor in run 13 seems to be that despite running for more than 36 hours before the steady state run was commenced, in fact steady state had not been reached. The very good mass balance in run 13 was thus to a certain extent fortuitous.

The volume balance for liquid and resin are within 1% and 5% respectively in this run (Table 21). The mass balance is good, the total calculated quantity of each of the alkali metal species (Table 22) being within 10%.

With the average composition of the rectification section liquid effluent known, a mass balance can be made over the elution and rectification sections in turn to calculate the

average composition of the extraction section resin product. A mass balance can now be made over the extraction section to provide a cumulative test of the accuracy of the measurements in the run, as the composition of all feed and product streams is known. The differences in the extraction section mass balances are within 5% i.e. smaller than the overall mass balance differences for Na and K. As deficits in the volume balance have been allowed for in the calculations, it can be said that the 10% differences in the overall mass balance are due in equal magnitude to errors in volume measurement and unrepresentative samples resulting from resin flowrate variation, coupled with analytical errors.

The equations of the operating lines for the rectification and extraction sections for Na and K can be solved to give the intersection points as $x_{Na} = 0.526$ and $x_K = 0.512$. Both values are satisfactorily close to the feed liquid composition.

The number of equivalent ideal stages in this run can be calculated by applying the separation performance and operating conditions to the equations given in section 2.2.3.

Equation (2.19) can be used to calculate the number of ideal stages for each of the cations in the elution section. As with the single section elution runs, n_K is greater than n_{Na} (Table 17). The calculated stage efficiency for

potassium elution is 110%. A stage efficiency of more than 100% is impossible but in view of the variation in the operating conditions during the run indicated by the changes in composition of the various liquid product streams, a 10% error in the stage efficiency is not unreasonable.

In the rectification section $x_o < x_n^*$ for both Na^+ and K^+ but E_{Na} and E_K were greater than unity so that elution of the cations from the resin was limited. The number of equivalent ideal stages for elution of each of the trace species was calculated out of interest. As the influent solution to this section contained alkali metal ions, equation (2.21) must be used to calculate n_{Na} and n_K. The rather low values of the corresponding stage efficiency of 55% and 57% respectively are to be expected with operation to give limited elution.

In the extraction section, E_{Na} and E_K were both greater than unity so that adsorption into the resin of both species was not limited. Equation (2.18) was used to calculate n_{Na} and n_K. The number of equivalent ideal stages was between 2 and 3 for sodium and 4 and 5 for potassium, with a corresponding stage efficiency of 42.2% and 71.6% respectively. With the value of E_{Na} approximately unity, errors in the measured values of the $\frac{L}{S}$ ratio and the Na enrichment make a large difference to the value of n_{Na} so this could be seriously in error.

The x - y diagram for Na^+/H^+ exchange in this run is shown in Figure 28. The rectification and extraction section operating lines intersect at (0.526, 0.787), well off the diagram. The flowrate of the feed relative to the liquid flowrates in the rectification and extraction sections is indicated by the difference in the slope of the operating lines for the two sections.

At the point in the equipment where the liquid feed is introduced between the rectification and extraction sections the composition of the resin remains unaltered, but the composition of the solution changes, with the concentration of sodium and potassium increased by the addition of the liquid feed. Thus y remains constant but x_{Na} and x_K increase. This is represented on the x - y diagram by a horizontal line from the point (A) on the rectification operating line corresponding to the composition of the liquid leaving the rectification section to the extraction section operating line (B). The sodium concentration in the extraction section liquid influent is represented by the x value at this point. It can be seen that the numbers of equivalent ideal stages for the elution and extraction sections match the calculated values (Table 17). There is a slight difference for the rectification section, but this may be explained by the fact that equation (2.21) is very sensitive to mass balance errors.

The 18% of the feed potassium not eluted from the

FIGURE 28. x - y DIAGRAM FOR Na^+/H^+ EXCHANGE IN THREE SECTION RUN 14

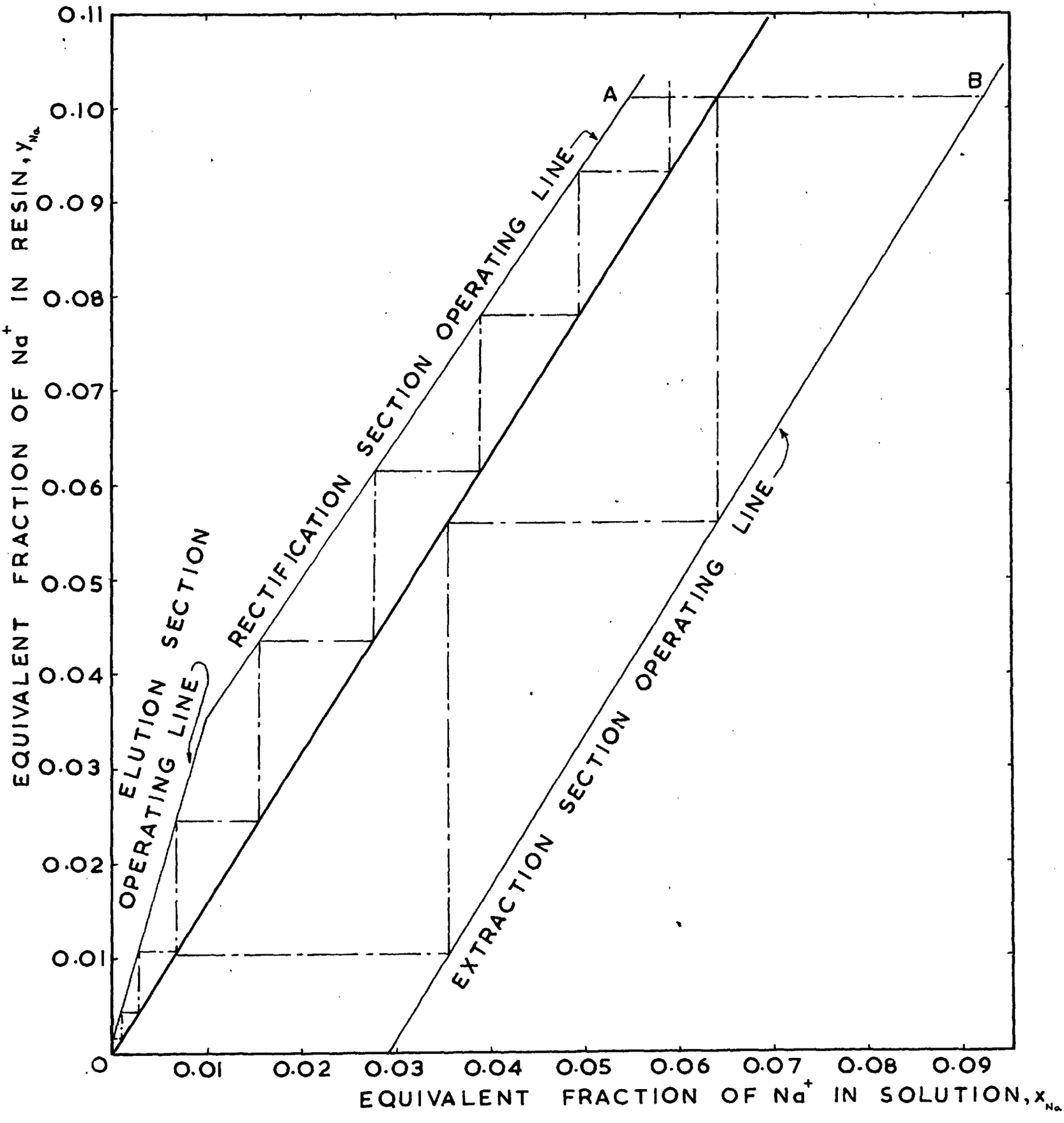

resin in this run was undesirably high. If this resin was recirculated to the extraction section, as it would be in a true countercurrent separation process, the potassium concentration in the resin in each section would increase until a different steady state was reached. In this new steady state the Na^+/K^+ separation performance of the contactor would be worse than it was in this run. It is thus obvious that the operating conditions used in run 14 cannot achieve a good separation of sodium and potassium.

Run 15

In this run the optimum operating conditions were used for the separation of sodium and potassium into two product streams and also for elution of sodium and potassium from the resin in the elution section, i.e. $E_{Na} < 1 < E_K$, or $\frac{L}{S} > 31.0$ in the extraction and rectification sections and E_{Na}, $E_K < 1$, or $\frac{L}{S} > 61.5$ in the elution section. The $\frac{L}{S}$ ratio in the various sections fulfilled these criteria (Table 17). The $\frac{L}{S}$ ratio in the elution section was appreciably greater than 61.5 in an attempt to get thorough elution of the resin.

The duration of the steady state run was long enough to ensure the complete replacement of the resin hold-up in the contactor. Because the resin flowrate was much less than in run 14, the run lasted $4\frac{1}{2}$ hours, or 273 cycles (Table 17).

TABLE 20 Liquid product concentrations during three section run 15

Description	Sample Number	Na^+ concentration (10^4N)	K^+ concentration (10^4N)	H^+ concentration (N)	Na^+ enrichment	K^+ enrichment
Na^+ rich Product	1	36.8	13.2	0.085	2.79	
	2	41.1	15.85	0.0842	2.6	
	3	37.2	14.53	0.085	2.56	
	4	35.3	13.2	0.085	2.68	
	5	36.3	12.52	0.085	2.9	
	6	33.2	10.55	0.086	3.15	
	7	35.0	10.55	0.085	3.32	
	8	34.1	10.3	0.086	3.31	
	9	34.4	11.9	0.085	2.89	
K^+ rich Product	Bulk	36.7	12.53	0.085	2.93	
	1	3.5	23.8	0.096		6.8
	2	2.37	21.1	0.097		8.9
	3	2.56	21.55	0.097		8.42
	4	2.85	23.1	0.097		8.1
	5	2.85	22.45	0.097		7.89
	6	3.98	25.0	0.096		6.29
	7	8.83	27.3	0.096		3.1
	8	6.63	24.0	0.096		3.62
	9	6.83	26.12	0.096		3.82
	Bulk	4.26	23.8	0.096		5.58
Rectification section effluent	1	30.0	63.5	0.090		2.11
	2	26.6	59.4	0.090		2.23
	3	28.6	61.4	0.090		2.15
	4	29.5	63.4	0.090		2.15
	5	30.0	61.4	0.090		2.05
	6	34.2	68.5	0.089		2.0
	7	34.4	66.8	0.089		1.94
	8	34.4	67.25	0.089		1.96
	9	33.4	66.0	0.089		1.98
	Average	31.23	64.2	0.090		2.06

The analyses of the various liquid streams (Table 20) show that the composition varied during the run, indicating that the resin flowrate increased and decreased several times during the run.

The variations of sodium enrichment in the Na rich product stream and of the K enrichment in the rectification section effluent stream are small, but the variation of potassium enrichment in the K rich product stream is considerable. As the quantity of alkali metal ions not eluted from the resin product (8.3% of the feed K and 0.5% of the feed sodium) was fairly small and the concentration of K in the K rich product stream was relatively high, elution was effective. The noted variation in the K enrichment was presumably due to a varying quantity of alkali metal ions in the resin entering the elution section. It can be concluded that variation in the resin flowrate affected the elution section far more than the other sections.

As mentioned above 8.3% of the potassium in the liquid feed was not eluted from the resin. Although this performance is considered to be very satisfactory for a 5 stage elution section, in a continuous ion exchange separation it is desirable that the quantity of K^+ in the eluted resin is less than 1% of the feed potassium. In any practical separation system, to allow for any variation in the resin flowrate and to ensure almost complete elution of the ions from the resin, the

TABLE 21 Volume balance for three section runs.

Run No.	Phase	IN		OUT	
		Description	Volume, (cm^3)	Description	Volume, (cm^3)
13	Liquid	Control $\frac{N}{10}$ HCl feed	555.0	Na^+ rich product	637.5
		Elution $\frac{N}{10}$ HCl feed	767.0	K^+ rich product	844
		Centre feed	42.0		
		Water feed to resin column	111.5		
		Total	1475.5	Total	1481.5
	Resin	Feed	17.4	Product	20.2
14	Liquid	Control $\frac{N}{10}$ HCl feed	819.0	Na^+ rich product	1199.5
		Elution $\frac{N}{10}$ HCl feed	1491.5	K^+ rich product	1334.0
		Centre feed	65.0	Samples taken	9.0
		Water feed to resin column	187.0		
		Total	2562.5	Total	2542.5
	Resin	Feed	36.0	Product	37.9
15	Liquid	Control $\frac{N}{10}$ HCl feed	1060	Na^+ rich product	1589.0
		Elution $\frac{N}{10}$ HCl feed	1780	K^+ rich product	1548.0
		Centre feed	85.5	Samples taken	9.0
		Water feed to resin column	214.0		
		Total	3139.5	Total	3146.0
	Resin	Feed	34.8	Product	37.1

elution section should have more stages than either the extraction or rectification sections. The actual number required will depend on the selectivity of the resin towards the two ions being separated, with respect to the gross ion.

The number of equivalent ideal stages for each cation in the elution section can be calculated from equation (2.19). As in the single section elution runs and run 14, $n_K > n_{Na}$ (Table 17). In fact the stage efficiency for Na and K is very similar to that for each species in run 14, although the quantity of alkali metal ions in the elution section in run 14 was much greater.

The influent solution to the rectification section contained alkali metal ions so that equation (2.21) must be used to calculate the number of equivalent ideal stages for this section. E_K was greater than unity, ensuring limited elution of K^+ ions from the resin. The number of equivalent ideal stages for Na^+ elution corresponded to a stage efficiency of 65% (Table 17). E_{Na} was less than unity in the extraction section, so that Na^+ adsorption into the resin was limited. Using equation (2.18) n_K was calculated to be about 3, with a corresponding stage efficiency of 60%.

The liquid volume balance for this run was very good, within 0.2% (Table 21). The disparity in the resin balance was 6.6% which is good considering the apparent resin

TABLE 22 Mass balance for three section runs

Run No.	IN						OUT					
	Description	Vol. (cm^3)	Na^+ Conc (meq/cm^3)	K^+ Conc (meq/cm^3)	Na^+ quantity (meq)	K^+ quantity (meq)	Description	Vol. (cm^3)	Na^+ Conc (meq/cm^3)	K^+ Conc (meq/cm^3)	Na^+ quantity (meq)	K^+ quantity (meq)
13	Centre feed	42	0.075	0.075	3.15	3.15	Na^+ rich liquid product	637.5	2.52×10^{-3}	3.205×10^{-4}	1.606	0.204
							K^+ rich liquid product	844	1.331×10^{-3}	2.542×10^{-3}	1.123	2.145
							Resin product	18.62	2.32×10^{-2}	4.16×10^{-2}	0.432	0.775
	Total				3.15	3.15	Total				3.161	3.124
14	Centre feed	64.98	0.075	0.075	4.873	4.873	Na^+ rich liquid product	1199.5	2.52×10^{-3}	2.648×10^{-4}	3.05	0.318
							K^+ rich liquid product	1334	9.87×10^{-4}	2.4×10^{-3}	1.318	3.208
							Resin product	36.95	2.42×10^{-3}	2.4×10^{-2}	0.0895	0.887
	Total				4.873	4.873	Total				4.4575	4.413
15	Centre feed	85.5	0.075	0.075	6.41	6.41	Na^+ rich liquid product	1589	3.67×10^{-3}	1.253×10^{-3}	5.83	1.99
							K^+ rich liquid product	1548	4.26×10^{-4}	2.38×10^{-3}	0.66	3.68
							Resin product	35.95	8.28×10^{-4}	1.48×10^{-2}	0.0297	0.531
	Total				6.41	6.41	Total				6.52	6.201

flowrate variation and the fact that it would take 260 minutes to replace the resin hold-up in the contactor at the average resin flowrate. The discrepancy in the overall mass balance of 4% for both sodium and potassium is small (Table 22).

As explained for run 14, from mass balances over the elution and rectification sections in turn the composition of the resin leaving the extraction section can be calculated. As volume balance errors are allowed for in this mass balance procedure, the source of errors in the overall process mass balance is indicated. The error in the extraction section Na balance is similar to that in the process mass balance so that the error in both cases is caused by unrepresentative product samples resulting from variation in the resin flowrate or analytical errors. The error in the extraction section potassium balance is half that in the overall mass balance so that the error in the latter is due in equal part to volume measurement errors and unrepresentative samples combined with K analysis errors.

The operating lines of the extraction and rectification sections intersect at $x_{Na} = 0.538$ and $x_K = 0.515$, reasonably close to the feed value of 0.5 for each cation.

The performance in this run can be compared with the calculated performance in the composite three section separation (Figure 26). The purity and recovery of sodium and

potassium in each of the two liquid product streams in this run were of the same order but rather lower than the calculated values of the composite process. The worse performance is to be expected. In the composite process each section had 15 actual stages. Assuming a stage efficiency of 60% for the glass stages, this was equivalent to 9 ideal stages per section. Assuming a stage efficiency of 90% for the perspex contactor stages, the number of equivalent ideal stages per section in run 15 was between 4 and 5. In addition, in the composite process the liquid feed contained only 26% K whereas the feed in run 15 contained equimolar quantities of sodium and potassium. The total concentration of alkali metal ions in the liquid entering the extraction section was 0.018 N compared with 0.025 N in the composite process, but the ratio in the liquid feed of Na:K of 1:1 instead of 3:1 was certainly a more difficult separation. The higher concentration of K in the eluted resin in run 15 was caused by the smaller number of equivalent ideal stages in the elution section and also by the greater proportion in the liquid feed of potassium, the most difficult component to elute from the resin.

The performance of this run was very satisfactory considering that only 5 stages were used in each section. With similar operating conditions and the use of more stages a very good separation of sodium and potassium in trace concentrations in the liquid feed into two liquid product streams could be

obtained with a 3 section contactor.

The calculated stage efficiency in the 3 section runs apart, from that for sodium enrichment in the extraction section in run 14, was between 60% and 110%. With the single section extraction runs 10 and 12 using the same contactor the stage efficiency was 100% and 80% respectively. Considering that these values applied to a wide range of operating conditions (e.g. $\frac{L}{S}$ ranged from 28.3 in run 14 extraction section to 80 in run 15 elution section) in a variety of ion exchange operations (resin elution and saturation, and enrichment of sodium in the liquid phase), the range is satisfactorily small. Further support has been provided for the conclusions reached after the single section trace runs with the glass stages that the equilibrium stage theory can be used to predict trace ion exchange separations in the new contactor and that as the number of stages is increased an additive improvement in the separation performance occurs.

..5.2.6. Mass transfer calculations

The liquid film mass transfer coefficient has only been calculated for runs with the glass contactor. Owing to the triangular shape of the contactor compartment in the perspex stages, the liquid velocity and voidage varied with the height in the resin bed.

The value of various physical properties of the resin and solution is required.

(i) Average diameter of resin particles.

In the H^+ form resin particle size determination (Figure 19), the peak in the histogram lies in the range 0.4952 to 0.5892 mm. The average H^+ resin particle diameter is taken to be 0.5422 mm.

From the relative density of the H^+, Na^+ and K^+ resin forms, the equivalent average size of resin particles in the other forms can be calculated.

Average diameter of Na^+ form resin particles

= 0.531 mm.

Average diameter of K^+ form resin particles

= 0.529 mm.

As the Na^+ and K^+ ions were only in trace concentrations, the average resin particle diameter in the trace runs was selected as 0.54 mm.

(ii) Voidage in the resin bed

In free settled state (section 3.2.1) mean voidage of H^+ form resin bed = 0.3628 x 1.015 = 0.3682

∴ Fraction of resin particles in free settled bed = 0.6318

A liquid flowrate of 65.5 cm^3/min. in glass contactor stages expanded the settled resin bed 100%.

∴ Voidage in expanded state = $\frac{2 - 0.6318}{2}$ = 0.684.

(iii) Viscosity of water = 0.0098 poise

(iv) Density of water = 1.0g/cm^3

(v) Diffusivity of Na^+ ions in liquid phase = 1.2×10^{-5} cm^2/sec (S5)

Diffusivity of H^+ ions in liquid = 8.35×10^{-5} cm^2/sec (S5)

The diffusivity of K^+ ions can be calculated using the Nernst-Einstein equation

$$D = \frac{RT}{\mathcal{F}} u' \qquad (5.5)$$

where u' is the mobility of the cation, and $\mathcal{F}$ is Faraday's constant.

$$u'_{Na} = 5.19 \times 10^{-4} \text{ cm/sec} \quad (G2)$$

$$u'_{K} = 7.61 \times 10^{-4} \text{ cm/sec} \quad (G2)$$

∴ $D_K = 1.2 \times 10^{-5} \times \frac{7.61}{5.19} = 1.76 \times 10^{-5}$ cm^2/sec by proportion.

Diffusivity of Na^+ ions in 8% DVB Zeo-Karb 225 = 1.21×10^{-6} cm^2/sec (S5)

Diffusivity of H^+ ions in 8% DVB Zeo-Karb 225 = 5.59×10^{-6} cm^2/sec (S5)

The values for self-diffusion in 10% DVB Dowex 50 (B6) are

$$\bar{D}_{Na} = 9.44 \times 10^{-7} \text{ cm}^2/\text{sec}$$

$$\bar{D}_{K} = 13.4 \times 10^{-7} \text{ cm}^2/\text{sec}$$

The values of $\bar{D}_{Na}$ in the two resins are very similar, and $\bar{D}_K$ in Zeo-Karb 225 will be calculated by proportion,

i.e $\bar{D}_K = \frac{13.4}{9.44} \times 1.21 \times 10^{-6} = 1.72 \times 10^{-6} \text{ cm}^2/\text{sec}$

The diffusivity values are not exact as they were not measured under experimental conditions. k_L is proportional to D_H (equation 2.32), so that any error in the value of D_H will affect k_L to the same extent. However any error in D_H is probably not greater than that introduced by the assumption of an average particle diameter, d, for the (-14 + 52) BSS resin. The diffusivity of the alkali metal ions is only used in the criterion for the rate determining step (equation 2.33) and any small error in the diffusivity values is unlikely to affect this.

Mass transfer coefficients

Run 1

Liquid flowrate = 65.5 cm^3/min. (The instantaneous value is used)

Radius of contactor compartment = 1 cm

$\therefore$ $u = \frac{65.5}{\pi} = 20.85$ cm/min.

$Re = \frac{\rho u_p d_m}{\mu}$

where d_m = mean hydraulic particle diameter, and

u_p = interstitial liquid velocity = $\frac{u}{e}$

$$d_m = \frac{ed}{6(1-e)}$$

$$\therefore \text{Re} = \frac{\rho ud}{6\mu(1-e)} = \frac{1 \times 20.85 \times 0.054}{6 \times 0.0098(1-0.6841)\times 60} = 1.01$$

$$Sc_H = \frac{\mu}{\rho D_H} = \frac{0.0098}{1 \times 8.35 \times 10^{-5}} = 117.6$$

From equation (2.32)

$$k_L = \frac{0.22\ D_H}{de} (\text{Re})^{\frac{1}{2}} (Sc_H)^{\frac{1}{3}}$$

$$= \frac{0.22 \times 8.35 \times 10^{-5} \times 1 \times 4.899}{0.054 \times 0.6841} = 2.42 \times 10^{-3} \text{ cm/sec.}$$

The nature of the rate determining step in the Na^+/H^+ and K^+/H^+ ion exchange can be found from equation (2.33).

The interdiffusion coefficients in the liquid film and resin must be calculated using equation (2.34).

The liquid feed end of the contactor in run 1 is considered.

In run 1, the resin product composition was $y_{Na} = 0.1171$,

$y_K = 0.125$, $y_H = 0.758$.

$$\therefore \bar{D}_{NaH} = 1.35 \times 10^{-6} \text{ cm}^2/\text{sec.}$$

$$\bar{D}_{KH} = 1.9 \times 10^{-6} \text{ cm}^2/\text{sec.}$$

For convenience the liquid film is assumed to have the same composition as the bulk liquid feed, i.e. $x_{Na} = 0.125$, $x_K = 0.125$, $x_H = 0.75$.

$\therefore D_{NaH^-} = 1.367 \times 10^{-5}$ cm^2/sec.

$D_{KH} = 1.97 \times 10^{-5}$ cm^2/sec.

For Na^+/H^+ exchange, $Sh_{NaH} = \frac{k_L d}{D_{NaH}} = \frac{2.456 \times 10^{-3} \times 0.054}{1.367 \times 10^{-5}} = 9.7$

$\therefore \frac{\bar{c}\,\bar{D}_{NaH}\,2}{c\,D_{NaH}Sh_{NaH}}(5+2K_{NaH}) = \frac{2 \times 1.82 \times 1.35 \times 10^{-6}}{0.1 \times 1.367 \times 10^{-6} \times 9.7}(5+2\overline{\times 1.7}) = 3.11$

i.e. film diffusion control.

For K^+/H^+ exchange.

$$Sh_{KH} = \frac{2.456 \times 10^{-3} \times 0.054}{1.97 \times 10^{-5}} = 6.71$$

$\therefore$

$$\frac{\bar{c}\,\bar{D}_{KH}\,2}{c\,D_{KH} \cdot Sh_{KH}}(5 + 2K_{KH}) = \frac{1.82 \times 1.9 \times 10^{-6}}{0.1 \times 1.97 \times 10^{-5} \times 6.71}(5 + \overline{2 \times 3.38}) = 6.16$$

i.e. film diffusion control.

Discussion

Snowdon[S5] found that, for Na^+/H^+ exchange with 8% D.V.B. Zeo-Karb 225, k_L varied from 5×10^{-3} cm/sec to 14×10^{-3} cm/sec as Re increased from 5.7 to 10.3. The value of k_L generally increased as Re increased and the H^+ saturation of the resin decreased. The mass transfer coefficient for our contactor is lower than Snowdon's values, but as Re is much lower, this is in line with Snowdon's conclusions.

Mass transfer model.

The value of various parameters required to apply equations (2.35), (2.36) and (2.37) to run 1 is as follows:

S = resin flowrate = 1.48 cm^3/min.

L = liquid flowrate = 27.25 cm^3/min.

Volume of settled resin in a stage = 6.27 cm^3 (Table 9)

Voidage of settled resin bed = 0.3682

∴ Absolute volume of resin in stage = 6.27 x 0.6318 = 3.88 cm^3

Specific surface of resin, s, = $\frac{6}{d} = \frac{6}{0.054}$ = 111.1 cm^{-1}

∴ Interfacial area in a stage, s', = 3.88 x 111.1 = 431.1 cm^2

k_L = 2.42 x 10^{-3} cm/sec.

x_{Na_6} = 0.00924

x_{K_6} = 0.00172

x_{Na_o} = 0.125

x_{K_o} = 0.125

From a mass balance

y_{Na_1} = 0.117

y_{K_1} = 0.125

From the equilibrium relationship,

$x_{Na_1}^{**}$ = 0.074

$x_{K_1}^{**}$ = 0.0458

Using equation (2.37) for stage 1

$$2.725\ (0.125 - x_1) = 6.264\ (x_1 - 0.074)$$

$$\therefore \quad x_1 = 0.0896$$

$\therefore$ From equation (2.36),

$$\Delta_1 = 0.0965 \text{ meq/min}$$

and from equation (2.35),

$$y_1 = 0.0606.$$

This procedure can be carried out for each stage until stage 5 to give the values of y_6 and x_5. x_6 can be calculated by a mass balance over stage 6. The concentrations of Na and K in the liquid product from run 1 have been estimated by this method. Values of the parameters are shown below.

Stage number	Na^+				K^+			
	x_i	x_i^*	Δ_i (meq/min)	y_i	x_i	x_i^*	Δ_i (meq/min)	y_i
1	0.0896	0.074	0.0965	0.117	0.07	0.0458	0.151	0.125
2	0.0631	0.0513	0.0723	0.0606	0.039	0.0253	0.0845	0.069
3	0.0431	0.0344	0.0545	0.0548	0.0214	0.0138	0.0478	0.0377
4	0.0282	0.0217	0.0406	0.0346	0.0116	0.00733	0.0267	0.02
5	0.0171	0.0122	0.0302	0.0195	0.00612	0.00372	0.015	0.01
6	0.00892			0.00826	0.0016			0.00457

The calculated values for x_{Na_6} and x_{K_6} can be compared with the measured values in the liquid product of 0.00924 and 0.00172 respectively, after allowing for dilution by water introduced with the resin feed.

The agreement appears to confirm that there is perfect mixing of both phases in forward flow in the glass contactor stages.

If this is the situation, it explains why the stage efficiency calculated from equations ((2.18),(2.19),(2.20) and 2.21)), which assume true countercurrent operation was in the range 36% to 70% for the glass stages.

5.3 Gross ionic fraction results and discussion

Results are shown in Tables 23, 24, 25, 26, 27 and 28. Extraction factors have not been included in Table 23 because they vary with resin composition.

5.3.1 10 stage runs.

In run 16, $\frac{\bar{Sc}}{Lc}$ is unity and the selectivity coefficient would have to decrease to a value less than 1 for the extraction factor for Na and K to be less than unity. It is probable that operating conditions were such that both cations were extracted into the resin and a low recovery of both cations in the liquid product would be expected. A sodium enrichment of 95 was obtained in the bulk liquid product from this run (Table 23). Although this is very satisfactory for a 10 stage run, the recovery of sodium was only about 2%.

Cycle times were different in runs 18 and 20.

The resin flowrate varied greatly during run 20 and $\frac{L}{S}$ values during the run were calculated for the intervening period from the time when the previous liquid sample was taken (Table 24). It can be seen from the liquid product analyses that the sodium enrichment increased as the resin flowrate increased and vice versa. The resin flowrate increased over the second half of the run. As the increased resin flowrate had not time over this period to reach the resin outlet, the volume of resin product

TABLE 23: Operating conditions and results of gross continuous countercurrent ion exchange extraction runs using the perspex contactor.

Run number	16	17	18	19	20	21	22	23	24	25	26	27	28	29
Number of stages	10	10	10	10	10	10	40	100	100	100	100	100	100	100
Forward flow period t_f(s)	39	39	46	39	46	39	39	37	46	37	37	37	37	45
No flow period t_s(s)	1	1	0	1	0	1	1	1	0	1	1	1	1	0
Reverse flow period t_r(s)	20	20	23	20	23	20	20	22	24	22	22	22	22	23
Liquid flowrate $U_f = U_r$ (cm^3/min)	15.8	15.9	16.44	15.7	17.05	15.4	17.1	17.04	17.6	15.76	16.64	15.1	16.84	16.82
Average liquid flowrate L (cm^3/cycle)	5.0	5.04	6.3	4.96	6.53	4.87	5.41	4.26	6.45	3.94	4.16	3.78	4.21	6.17
Average resin flowrate S (cm^3/cycle)	0.29	0.185	0.175	0.116	0.157	0.098	0.143	0.0895	0.184	0.0945	0.0959	0.0878		0.146
*Ratio L/S	18.24	28.7	35.2	43.1	44.5	53.4	41.5	45.15	39.9	40.5	43.6	43.1		43.2
*Resin hold-up (cm^3/stage)					2.25			1.7						
Number of cycles	150	150	150	156	180	154	131	150	252	156	144	212		128
Total liquid feed (cm^3)	750	755	945	775	1175	750	710	640	1625	615	600	800		790
Total resin feed (cm^3)	43.5	27.8	26.2	18.15	28.2	15.1	18.7	13.4	46.3	14.75	13.8	18.6		18.7
Liquid feed concentration c_{Na} (N)	0.05	0.05	0.05	0.05	0.05	0.05	0.04	0.05	0.05	0.05	0.05	0.05		0.05
Liquid feed concentration c_K (N)	0.05	0.05	0.05	0.05	0.05	0.05	0.05	0.05	0.05	0.05	0.05	0.05		0.05
Liquid feed concentration c_H (N)	0	0	0	0	0	0	0	0	0	0	0	0		0
Resin feed concentration $\bar{c}_{Na}$(meq/cm^3)	0	0	0	0	0	0	0	0	0	0	0	0		0
Resin feed concentration $\bar{c}_K$ (meq/cm^3)	0	0	0	0	0	0	0	0	0	0	0	0		0

/Cont'd.....

Table 23 ..... Continued

Run number	16	17	18	19	20	21	22	23	24	25	26	27	28	29
Resin feed concentration $\bar{c}_H$ (meq/cm^3)	1.82	1.82	1.82	1.82	1.82	1.82	1.82	1.82	1.82	1.82	1.82	1.82	1.82	1.82
Liquid product concentration c_{Na} (10^4N)	9.7	165	213.5	260	294	298	329.5	392	410	448.5	410	268		405
Liquid product concentration c_K (10^4N)	0.102	60.3	121	168.5	192.6	210	89.7	0.215	8.62	2.05	18.7	163		32.45
Liquid product concentration c_H (N)	0.082	0.0614	0.0505	0.0419	0.0353	0.0372	0.0429	0.0451	0.0453	0.0394	0.0434	0.0416		0.0428
Enrichment of Na in liquid product (f_1)	95.0	2.74	1.761	1.54	1.53	1.42	4.6	1820	47.5	218.5	21.9	1.645		12.5
Recovery of Na in liquid product (%)	1.94	33.0	42.7	52.0	58.8	59.6	65.9	78.4	82.0	89.7	82.0	53.6		81.0

* Based on the average of the feed and product resin volumes.

TABLE 24: Liquid product concentrations during 10 stage gross ionic fraction runs

(Samples taken every 30 minutes. Bulk product mixed and analysed for each run).

Sample number	RUN 16				RUN 17				RUN 18			
	Na^+ conc (10^4N)	K^+ conc (10^4N)	H^+ conc (N)	Na enrich-ment	Na^+ conc (10^4N)	K^+ conc (10^4N)	H^+ conc (N)	Na enrich-ment	Na^+ conc (10^4N)	K^+ conc (10^4N)	H^+ conc (N)	Na enrich-ment
N.S.S. (-30) (mins)									203.0	107.7	0.0529	1.89
1	10.65	0.1105	0.082	96.5	178.5	66.4	0.0594	2.69	220.5	134.8	0.0485	1.64
2	8.52	0.0829	0.082	103.0	169.0	66.4	0.0604	2.55	212.0	134.8	0.0493	1.572
3	7.85	0.0665	0.082	118.0	169.0	65.2	0.0605	2.595	169.0	101.0	0.057	1.672
4	8.56	0.0746	0.082	114.8	162.0	58.7	0.0618	2.76	150.0	80.6	0.061	1.86
5	10.58	0.0885	0.082	119.5	158.0	53.8	0.0627	2.94	203.0	107.7	0.053	1.89
6									306.0	183.3	0.0346	1.625
Bulk	9.7	0.1022	0.082	95.0	165.0	60.3	0.0614	2.74	213.5	121	0.0505	1.763

/Cont'd.....

TABLE 24: Continued

Sample Number	RUN 19				RUN 20					RUN 21			
	Na^+ conc (10^4N)	K^+ conc (10^4N)	H^+ conc (N)	Na enrich-ment	Na^+ conc (10^4N)	K^+ conc (10^4N)	H^+ conc (N)	Na enrich-ment	L/S ratio over sample period	Na^+ conc (10^4N)	K^+ conc (10^4N)	H^+ conc (N)	Na enrich-ment
1	258.5	157.0	0.0432	1.647	304.0	206.0	0.033	1.475	59.5	288.5	200.0	0.0392	1.44
2	256.0	160.7	0.0431	1.594	344.0	252.6	0.0243	1.36	81.0	298.0	213.0	0.0381	1.40
3	266.7	170.4	0.041	1.565	310.0	214.0	0.0316	1.45	53.0	298.0	215.5	0.0367	1.39
4	272.0	184.0	0.0392	1.48	270.0	174.0	0.0396	1.55	32.9	293.0	207.0	0.0380	1.42
5	234.0	153.0	0.0461	1.53	204.8	118.1	0.0517	1.73	29.9	303.0	215.5	0.0362	1.41
6					221.5	114.8	0.0504	1.93	32.3				
Bulk	260.0	168.5	0.0419	1.54	294.0	192.6	0.0353	1.53	41.75	298.0	210.0	0.0372	1.42

** Based on volume of feed resin

N.S.S. means sample taken before start of steady state run

was markedly less than that of the feed volume.

Despite the fluctuations in the resin flowrate and the use of a different time cycle, with higher average and instantaneous liquid flowrates, the sodium enrichment in the liquid product of 1.53 was very close to the value of 1.54 for run 19 where the flowrate ratio $\frac{L}{S}$ was slightly lower (Table 23).

All 10 stage runs show the trend of decreasing sodium enrichment and increasing sodium recovery as the $\frac{L}{S}$ ratio increased. Although poor mass balances were generally obtained in these runs (i.e. the sum of $(y_{Na_1} + y_{K_1})$ is greater than unity) the consistent change in the Na enrichment and recovery shows that the sodium-potassium separation achieved was reproducible.

A good liquid volume balance (Table 25) was achieved in all 10 stage runs. Difficulty was experienced in keeping the low resin flowrate constant. The resin feed and product volumes were never equal, but only in run 20 where the resin flowrate fluctuated markedly was the difference greater than 10%.

5.3.2. Run 22

During run 22, a 40 stage run, the composition of the liquid product changed continuously (Table 26), to give a decreasing sodium enrichment in the liquid product. The resin flowrate remained constant during the steady state run and the

TABLE 25: Volume balance for 10 stage gross ionic fraction runs

Run No.	Phase	IN		OUT	
		Description	Volume (cm^3)	Description	Volume (cm^3)
16	Liquid	Feed	750		
		Water feed to resin column	155		
		Total	905	Product	925
	Resin	Feed	43.5	Product	40.0
17	Liquid	Feed	755		
		Water feed to resin column	145		
		Total	900	Product	931
	Resin	Feed	27.8	Product	26.1
18	Liquid	Feed	945		
		Water feed to resin column	181		
		Total	1126	Product	1087
	Resin	Feed	26.2	Product	26.5
19	Liquid	Feed	775		
		Water feed to resin column	140		
		Total	915	Product	904
	Resin	Feed	18.15	Product	17.5
20	Liquid	Feed	1175		
		Water feed to resin column	225		
		Total	1400	Product	1375
	Resin	Feed	28.2	Product	24.3
21	Liquid	Feed	750		
		Water feed to resin column	102		
		Total	852	Product	880
	Resin	Feed	15.1	Product	13.6

TABLE 26: Liquid product concentrations during 40 and 100 stage gross ionic fraction runs

Samples taken every 30 minutes. Bulk product mixed and analysed for each run

Sample Number	RUN 22				RUN 23				RUN 24			
	Na^+ conc (10^4N)	K^+ conc (10^4N)	H^+ conc (N)	Na^+ enrich-ment	Na^+ conc (10^4N)	K^+ conc (10^4N)	H^+ conc (N)	Na^+ enrich-ment	Na^+ conc (10^4N)	K^+ conc (10^4N)	H^+ conc (N)	Na^+ enrich-ment
NSS 1 (-210 mins)									247.0	0.350	0.0624	705
NSS 2 (-150 mins)									340.0	0.735	0.0531	462
NSS 3 (-30 mins)									451.0	3.5	0.0416	129
1	378.0	76.0	0.0404	6.21	252.0	0.148	0.0591	1700	451.0	4.85	0.0415	93.0
2	370.0	98.3	0.0380	4.7	306.0	0.170	0.0537	1800	380.0	5.75	0.0485	66.1
3	307.0	100.3	0.0441	4.63	291.5	0.256	0.0551	1137	321.0	5.61	0.0544	57.2
4	258.6	93.4	0.0496	3.46	410.0	0.363	0.0433	1130	306.0	5.94	0.0559	51.6
5	258.6	105.0	0.0484	3.08	420.0	0.458	0.0423	918	346.0	8.45	0.0517	41.0
6									321.0	9.41	0.054	34.1
7									360.0	11.59	0.050	31.1
8									372.5	15.12	0.0484	24.6
9									370.0	17.8	0.0483	20.8
Bulk	329.5	89.7	0.0429	4.6	392.0	0.215	0.0451	1820	410.0	8.62	0.0453	47.5

/Cont'd.....

TABLE 26: Continued

Sample Number	Run 25				Run 26				Run 27				Run 29			
	Na^+ conc (10^4N)	K^+ conc (10^4N)	H^+ conc (N)	Na enrich-ment	Na^+ conc (10^4N)	K^+ conc (10^4N)	H^+ conc (N)	Na enrich-ment	Na^+ conc (10^4N)	K^+ conc (10^4N)	H^+ conc (N)	Na^+ enrich-ment	Na^+ conc (10^4N)	K^+ conc (10^4N)	H^+ conc (N)	Na^+ enrich-ment
S 1 (360 mins)													116.1	1.183	0.0748	98.2
S 2 (240 mins)													116.1	1.293	0.0748	90.0
S 3 (150 mins)													212.6	2.725	0.065	78.0
S 4 (90 mins)													301.5	8.61	0.0545	35.0
S 5 (30 mins)													445.0	21.55	0.0399	20.65
1	426.0	1.12	0.0418	380	388.0	12.9	0.0488	30.0	264.0	137.0	0.0446	1.93	445.0	28.1	0.0392	15.85
2	473.0	1.845	0.037	256	394.0	15.35	0.0484	25.65	256.5	141.0	0.0449	1.82	380.0	32.06	0.0453	11.86
3	486.0	2.66	0.0356	183	419.0	20.45	0.0464	20.5	264.0	155.0	0.0428	1.7	351.5	31.65	0.0482	11.1
4	462.0	3.615	0.0379	128	435.0	29.0	0.0399	15.0	284.0	181.5	0.0381	1.57	380.0	33.9	0.0451	11.2
5	398.0	3.90	0.0443	102	431.5	34.2	0.0397	12.6	283.0	188.2	0.0376	1.5	351.5	39.6	0.0474	8.88
6									265.5	188.2	0.0393	1.41				
7									242.0	160.0	0.0445	1.51				
Total	448.5	2.053	0.0394	218.5	410.0	18.7	0.0434	21.9	268.0	163.0	0.0416	1.65	405.0	32.45	0.0428	12.49

NSS means sample taken before start of steady state run

change in liquid product composition indicates that steady state had not in fact been attained although the run had been conducted for 12 hours and the H^+ concentration remained at between 0.0421N and 0.0408N for one hour before the steady state run was commenced.

The volume balance for liquid was good; the resin product was 2.7 cm^3 less than the feed volume but as the hold-up was about 80 cm^3 resin, this discrepancy was caused by variation in the resin flowrate many hours before the start of the steady state run (Table 28).

5.3.3. Run 23

The 100 stage contactor was operated for about 40 hours and the H^+ concentration had been constant at 0.06N for one hour before the steady state run was commenced. However, during the run the liquid product composition changed and the liquid product sodium enrichment decreased (Table 26). Although the maximum potassium concentration was only 1.79 ppm, it is believed that steady state was not attained in the 43 hours that the equipment was operated.

The good agreement between feed and product resin volumes shows that steady operating conditions were maintained over a long period, as the total resin hold-up in the contactor was about 200 cm^3 (Table 28).

5.3.4. Run 24

The liquid product was sampled and analysed over an 8 hour period after the contactor had been operating continuously for about 40 hours to establish that the continuous change in the liquid product was an approach to steady state (Table 26). The run was terminated when no feed liquid was left. The sodium enrichment in the liquid product decreased from 705 to 20.8, mainly because the K concentration increased continuously from 1.37 ppm to 0.00178N. It must be concluded that in runs 22, 23 and 24 a steady state had not been attained and the steady state sodium enrichment in the liquid product was much lower than 20.

The large disparity in run 24 in the resin feed and product volumes (Table 28) over the steady state run was due to decrease in the resin flowrate during a period 12 hours before the steady state run was commenced.

5.3.5. Runs 25, 26, 27 and 28.

These runs were the nearest that could be practically achieved to a continuous run to steady state conditions. In view of the long operating time involved and limitations imposed by the 15 litre capacity of the liquid feed tank, the run was broken into operating periods of 40 hours for run 25, 15 hours for runs 26 and 27 and 40 hours for run 28. The liquid product samples from runs 25, 26 and 27 (Table 26) show a decreasing

sodium enrichment. In run 28, when steady state had undoubtedly been attained, the sodium enrichment (Table 27) was more or less constant although it varied slightly due to resin flowrate variation. It tended to increase in the period following a resin flowrate increase and vice versa. It is concluded that the steady state enrichment for a 100 stage run with an $\frac{L}{S}$ ratio of about 45 is 1.4 to 1.5. This is very similar to the enrichment obtained with 10 stages.

The concentrations of Na and K in the liquid product are also similar to those obtained with the 10 stage runs at the same $\frac{L}{S}$ ratio.

5.3.6. Run 29

The contactor was initially filled with resin partially saturated with sodium and potassium ($y_{Na} = 0.2$, $y_K = 0.27$) but operated in the same way as other 100 stage runs with a H^+ resin feed. The aim was to show that runs 25, 26, 27 and 28 were in fact equivalent to a continuous run to steady state conditions and not 4 separate runs in which the decreasing Na enrichment in the liquid product was adventitious. From Table 26 it can be seen that after 40 hours running the product sodium enrichment decreased continuously over a period of $8\frac{1}{2}$ hours from 98 to 9. Thus although the resin initially contained Na and K, the liquid product shows the same concentration history as the 100 stage runs (23 and 24) where the resin was initially

TABLE 27: Liquid product concentrations during run 28

Run commenced at 22.30 hrs. - 4th October 1966

Time Sample taken		Na^+ conc (10^{-4}N)	K^+ conc (10^{-4}N)	H^+ conc (N)	Na^+ enrich-ment	$\frac{L}{S}$ * ratio
Date	Time					
5.10.1966	14.00	130.5	85.0	0.0631	1.54	31.8
	15.00	222.5	155.0	0.0469	1.44	46.3
	16.00	265.0	202.0	0.0380	1.31	45.2
	17.00	222.5	168.0	0.0456	1.33	45.5
	18.00	174.0	117.0	0.0556	1.49	}
	21.40	161.0	107.8	0.0578	1.50	}46.25
	23.00	74.0	45.8	0.0727	1.615	}
6.10.1966	00.50	267.0	188.0	0.0395	1.42	}
	04.40	247.0	190.0	0.041	1.30	}52.5
	09.20	336.0	295.0	0.0216	1.14	}
	10.20	272.0	189.0	0.0386	1.44	34.8
	11.15	234.0	177.0	0.0436	1.32	46.6
	12.20	215.0	150.0	0.0482	1.43	41.0
	13.35	235.0	156.0	0.0456	1.50	37.4
	14.20	247.0	175.0	0.0425	1.41	46.2
	15.20	195.0	144.5	0.0507	1.35	34.8
	16.20	252.0	171.5	0.0423	1.47	38.0
	17.20	218.0	144.5	0.0484	1.51	38.3
	19.40	275.0	202.0	0.0370	1.36	
	20.40	286.5	215.0	0.0345	1.33	

* This is an average value which applies to the intervening period since the last sample was taken, based on the volume of feed resin.

TABLE 28: Volume balance for 40 and 100 stage gross ionic fraction runs

Run no.	Phase	IN		OUT	
		Description	Volume (cm^3)	Description	Volume (cm^3)
22	Liquid	Feed	710		
		Water feed to resin column	127		
		Total	837	Product	852
	Resin	Feed	18.7	Product	16.0
23	Liquid	Feed	640		
		Water feed to resin column	120		
		Total	760	Product	746
	Resin	Feed	13.4	Product	14.75
24	Liquid	Feed	1625		
		Water feed to resin column	240		
		Total	1865	Product	1852
	Resin	Feed	46.3	Product	36.0
25	Liquid	Feed	615		
		Water feed to resin column	113		
		Total	728	Product	703
	Resin	Feed	14.75	Product	15.0
26	Liquid	Feed	600		
		Water feed to resin column	95		
		Total	695	Product	707
	Resin	Feed	13.8	Product	14.0
27	Liquid	Feed	800		
		Water feed to resin column	145		
		Total	945	Product	928
	Resin	Feed	18.6	Product	18.5
29	Liquid	Feed	790		
		Water feed to resin column	123		
		Total	913	Product	875
	Resin	Feed	18.7	Product	17.0

in the H^+ form. As runs 25, 26, 27 and 28 showed a different history it is concluded that they were equivalent to a continuous run.

5.3.7. Discussion

A notable feature of the 10 stage runs was the decrease of sodium enrichment as the $\frac{L}{S}$ ratio increased.

Steady state was not attained in the 40 stage run. The enrichment was 3.08 at the end of the run and the steady state value apparently would be much lower than this. The 100 stage runs appeared to have a steady state liquid product composition similar to that obtained with 10 stages operating with the same flowrate ratio. It is reasonable to suppose that 40 stages would give the same product composition with steady state operation.

A possible explanation of these results is that a pinch point was obtained in the runs using more than 10 stages so that the same liquid product composition was obtained as with 10 stages.

The equilibrium data show that a complex situation exists (Figures 14, 15, 16 and 17). The binary Na^+/H^+ and K^+/H^+ equilibrium curves are markedly curved due to the decrease in selectivity for the alkali metal ions as the equivalent fraction of the alkali metal species in the resin increases. Also the equilibrium lines for both the Na^+/H^+ and K^+/H^+ systems are

different when the other alkali metal ion species is also competing for the exchange sites. In both cases the resin shows less selectivity for the alkali metal ions with respect to H^+ ions in the ternary system than it does in the binary systems.

If the capacity of the resin phase is not sufficient to remove all the solute most easily extracted, i.e. the potassium, then the extraction of K into the resin is limited, and a pinch point will occur on the K^+/H^+ equilibrium line at the potassium concentration in the liquid feed. From the relative cation concentrations in the resin and liquid phases, expressed as meq/cm^3, it can be calculated that when $\frac{L}{S} > 36.5$, the resin cannot adsorb all the potassium in the liquid feed and a pinch point can be expected.

The results can best be discussed by reference to x - y diagrams, the binary K^+/H^+ and Na^+/H^+ equilibrium lines and Na and K operating lines for each of the 10 stage runs are shown in Figures 29 to 34 inclusive. Only the binary equilibrium lines have been shown to simplify the diagrams. Although both Na^+ and K^+ ions are adsorbed by the resin in preference to H^+ ions, the extraction factor for potassium is higher and the pinch point will occur on a K^+/H^+ equilibrium line to give maximum extraction of K^+ into the resin. It can be seen from Figures 30 to 34 that in runs 17 to 21 the K^+ operating lines cut the binary K^+/H^+ equilibrium line at approximately $x_K = 0.5$, i.e. the K^+

FIGURE 29. x - y DIAGRAM FOR GROSS IONIC FRACTION RUN 16

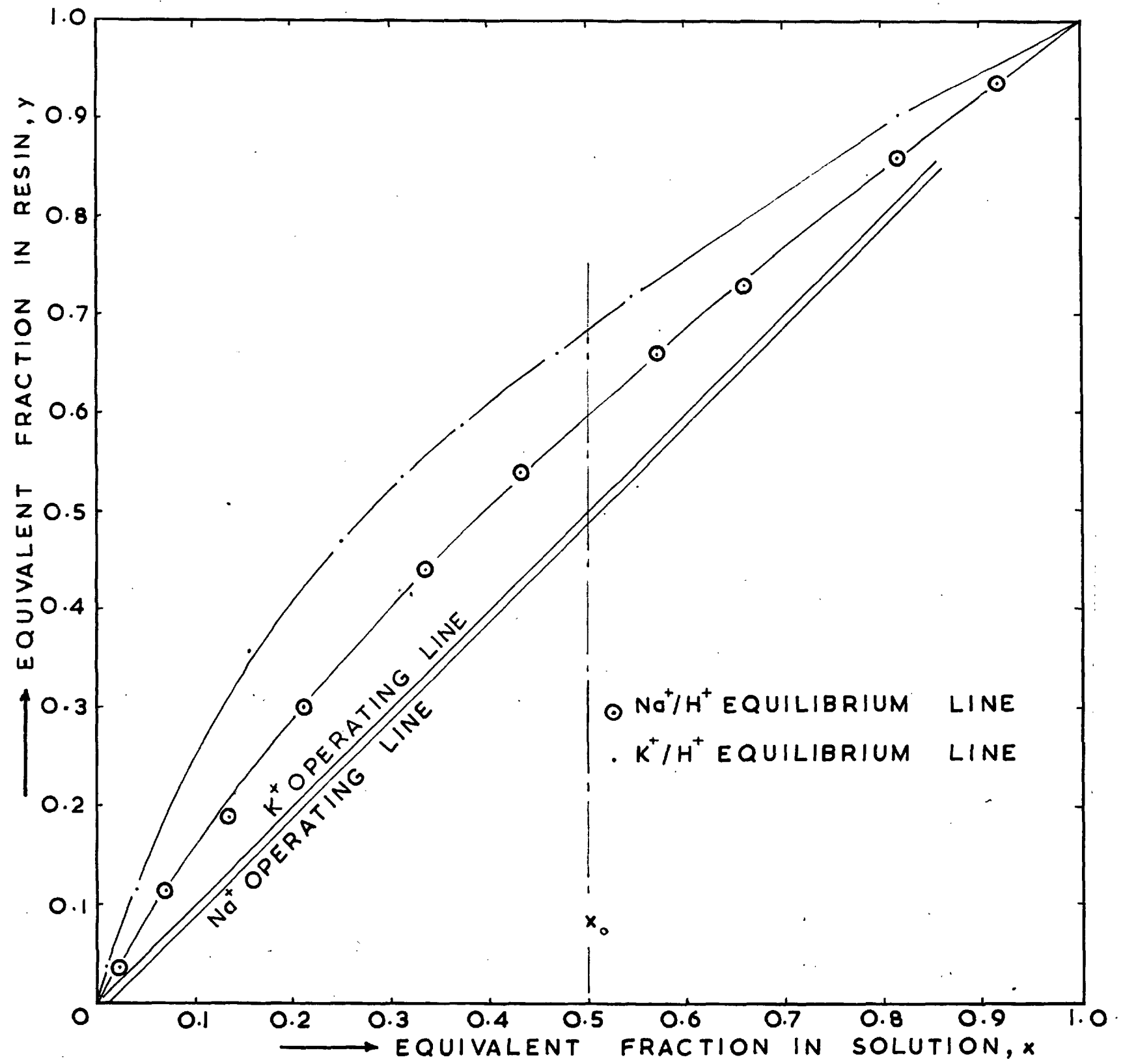

FIGURE 30. x - y DIAGRAM FOR GROSS IONIC FRACTION RUN 17

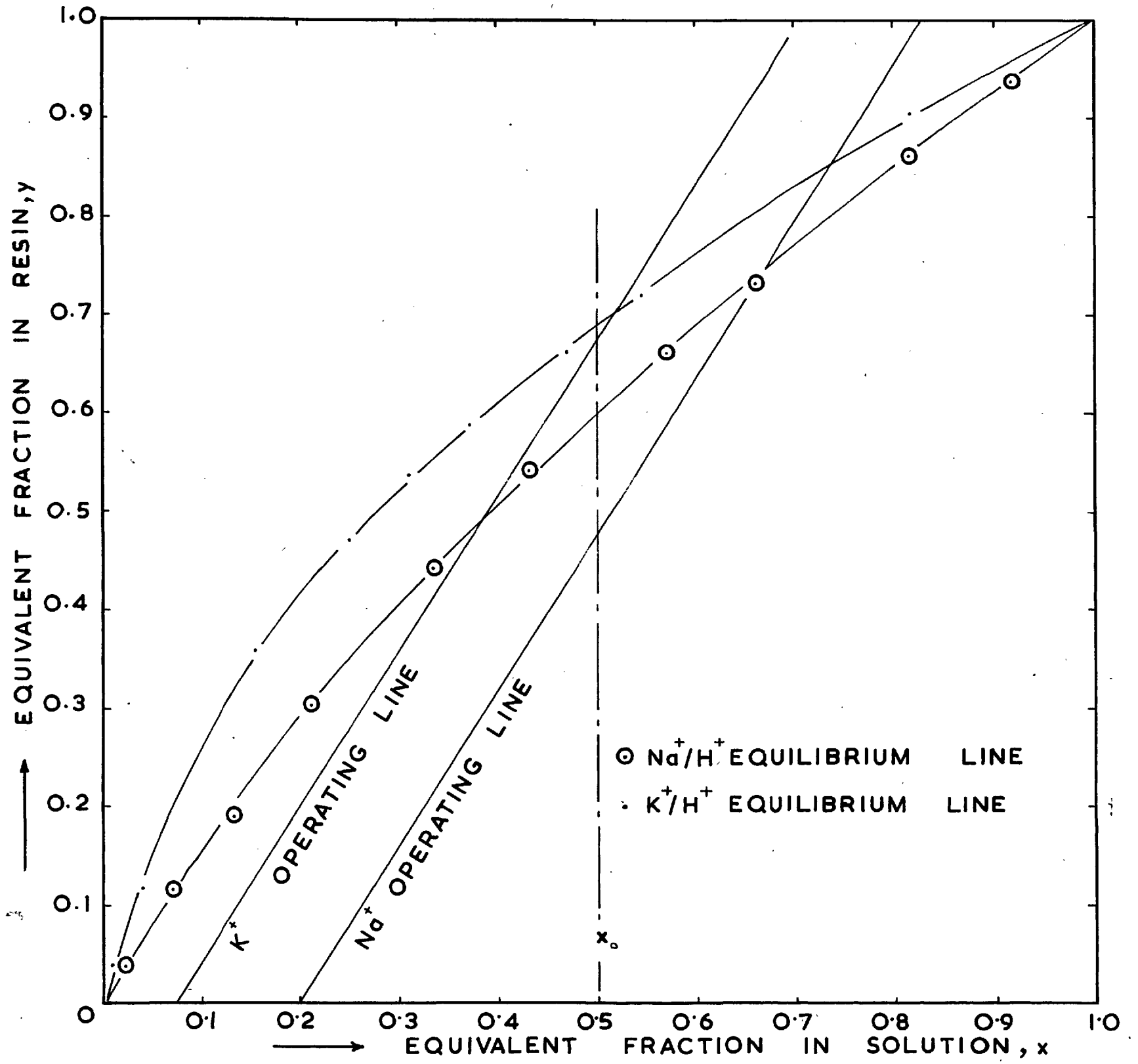

FIGURE 31. x - y DIAGRAM FOR GROSS IONIC FRACTION RUN 18.

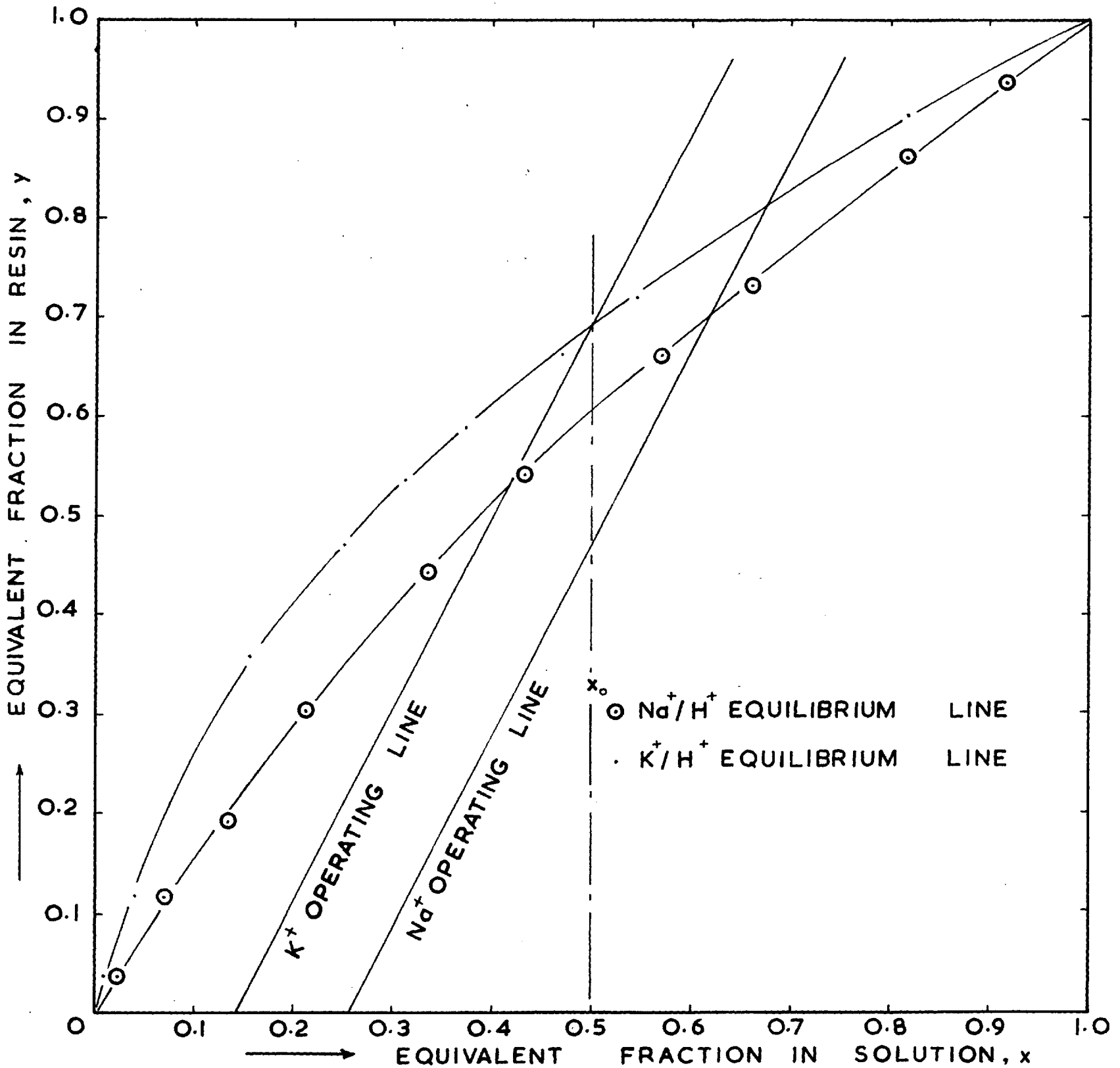

FIGURE 32. x - y DIAGRAM FOR GROSS IONIC FRACTION RUN 19

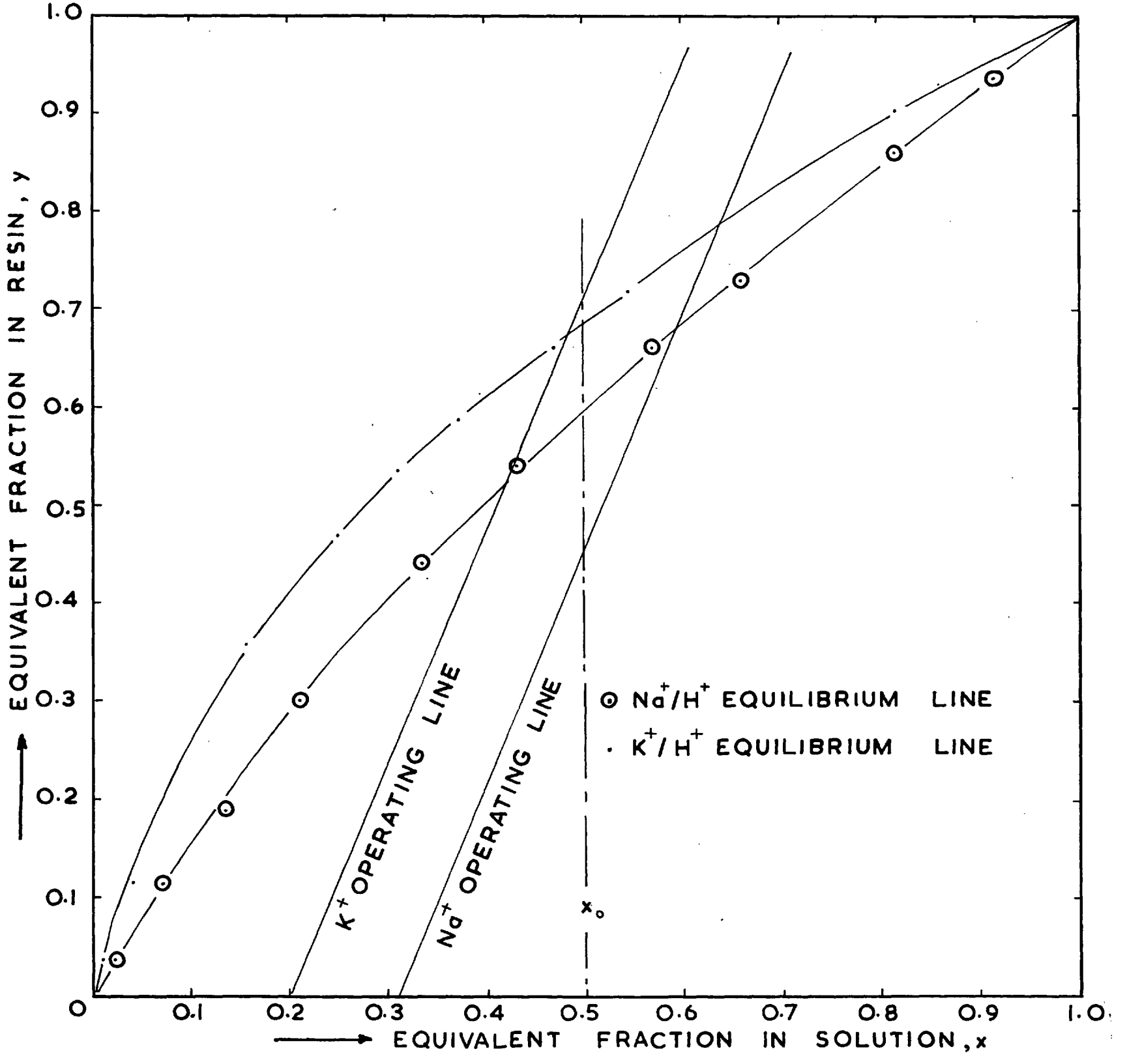

FIGURE 33. x - y DIAGRAM FOR GROSS IONIC FRACTION RUN 20.

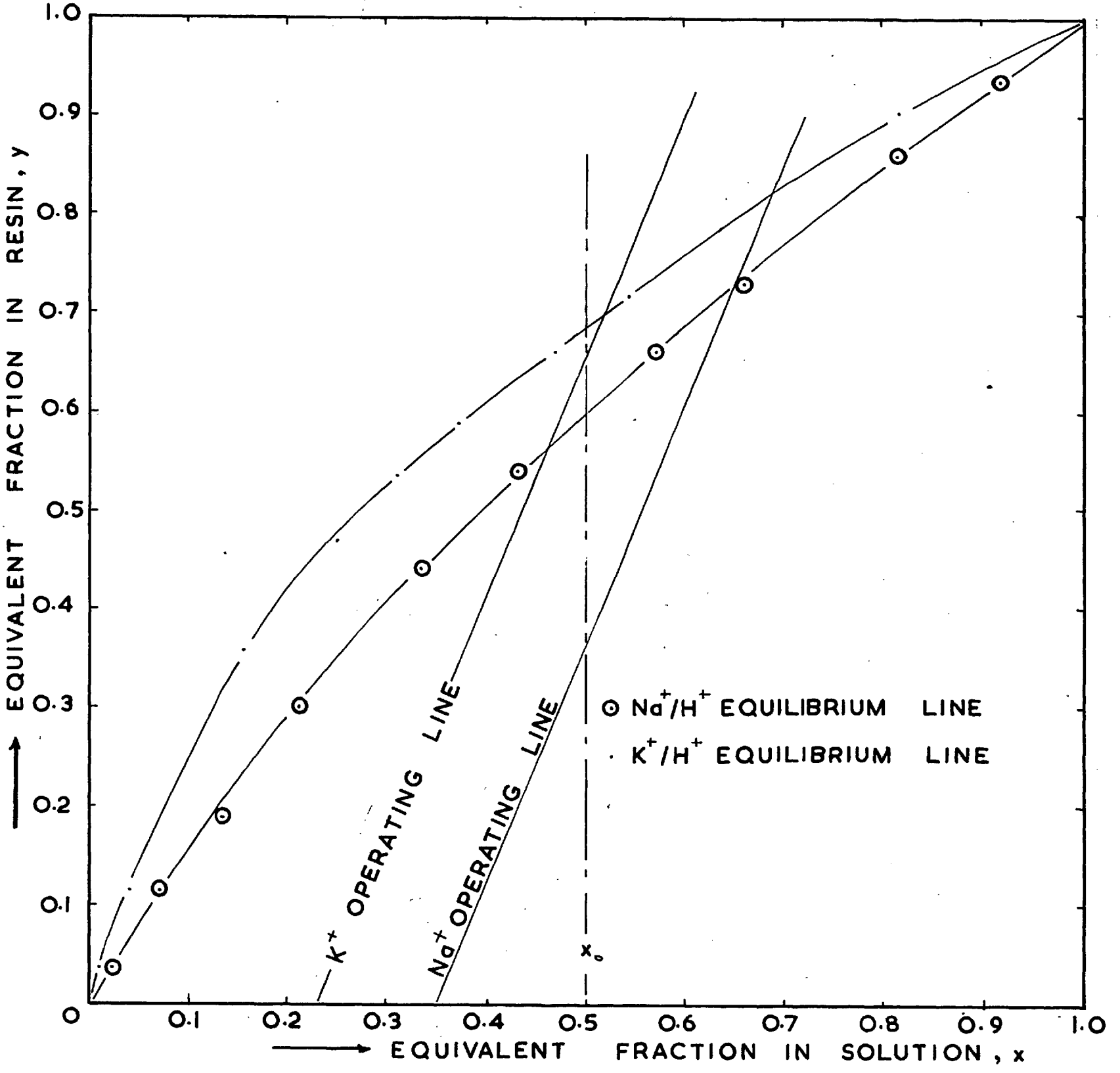

FIGURE 34. x - y DIAGRAM FOR GROSS IONIC FRACTION RUN 21.

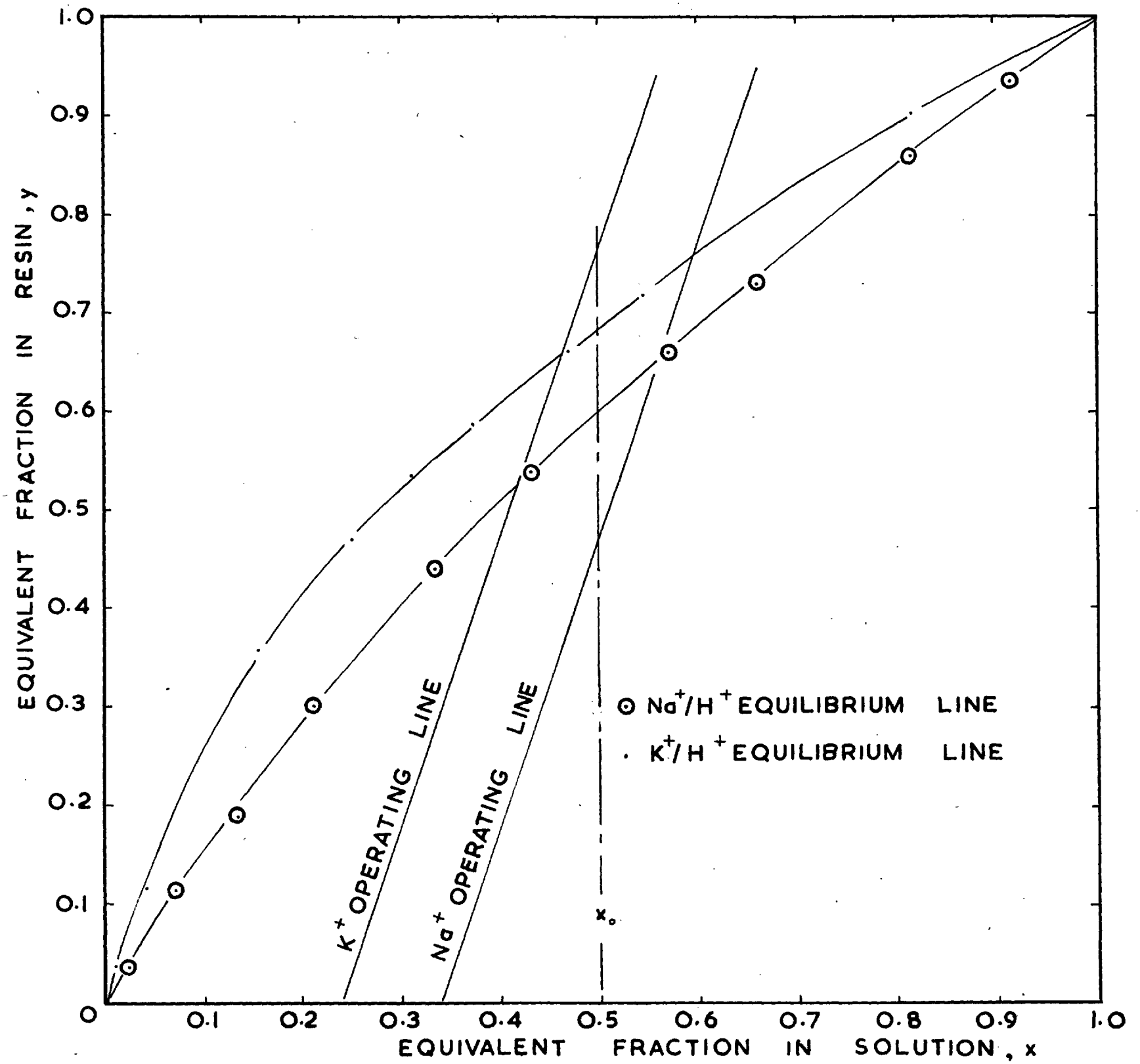

feed concentration.

This may seem surprising at first sight because

(a) in all the 10 stage gross ionic fraction runs except 16 neither the liquid nor the resin phases contain H^+ ions at the liquid feed end of the contactor.

(b) the batch equilibrations have shown that the K^+/H^+ equilibrium line in ternary systems differs from that for the binary K^+/H^+ system. Also the concentration of sodium in both phases at the liquid feed end of the contactor is appreciable.

With respect to point (a), this is a countercurrent process and although there are no H^+ ions at the liquid feed end of the contactor in runs 17 to 21, there are plenty of H^+ ions in the contactor as a whole (e.g. in a run with a $\frac{L}{S}$ ratio of 36.4 there are equimolar quantities of Na^+, K^+ and H^+ ions entering the contactor) so the use of a K^+/H^+ equilibrium line for the whole contactor is reasonable.

Regarding point (b), if the positive mass balance errors (i.e. the sum $(y_{Na_1} + y_{K_1})$ is greater than unity in runs 17, 18, 19 and 21) are allowed for, the position of the K^+ operating line is closer to the ternary system K^+/H^+ equilibrium lines. A consistent error of the potassium analyses of 15% would be necessary for the K^+ operating line in all runs to cut the ternary K^+/H^+ equilibrium line for equimolar quantities of Na^+ and K^+. Of course as the resin product contained a higher proportion of K^+

than Na^+, and the liquid feed contained equimolar quantities of Na^+ and K^+, there was in fact more K^+ than Na^+ in the two phases at the liquid feed end of the contactor in these runs. The ternary K^+/H^+ equilibrium points of this system would be closer to the binary K^+/H^+ equilibrium line.

Although mass balance errors up to 20% can be expected (Appendix 1), it cannot be concluded with certainty that the K^+ operating line in runs 17 to 21 forms a pinch point on the binary K^+/H^+ equilibrium line, in view of the mass balance errors. If the pinch point is formed on the binary K^+/H^+ line in these runs the greatest adsorption of K^+ ions into the resin occurs.

The 100 stage runs gave the same Na^+/K^+ separation and liquid product composition as the 10 stage runs, under the same operating conditions, confirming the position of the pinch point.

The intersection of the K^+ operating line with the K^+/H^+ equilibrium line at the potassium concentration in the liquid feed fixed the concentration of K^+ in the liquid (x_{K_n}) and resin (y_{K_1}) product streams. As the entering resin only contacted Na^+ and K^+ ions in the liquid feed the rest of the exchange sites in the resin would be occupied by sodium ions, so that y_{Na_1} was also fixed. This locates the position of the Na^+ operating line as it cuts the line corresponding to the Na^+ feed

concentration at this value of y_{Na_1}. The sodium enrichment is therefore limited by the relative disposition of the equilibrium lines for the K^+/H^+ and Na^+/H^+ systems.

It is apparent that a good separation of Na and K i.e. almost complete adsorption of the potassium, can only be achieved when the gradient of the operating line is less than the gradient of the line connecting the origin with the point on the K^+/H^+ equilibrium line corresponding to x_K in the liquid feed. If the pinch point is formed on the binary K^+/H^+ equilibrium line, this is when $\frac{L}{S} < 25$. If it is formed on a ternary K^+/H^+ equilibrium line it is at a lower value of $\frac{L}{S}$. For values of the flowrate ratio less than 25, the extraction factor for sodium is probably greater than unity for all values of the resin composition in the contactor, so that both sodium and potassium ion species are preferentially extracted by the resin. It is thus inevitable with the alkali metal ions in gross ionic fractions in the liquid feed that a poor sodium recovery will be associated with a good sodium enrichment in the liquid product with a single section ion exchange separation.

6. Conclusions.

The batch equilibration results show that the relative quantities of Na^+, K^+ and H^+ in the binary Na^+/H^+, K^+/H^+ and K^+/Na^+ and ternary $Na^+/K^+/H^+$ cation systems significantly affect the equilibrium distribution of the component cations between the resin and solution phases.

Although some of the experimental trends are contrary to published work they are in general qualitative agreement with swelling pressure theory considerations.

It has been established in the trace and gross ionic fraction runs, using the sodium enrichment and recovery in the liquid phase as the criteria, that the Na^+/K^+ separation performance was reproducible.

In addition to this the stage efficiency, calculated on the basis of sodium enrichment in the liquid phase or potassium enrichment in the resin phase, for both the glass and the perspex stage designs has been fairly constant over a wide range of operating conditions with trace ion concentrations. The calculated stage efficiency of the glass stages varied from 36% to 70% in extraction and rectification runs, with one exception, with the $\frac{L}{S}$ ratio ranging from 18 to 54. The calculated stage efficiency of the perspex contactor in extraction and elution runs varied from 60% to 110% except in one case, with the $\frac{L}{S}$ ratio varying from 28 to 80.

It can be concluded that the equilibrium stage theory can be used to predict the trace ion exchange separations achieved in the new contactor, and also that as the number of stages in this contactor is changed, the ion exchange separation performance will be altered in a predictable way.

The application of the principle of extraction factors to the Na^+/K^+ separations has been very useful. In the single section separations a good enrichment and recovery of sodium in the liquid phase and of potassium in the resin phase were obtained in extraction and rectification runs respectively. In the three section work ... two runs were carried out, only one of which was under optimum operating conditions. In this run the recovery and purity of sodium in the Na rich product and potassium in the K rich product were improved and the proportion of alkali metal ions not eluted from the resin was much smaller, in comparison with the run where optimum operating conditions were not used. The superior performance was gained using a lower resin flowrate relative to the liquid feed. The better utilisation of resin also emphasized the utility of extraction factor principles.

In the gross runs an interesting feature was the same Na^+/K^+ separation achieved in the 100 stage runs as with the 10 stage runs. The existence of a pinch point on the K^+/H^+ equilibrium line is indicated. This makes it inevitable that a poor sodium recovery will be associated with a high sodium

enrichment in the liquid phase with a single section separation with gross ionic fractions of the alkali metals in the liquid feed.

The compact contactor stage developed in this work could be very useful in many small scale continuous ion exchange applications, for example the purification of pharmaceutical preparations or the purification of solutions containing valuable metal ions or in separation, concentration or purification for chemical analysis.

7. References

A1 Anon. Chem. Engng, 1953, 62(9), 248.

A2 Arden, T.V., Davis, J.B., Herwig, G.L., Stewart, R.M., Swinton, E.A. and Weiss, D.E. Proc. 2nd Int. Conf. peaceful Uses atmm. Energy, 1958, 3, 396.

A3 Arehart, T.A., Bresee, J.C., Hancher, C.W. and Jury, S.H. Chem. Engng. Prog., 1956, 52, 353.

A4 Asahi Kasei K.K.K., F.P. 1,352,622 (4.4.1963)

A5 Asahi Kasei K.K.K., B.P. 1,036,429 (20.7.1966)

B1 Bennett, B.A. Private communication, 1967.

B2 Bonner, O.D. J. phys. Chem., 1954, 58, 318.

B3 Bonner, O.D., Holland, V.F. and Smith, L.L. J. phys. Chem., 1956, 60, 1102.

B4 Bonner, O.D., and Smith, L.L., J. phys. Chem., 1957, 61, 1614.

B5 Boyd, G.E., Vaslow, F. and Lindenbaum, S. J. phys. Chem., 1964, 68, 590.

B6 Boyd, G.E. and Soldano, B.A. J. Amer. Chem. Soc., 1953, 75, 6091.

C1 Carberry, J.J. A.I.Ch. E. Jl, 1960, 6, 460.

C2 Cloete, F.L.D. and Streat, M. Nature, London, 1963, 200, 1199.

C3 Cloete, F.L.D., Streat, M. and Miller, A.I. A.I. Ch.E. -I. Ch. E. Symp. Ser., 1965, No.1, 54.

C4 Collins, G.C. and Polkinhorne, H. Analyst, 1952, 77, 430.

C5 Coulson, J.M. and Richardson, J.F. "Chemical engineering", Vol. 1, 1st Ed. 1954 (Pergamon).

C6 Coulson, J.M. and Richardson, J.F. "Chemical engineering", Vol. 2, 1st Ed. 1955 (Pergamon).

C7 Cruickshank, E.H. and Meares, P. Trans. Faraday Soc., 1958, 54, 174.

D1 Davies, O.L. "Statistical methods in research and production", 3rd Ed. 1957 (Oliver and Boyd).

D2 Dean, J.A. "Flame photometry", 1960 (McGraw-Hill).

D3 Dranoff, J. and Lapidus, L. Industr. Engng Chem., 1957, 49, 1297.

D4 Duncan, J.F. and Lister, B.A.J. J. Chem. Soc., 1949, 3285.

E1 Elwell, W.T. and Gidley, J.A.F. "Atomic absorption spectrophotometry", 1961 (Pergamon).

E2 Erickson, E.E. Diss. Abstr., 1960, 20, 4353.

F1 Flagg, J.F. (Ed.) "Chemical processing of reactor fuels", 1961 (Academic).

F2 Flett, D.S. and Meares, P. Trans. Faraday Soc., 1966, 62, 1469.

G1 Ghate, M.R., Gupta, A.R. and Shankar, J. Indian J. Chem., 1966, 4, 64.

G2 Glasstone, S. "Introduction to electrochemistry", 2nd ed. 1946 (D. Van Nostrand).

G3 Glueckauf, E. Proc. roy. Soc. 1952 214A 207.

G4 Glueckauf, E. Proc. roy. Soc. 1962. 268A 350.

G5 Glueckauf, E. and Watts, R.E. Proc. roy. Soc. 1962. 268A 339

G6 Gorshkov, V.I., Kuznetsov, I.A. and Panchenkov, G.M. Proc. Acad. Sci. U.S.S.R. Phys. Chem. Section. 1962 143 241.

G7 Gorshkov, V.I., Martynenko, L.I. and Chumakov, V.A. J. App. Chem. U.S.S.R. 1964 37 1183

G8 Gorshkov, V.I. Kuznetsov, I.A. and Panchenkov, G.M. Russ. J. phys. Chem. 1964 38 1347.

G9 Gorshkov, V.I., Kuznetsov, I.A., Panchenkov, G.M. and Kustova, L.V. Russ. J. inorg. Chem. 1963 8 1465.

G10 Grimmett, E.S. and de Nevers, N. USAEC Rept. IDO-14648 (March 1965).

G11 Grimmett, E.S. and Brown, B.P. Industr. Engng Chem., 1962 54(11), 24.

H1 Helfferich, F. 'Ion exchange", 1962 (McGraw-Hill).

H2 Hiester, N.K., Phillips, R.C., Fields, E.F., Cohen, R.K. and Radding, S.B. Industr. Engng Chem., 1953, 45, 2402.

H3 Hiester, N.K, Fields, E.F., Phillips, R.C. and Radding, S.B. USAEC Rept. AECU - 2737 (1953).

H4 Hiester, N.K., Phillips, R.C. and Cohen, R.K. USAEC Rept. AECU-2738 (1953).

H5 Hiester, N.K., and Phillips, R.C. Chem. Engng, 1954, 61 (10), 161.

H6 Higgins, I.R. and Roberts, J.T. Chem. Engng Prog. Symp. Ser., 1954, 50 (No. 14), 87.

H7 Higgins, I.R. and Messing, A.F. USAEC Rept. ORNL - 2491 (1958).

H8 Higgins, I.R. Industr. Engng Chem. 1961 53 635, 999.

H9 Higgins, I.R., Phillippi, C.G. and Jones, J.D. USAEC Rept. ORO - 604 (1963).

H10 Higgins, I.R. Private communication, 1967.

H11 Högfeldt, E. Ark. Kemi, 1959, 13, 491.

J1 Jasz, A. and Lengyel, T. Int. Chem. Engng, 1963, 3, 55.

K1 Komarovskii, A.A. J. app. Chem. USSR, 1963, 36, 1167.

K2 Kremser, A. Nat. Petrol. News, 1930, May 21, 43.

M1 McCormack, R.H. and Howard, J.F. Chem. Engng Prog., 1953 49, 404.

M2 Matthieson, F.O. U.S. Pat. 329, 185 (18.5.1885).

M3 Mavrodineanu, R. and Boiteux, H. 'Flame spectroscopy", 1965 (J. Wiley and Sons).

M3 Meyer, W. and Olsen, R.S. Nucl. Sci. Abstr., 1965 19 No. 9277.

M4 Mihara, S. and Terasaki, Y. Jap. Pat. 2,223 (1951).

M5 Miller, A.I. Ph.D. Thesis, Uni. of London (1966).

M6 Mixon, F.O. and Carberry, J.J. Chem. Engng Sci., 1960, 13, 30.

M7 Moelwyn-Hughes, E.A. "Physical chemistry", 1957, (Pergamon).

M8 Myers, G.E. and Boyd, G.E., J. phys. Chem., 1956, 60, 520.

N1 Nordell, C.H. U.S. Pat. 1,608,661 (30.11.1926).

N2 Nordell, C.H. U.S. Pat. 1,740,199 (17.12.1929).

O1 Olin, J. Koenig, W.W., Babb, A.L. and McCarthy, J.L. Chem. Engng Prog. Symp. Ser., 1954, 50 (No. 14), 103.

P1 Pepper, K.W., Reichenberg, D. and Hale, D.K. J. chem. Soc., 1952, 3129.

P2 Permutit Co. Ltd. Private communication, 1967.

P3 Perry, S.F. U.S. Pat. 2,632,720. (24.3.1953).

P4 Pike, F.P. and Erickson, E.E. U.S. Pat. 3,092,515 (4.6.1963).

P5 Poluektov, N.S., Nikonova, M.P. and Vitkun, R.A., Zh. analit. Khim, 1958, 13, 53.

P6 Porter, R. Chem. Week, 1956, 78, (June 9), 74.

R1 Redinha, J.S. and Kitchener, J.A. Trans. Faraday Soc., 1963, 59, 515.

R2 Reichenberg, D., Pepper, K.W. and McCauley, D.J. J. chem. Soc., 1951, 493.

R3 Reichenberg, D. and McCauley, D.J. J. chem. Soc. 1955, 274.

S1 Selke, W.A. and Bliss, H. Chem. Engng Prog., 1951, 47, 529.

S2 Selke, W.A. and Muendel, C.H. USAEC Rept. NYO - 962 (1953).

S3 Shell Development Co. Aust. Pat. 129,885 (25.11.1948).

S4 Shulman, H.L., Youngquist, G.R. and Covert, J.R. Industr. Engng Chem., Proc. Design Devt., 1966, 5, 257.

S5 Snowdon, C.B. Ph. D. Thesis, Uni. of Cambridge (1966).

S6 Souders, M. and Brown, G.G. Industr. Engng. Chem., 1932, 24, 519.

S7 Stanton, L.S., M.S. Thesis, Uni. of Washington (1950).

S8 Sun Oil Co. U.S. Pat. 2,813,781 (19.11.1957).

S9 Swinton, E.A. and Weiss, D.E. Aust. J. App. Sci., 1953, 4, 316.

T1 Turner, J.C.R. and Church, M.R. Trans. Instn Chem. Engrs., Lond., 1963, 41, 283.

T2 Turner, J.C.R., Church, M.R., Johnson, A.S.W. and Snowdon, C.B. Chem. Engng Sci., 1966, 21, 317.

V1 Vaslow, F. and Boyd, G.E., J. Phys. Chem., 1966, 70, 2.295.

V2 Vogel, A.I. "A textbook of quantitative inorganic analysis" 3rd ed. 1961 (Longmans).

W1 Whitcombe, J.A., Banchero, J.T. and White, R.R. Chem. Engng Prog. Symp. Ser., 1954, 50 (No. 14), 73.

Z1 Zsigmond, A. and Gryllus, L. Elelm. Ipar, 1963, 17(6), 169.

8. Nomenclature

a	valency of ionic species A	(dimensionless)
A	constant in equation (3.2)	(dimensionless)
b	valency of ionic species B	(dimensionless)
B	constant in equation (3.2)	(dimensionless)
c	concentration referred to the liquid phase	(meq/cm^3)
$\bar{c}$	concentration referred to the resin phase	(meq/cm^3 free settled swollen resin)
$\bar{c}_{vol}$	volume exchange capacity of resin	(meq/cm^3 swollen resin)
$\bar{c}_{wt.}$	weight exchange capacity of resin	(meq/g)
C	constant in equation (3.2)	
d	swollen resin bead diameter	(mm or cm)
d_m	mean hydraulic swollen resin bead diameter	(cm)
D	diffusivity of an ion in solution	(cm^2/sec)
$\bar{D}$	diffusivity of an ion in the swollen resin	(cm^2/sec)
D_{eff}	effective diffusivity used in mass transfer correlations	(cm^2/sec)
e	fractional void volume of swollen resin	(dimensionless)
E	extraction factor	(dimensionless)
f_1	enrichment factor for sodium in solution product	(dimensionless)
f_2	enrichment factor for potassium in resin product	(dimensionless)
$\mathcal{F}$	Faraday's constant	(2.3×10^4 cal/(volt)(g.eq))

$F_1(x_A)$ factor used in definition of D_{eff}

$$= \frac{2 \quad (1 + \alpha' \bar{x})^{\frac{1}{3}}}{\sqrt{(1+\alpha' x_{in})(1+\alpha' x)+(1+\alpha' x_{in})}} \qquad \text{(dimensionless)}$$

g	valency of gross ionic species G.	(dimensionless)
H	volume of free settled swollen resin initially present in a contacting stage	(cm^3)
$H_{critical}$	the smallest value of H to give W_{max}	(cm^3)
k_L	liquid film mass transfer coefficient	(cm/sec)
K_3	constant in equation (2.13)	(dimensionless)
K_{AB}	selectivity coefficient	(dimensionless)
L	average liquid phase volumetric flowrate	(cm^3/min)
m	gradient of equilibrium distribution line	(dimensionless)
n	calculated number of equivalent ideal contacting stages	(dimensionless)
P	purity of sodium or potassium in a solution product	(dimensionless)
R	Universal gas constant = 0.0821 l.atm/(mole)(^oK)	
Re	Reynolds number ($\frac{\rho ud}{\mu}$)	(dimensionless)
s	surface area of swollen resin per unit absolute resin volume	(cm^{-1})
s'	interfacial area in a contacting stage	(cm^2)
S	average free settled swollen resin volumetric flowrate	(cm^3/min)
Sc	Schmidt number ($\frac{\mu}{\rho D}$)	(dimensionless)
Sh	Sherwood number ($\frac{k_L d}{D}$)	(dimensionless)
t_f	forward flow cycle time	(sec)
t_r	reverse flow cycle time	(sec)
t_s	no flow cycle time (secs)	
T	absolute temperature	(^oK)

u	superficial velocity of liquid in a contacting stage (cm/sec)
u_p	interstitial velocity of liquid in a contacting stage (cm/sec)
u'	mobility of an ion in solution (cm/sec over 1 volt/cm potential gradient)
U_f	instantaneous liquid flowrate in forward flow (cm^3/min)
U_r	instantaneous liquid flowrate in reverse flow (cm^3/min)
v	volume of solution used in batch equilibrations (Appendix 1)(cm^3)
$\bar{V}$	partial molal volume of ionic species in swollen resin (litre/mole)
W	volumetric increment of free settled swollen resin transferred per cycle (cm^3)
W_{max}	maximum value of W when W becomes independent of further increases in H (cm^3)
x	equivalent fraction of an ionic species in solution phase
x_i^*	equivalent fraction of an ionic species in solution in a contacting stage in equilibrium with the mean composition of the resin entering the stage (dimensionless)
x_i^{**}	equivalent fraction of an ionic species in solution in a contacting stage in equilibrium with the mean composition of the resin in the stage (dimensionless)
$\bar{x}$	mean equivalent fraction of an ionic species in the liquid boundary layer (dimensionless)
y	equivalent fraction of an ionic species in the resin phase (dimensionless)
y^*	equivalent fraction of an ionic species in the resin in a contacting stage in equilibrium with the composition of the solution entering the stage (dimensionless)
Z	fractional water content of swollen resin expressed as weight (dimensionless)

α	separation factor = $\frac{K_{KH}}{K_{NaH}}$	(dimensionless)
α'	factor used in definition of $F_1(x_A) = \frac{D_A}{D_B} - 1$	(dimensionless)
β	overall stage efficiency in a multistage contactor	(dimensionless)
ϕ	constant in equations (2.27) and (2.28)	(dimensionless)
σ	activity of ionic species in solution	(dimensionless)
$\bar{\sigma}$	activity of ionic species in a swollen resin	(dimensionless)
Δ	rate of ion exchange in a contacting stage	(meq/min)
λ	distribution coefficient of an ionic species	(dimensionless)
π	resin swelling pressure	(atm.)
ρ	density of liquid	(g/cm^3)
ρ_s	density of swollen resin	(g/cm^3)
μ	viscosity	(g/(cm)(sec))

Subscripts.

A,B,G	refer to ionic species
AB	refers to the interdiffusion of ionic species A and B when applied to the diffusion coefficient
co	refers to co-ions
i	refers to a general stage in a multistage contactor
in	refers to the resin-solution interface
n	refers to contacting stage n
o	refers to the liquid stream entering contacting stage 1

Abbreviations

BSS	British Standard sieve
DVB	divinyl benzene
EEL	Evans Electroselenium Ltd.

Appendix 1. An estimate of the errors involved in the work.

The error formulae used are

$$A \pm B, \quad \delta(A \pm B) = \sqrt{(\delta A)^2 + (\delta B)^2}$$

$$AB \text{ or } \frac{A}{B}, \quad \frac{\delta(AB)}{AB} = \frac{\delta\left(\frac{A}{B}\right)}{\frac{A}{B}} = \sqrt{\left(\frac{\delta A}{A}\right)^2 + \left(\frac{\delta B}{B}\right)^2}$$

(i) Batch equilibrations

The Na^+/H^+ ion exchange system is considered. The estimated maximum value of various experimental errors is as follows:

(a) Error in making up standard NaCl solutions = ± 0.05%

(b) Overall error in the measurement of the Na^+ concentration in the equilibrated supernate (c_{Na_t}) = ± 2.0%

(c) Error in exchange capacity of resin = ± 1.0%

(d) Error in volume of solution used in batch equilibrations = ± 0.5%

(this includes pipetting errors and variation in the quantity of interstitial water left on the resin particles after centrifugation).

Two cases will be considered

(a) c_{Na_o} = 0.1N c_{Na_t} = 0.033 N

(b) c_{Na_o} = 0.1N c_{Na_t} = 0.01 N

To simplify the calculations the volume of solution used in the equilibrations, $\mathcal{V}$, is $\frac{\bar{c}}{c}$ or 18.2 cm^3.

(a) $$y_{Na} = \frac{v\,(c_o - c_t)}{\bar{c}}$$

$$c_o - c_t = 0.1N \pm 0.05\% - 0.033N \pm 2.0\%$$
$$= 0.1N \pm 0.00005 - 0.033N \pm 0.00067$$
$$= 0.067N \pm \sqrt{0.00005^2 + 0.00067^2}$$
$$= 0.067N \pm 0.00067N \simeq 0.067N \pm 1.00\%$$

$$y_{Na} = \frac{18.2 \pm 0.5\% \times 0.067N \pm 1.0\%}{\bar{c} \pm 1\%}$$

$$y_{Na} = 0.67$$

$$\frac{\partial y_{Na}}{y_{Na}} = \sqrt{0.5^2 + 1.0^2 + 1.0^2} = \pm 1.5\%$$

$$\therefore\ y_{Na} = 0.67 \pm 0.01005$$

$$\therefore\ y_H = 0.33 \pm 0.01005 = 0.33 \pm 3.0\%$$

$$x_{Na} = \frac{c_t}{c} = \frac{c_t \pm 2.0\%}{c \pm 0.05\%}$$

$$\frac{\partial x_{Na}}{x_{Na}} = \sqrt{2.0^2 + 0.05^2} = \pm 2.0\%$$

$$x_{Na} = 0.33 \pm 0.0067$$

$$x_H = 0.67 \pm 0.0067 = 0.67 \pm 1.0\%$$

$$K_{NaH} = \frac{y_{Na} \times x_H}{y_H \times x_{Na}} = \frac{0.67 \pm 1.5\% \times 0.67 \pm 1.0\%}{0.33 \pm 3.0\% \times 0.33 \pm 2.0\%}$$

$$\frac{\partial K_{NaH}}{K_{NaH}} = \sqrt{1.5^2 + 1.0^2 + 3.0^2 + 2.0^2} = \pm 4.05\%$$

(b) $c_o = 0.1N \qquad c_t = 0.01N$

$$c_o - c_t = 0.1N \pm 0.05\% - 0.01N \pm 2.0\%$$
$$= 0.1N \pm 0.00005 - 0.01N \pm 0.0002$$

$$\partial(c_o - c_t) = \sqrt{0.00005^2 + 0.0002^2} \simeq \pm 0.0002N$$

$$\therefore (c_o - c_t) = 0.09N \pm 0.0002 = 0.09N \pm 0.2\%$$

$$y_{Na} = \frac{18.2 \pm 0.5\% \times 0.09N \pm 0.2\%}{1.82 \pm 1\%}$$

$$\frac{\partial y_{Na}}{y_{Na}} = \sqrt{0.5^2 + 0.2^2 + 1^2} = \pm 1.14\%$$

$$y_{Na} = 0.9 \pm 1.14\% = 0.9 \pm 0.01026$$

$$y_H = 0.1 \pm 0.01026 = 0.1 \pm 10.26\%$$

$$x_{Na} = \frac{c_t}{c} = \frac{0.01 \pm 2.0\%}{0.1 \pm 0.05\%}$$

$$\frac{\partial x_{Na}}{x_{Na}} = \sqrt{2.0^2 + 0.05^2} = \pm 2.0\%$$

$$x_{Na} = 0.1 \pm 2.0\% = 0.1 \pm 0.0020$$

$$x_H = 0.9 \pm 0.002 = 0.9 \pm 0.22\%$$

$$\frac{\partial K_{NaH}}{K_{NaH}} = \sqrt{(\partial y_{Na})^2 + (\partial y_H)^2 + (\partial x_{Na})^2 + (\partial x_H)^2}$$

$$= \sqrt{1.14^2 + 10.26^2 + 2.0^2 + 0.22^2}$$

$$= \pm 10.5\%$$

It can be concluded that the calculation of y_{Na} by difference yields results accurate to within a few percent in the mid-concentration range. However at high or low values of x (or y) the errors become substantial, with similar errors in the value of the selectivity coefficient K_{NaH}.

The errors in the ternary equilibrations will be even higher.

(ii) Gross ionic fraction Na^+/K^+ separation runs

(a) Error in the measured volume of resin.

The difference between the resin feed and product volumes has been 3.9 cm^3 when the average resin volume was 26.2 cm^3 (run 20)

$\therefore$ Volume measurement error = $\pm \frac{1.95}{26.2} = \pm 7.5\%$

(b) Error in liquid volume measurement.

The disparity in the volume balance has been 31 cm^3 with an average total liquid volume of 915 cm^3 (run 17)

$\therefore$ Volume measurement error = $\pm \frac{15.5}{915} = \pm 1.7\%$

(c) Overall error in flame photometric determination of sodium or potassium concentrations in liquid product = $\pm$ 3% (less care was taken than with the batch equilibration work).

(d) Error in making up liquid feed solution = $\pm$ 2%

(e) Error in resin exchange capacity = $\pm$ 1%

(f) Error in the quantity of each alkali metal in the resin caused by unrepresentative samples = $\pm$ 5%

(g) Overall error in mass balance for sodium:

Quantity of sodium in liquid product

= volume x concentration

= volume $\pm$ 1.7% x c_{Na_n} $\pm$ 3%

$\therefore$ $\frac{\delta(\text{quantity of sodium in liquid product})}{\text{quantity of sodium in liquid product}}$

$= \sqrt{1.7^2 + 3^2} \simeq 3.45\%$

$\frac{\delta(\text{quantity of sodium in resin product})}{\text{quantity of sodium in resin product}}$

$= \sqrt{7.5^2 + 3^2 + 1^2 + 5^2}$

$= \pm 9.55\%$

Assuming an equal quantity of sodium in each phase

Error in mass balance for sodium $= \sqrt{3.45^2 + 9.55^2}$

$= \pm 10.1\%$

The potassium mass balance error will be comparable.

(iii) Trace Na^+/K^+ separation runs.

The overall mass balance error for each of the alkali metals should be less than $\pm$ 10% as there was only a small proportion of the total sodium and potassium in the resin product.

ION EXCHANGE PRE-TREATMENT FOR SEA WATER DESALINATION PLANTS*

G. K. KUNZ

Maschinenfabrik Augsburg-Nürnberg, Aktiengesellschaft Werk Gustavsburg, Gustavsburg/Hessen (Germany)

SUMMARY

The range of optimization for sea water desalination plants, using thermal processes, is considerably restricted by scale-formation, especially that of calcium sulphate. A study is made of the dependence of the saturation concentrations of the anhydrite and hemihydrate modifications on temperatures and concentration factors. The conversion of the hemihydrate phase into the anhydrite phase, whose speed was measured, proved to be of particular importance.

Partial softening of sea water by means of ion exchange, using the brine concentrated in the evaporators as a regenerant, reduces calcium ion concentration to such an extent that no deposits occur. Results obtained in discontinuous laboratory experiments show the dependence on the various limiting quantities.

The degree of softening can be considerably increased if the ion exchange is carried out continuously, countercurrently. The apparatus used for a typical plant consists of countercurrent columns, the absorption column operating by stages. No pumps are required for the circulation of the resin; regulation is by automatic control of a single valve.

The results of the operation of a pilot plant are given with particular reference to the exchange efficiency. The combination with the saturation concentrations of calcium sulphate shows that even with low concentration factors the maximum operating temperatures can be as high as 160° C without the solubility limit of the calcium sulphate hemihydrate being exceeded.

THE INFLUENCE OF CALCIUM SULPHATE DEPOSITS ON THE ECONOMICS OF THERMAL DESALINATION PROCESSES

Among the economically attractive processes for the conversion of sea water to fresh water the thermal processes have become increasingly important in recent years. The conditions under which they operate, however, can be chosen freely only within certain limits; the range of optimization is thus limited. Temperatures and concentration factors, for example, are restricted by the saturation concentrations of the scale-forming agents which adversely affect the economic operation of sea water desalination plants.

Calcium sulphate is a particularly unpleasant scale-forming agent. Unlike the solubility of the carbonates and hydroxides of calcium and magnesium, its solubility cannot be influenced by changing the hydrogen ion concentration. Deposits are particularly encouraged by the fact that the solubility of $CaSO_4$ diminishes rapidly at elevated temperatures. During the operation of multi-stage flash evaporators no $CaSO_4$ deposits occurred at a temperature of 120°C and a concentration factor of 1.7.

* Paper presented at the Second European Symposium on Fresh Water from the Sea, May 9–12, 1967, Athens, Greece. European Federation of Chemical Engineering.

At higher temperatures and concentration factors, however, $CaSO_4$ layers form which impede the heat flow.

On the other hand, increased temperatures lead to a reduction in energy requirements and hence, under certain circumstances, also in the production costs of fresh water. As the concentration factor increases, the costs of pretreating the sea water such as those of pumping, pre-cleaning, control of chemicals, and degasification go down.

Fig. 1 shows the fresh water costs as a function of the steam temperature for a rate of production of 200 m^3/h.

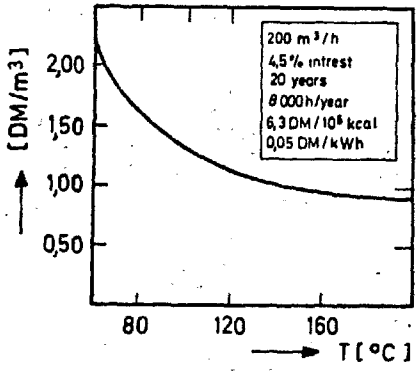

Fig. 1. Water cost, vs. steam temperature.

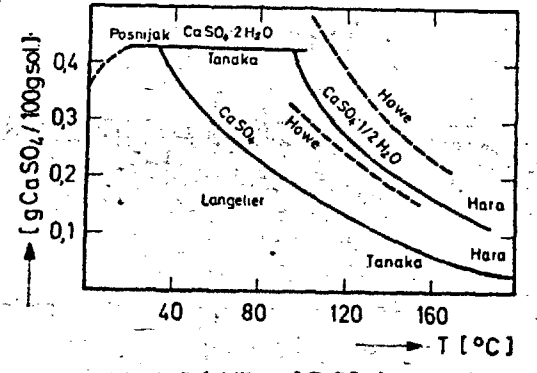

Fig. 2. Solubility of $CaSO_4$ in sea water.

2. THE BEHAVIOUR OF $CaSO_4$ AND ITS MODIFICATIONS IN SEA WATER OF DIFFERENT TEMPERATURES AND CONCENTRATION FACTORS

If $CaSO_4$ is in solubility equilibrium with water or aqueous NaCl solutions it may occur in two stable modifications, or one metastable one, over the entire range of temperature up to the critical point. Below 42°C the dihydrate is stable, above this temperature the anhydrite is stable. While the hemihydrate can exist as a metastable phase over the entire range of temperature, the dihydrate is stable only between 42° and approximately 98°C for a certain period of time. At higher temperatures it is converted into the hemihydrate phase.

The solubility of the various $CaSO_4$ modifications in sea water are shown in Fig. 2. The dependence of these values on the concentration factors was determined in several test runs. The Battelle Institute at Frankfurt-on-Main was in charge of these measurements.

2.1 *Measuring technique*

The mixtures consisting of solution and solid phase were brought to the desired temperature in a 5 liter silver-plated autoclave with a magnetic stirrer. The samples were taken by means of a cooler, the analysis was made titrimetrically. Equilibrium was assumed to have occurred when there was a constant concentration.

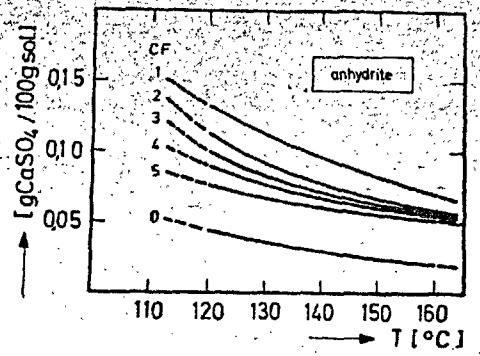

Fig. 3. Solubility of $CaSO_4$.

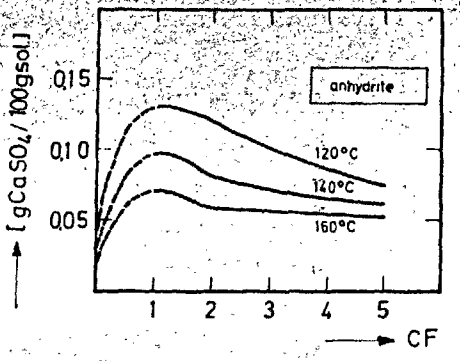

Fig. 4. Solubility of $CaSO_4$.

2.2 *The solubility of the* $CaSO_4$ *anhydrite modification*

The measurements were taken at temperatures ranging from 120° to 160°C, four concentrations 2, 3, 4 and 5 times those of sea water. The mean error of measurement is about 3%.

Fig. 3 shows that solubility decreases with the temperature for all concentrations. Solubility is small in distilled water and increases considerably due to the influence of the salts dissolved in the sea water. As the concentration increases, however, it decreases again, the decrease being slower at elevated temperatures than at lower temperatures. This is shown in Fig. 4.

2.3 *The solubility of the* $CaSO_4$ *hemihydrate modification and its conversion rate in anhydrite*

Further measurements were made to study how the calcium ion concentration of the initial hemihydrate equilibrium approaches the calcium ion concentration of the anhydrite equilibrium in solutions 2−, 3−, 4−, and 5 times more concentrated than sea water.

This conversion can be explained by the relevant rule established by Ostwald; apart from the rate of nucleation and crystal growth, its rate is largely dependent on the temperature. Figs. 5, 6 and 7 show the change in $CaSO_4$ saturation concentration as a function of the time at 120, 140 and 160°C for different concentration factors. These figures show that, e.g. in an evaporator, anhydrite will form in a comparatively short time although only small quantities of hemihydrate have at first been precipitated. This results in a highly oversaturated condition of the system which causes the anhydrite to crystallize rapidly. This behaviour is shown in Fig. 8. While run A contained only hemihydrate as solid phase at the beginning of the experiment, small quantities of anhydrite were added to run B.

When determining the evaporator service conditions, care should therefore be taken to ensure that there is a sufficient difference in concentration compared with the saturation concentration of the hemihydrate to avoid the critical oversaturated condition of the anhydrite.

A fact worth noting is the dependence of the $CaSO_4$ saturation concentration on the total salt content of the solution. Fig. 9 shows that it reaches a maximum at concentration factors 2 and 3.

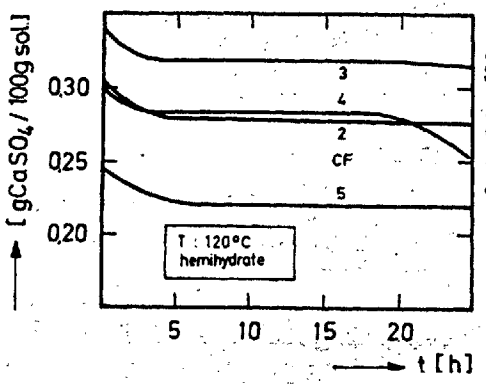

Fig. 5. $CaSO_4$ solubility modification.

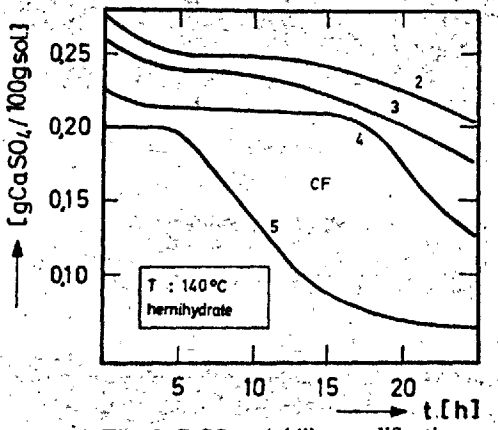

Fig. 6. $CaSO_4$ solubility modification.

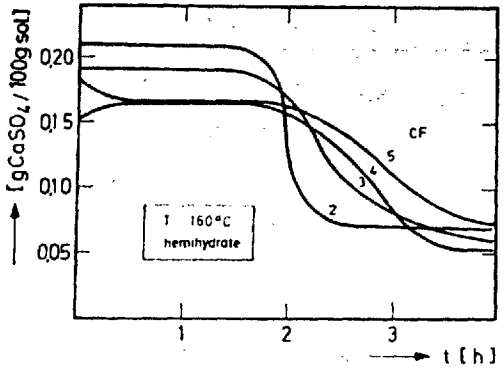

Fig. 7. $CaSO_4$ solubility modification.

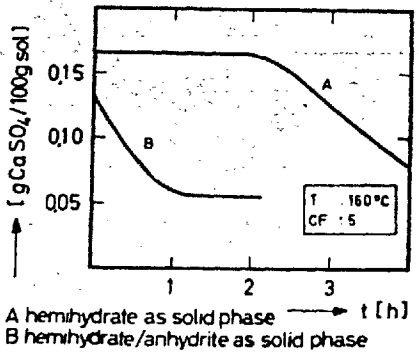

Fig. 8. $CaSO_4$ solubility modification.

3. PARTIAL SOFTENING OF SEA WATER BY MEANS OF ION EXCHANGE

As was mentioned previously, the $CaSO_4$ solubility cannot be influenced by pH control. The Ca ion concentration of the feed water can however be reduced with the aid of ion exchange resins. Although the high Na ion concentration permits only partial softening of the water, it is sufficient if, under the proposed evaporator service conditions, the remaining concentration is lower than the solubility equilibrium concentration of the Ca ions. The use of the brine concentrated in the evaporator as a regenerant results in economic operation.

3.1 *Intermittent ion exchange in a fixed-bed filter; laboratory tests*

To determine the influence of different operating conditions on the Ca and Mg ion

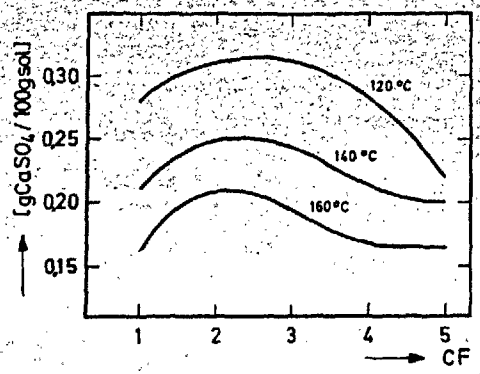

Fig. 9. Hemihydrate solubility of $CaSO_4$ vs. concentration factors.

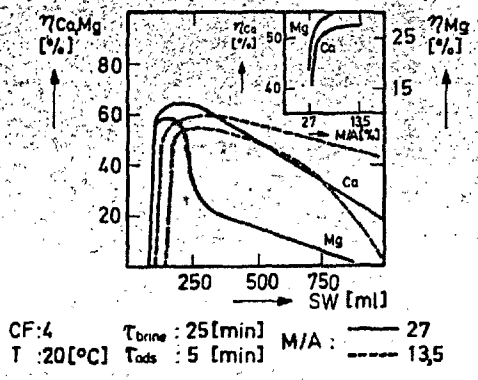

Fig. 10. ηCa, ηMg, quantity ratio M/A.

concentrations during adsorption, a laboratory column filled with the cation resin Dowex 50 W was filled with sea water. Brine of a concentration four times that of sea water served as a regenerant. Its calcium and magnesium contents corresponded to a 50% and a 33% exchange in sea water respectively. Adsorption and regeneration were carried out in the downflow; the mean contact time of the sea water was 5 minutes under all conditions.

The efficiency (η) of the calcium and magnesium exchange is expressed as a ratio of the final concentrations (C) of calcium and magnesium and the initial concentrations (C_0). Fig. 10 shows the change in Ca and Mg efficiency during the adsorption cycle for two quantitative relations of sea water (M) to resin (A). The strong dependence of the mean efficiency on the M/A ratio at a constant column diameter is mainly due to the well-known influence of the fixed-bed filter geometry on the exchange kinetics. The value 27 in the inset graph corresponds to a complete utilization of the exchange capacity.

Fig. 11 shows the efficiency of the Ca and Mg exchange after regeneration for different mean brine contact times. The inset graph shows the relatively small dependence.

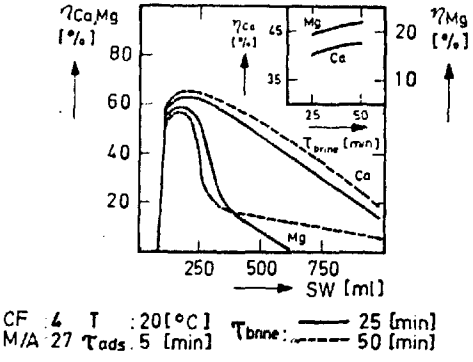

Fig. 11. ηCa, ηMg, middle r brine.

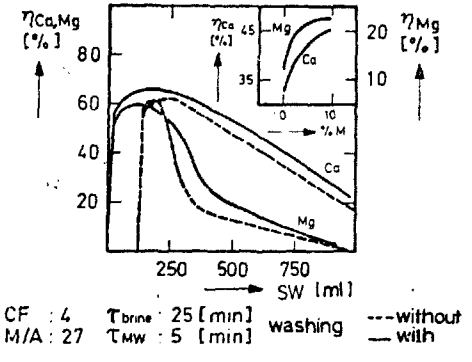

Fig. 12. ηCa, ηMg, as water volumes.

The mean efficiency is strongly influenced by the quantity of wash water used. The percentages given in Fig. 12 refer to the product quantity. The temperature of the regenerant brine has only a minor effect on the ion exchange equilibrium (Fig. 13).

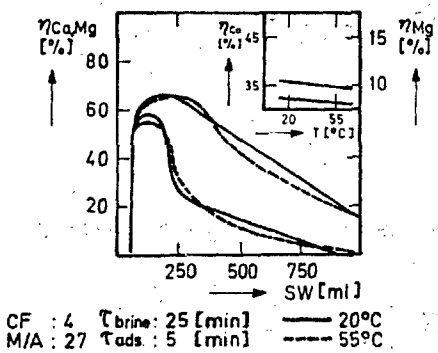

Fig. 13. ηCa, ηMg, brine temperatures.

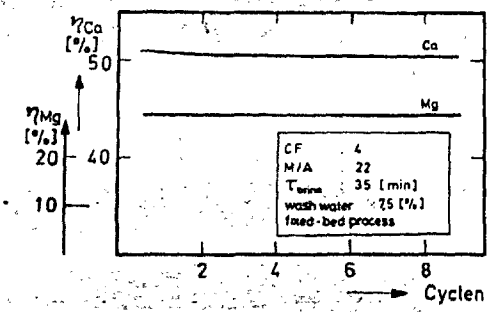

Fig. 14. ηCa, ηMg, adsorption cycles.

Fig. 14 shows the efficiencies of adsorption cycles carried out repeatedly one after the other. It indicates that in a fixed-bed filter 50% of the calcium and approx. 29% of the magnesium can be removed from the sea water under the operating conditions given.

About the same results were obtained from a small-scale plant built by the Dow Chemical Co. on behalf of the OSW *(1)* and operated in combination with thermo-compression plants for a prolonged period of time. Operation was intermittent and adsorption was effected in the fluidized bed cotercurrently and regeneration in accordance with the fixed-bed process.

3.2 *Working principle and arrangement of apparatus of a fully continuous counter-current ion exchange plant*

Of the various possibilities of a continuous or near-continuous process we selected the arrangement shown in Fig. 15 where adsorption and regeneration are effected in the countercurrent. Fully continuous operation is achieved by carrying the regenerated and washed resin to the adsorption column and the exhausted resin to the regenerating column. Exhausting of the resin, regeneration, and washing are effected in one column each, the regenerating column and the washing column forming one unit (Fig. 16).

The adsorption column and the washing column are fitted with outlets at their bottom ends, counter-pressure chambers as they are called, to which the feed pipes are connected. A counter-pressure pipe leads to each of the counter-pressure chambers, and a washpipe leads to the bottom part of the washing column. The softened sea water is drawn off through the top of the adsorption column. The adsorption column is equipped with trays and overflow pipes which, in accordance with the extraction,

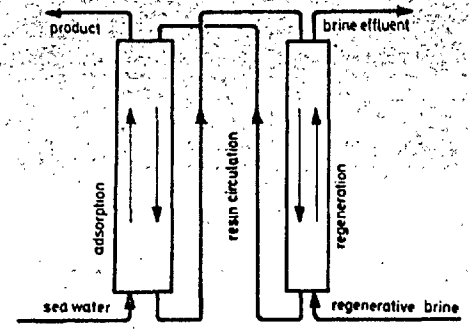

Fig. 15. Continuous countercurrent principle.

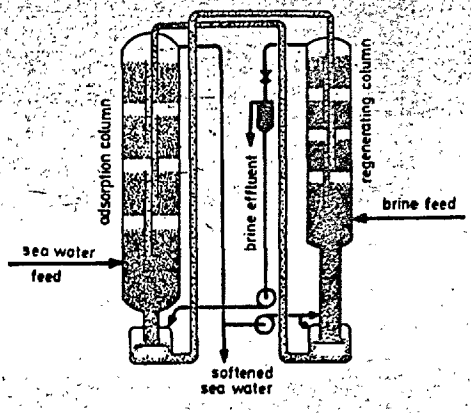

Fig. 16. Plant diagram.

divide the column into stages. The raw water enters the adsorption column through a distribution tray and flows through the stages from the bottom to the top. On its way up the resin forms a highly turbulent fluidized bed on each tray in which the exchange occurs from one stage to the next. The fluidized bed flowing through the column in an opposite direction to that of the sea water is increasingly exhausted and finally reaches the top of the regenerating column via the counter-pressure chamber through a feed pipe. The brine at the top of the regenerating column, being a counter-pressure or the feed fluid, acts as a recycle for the exhausted resin from which the brine is removed. The function of the regenerating and washing unit is the same as that of the adsorption column. Of particular interest is the fact that no pumps are required for the transport of the resin.

The regulation of the sea water throughput and of the streams which are equivalent to the throughput is achieved by means of the well-known techniques of automatic quantity and pressure control. The fluidized beds are maintained at a constant level by means of a single valve, the brine discharge valve. Control is based on a specially developed ultrasonic measurement of the level of the fluidized bed.

The plant requires no operators.

3.3 *Results of operation of a pilot plant*

The fully continuous countercurrent process described above has only little in common with conventional filter processes. It is a kind of extraction or absorption process where the resin must be regarded as an extraction or absorption agent having the properties of a fluid. This is particularly evident from Fig. 17 where the progress of ion exchange in the columns is represented graphically between operating lines and equilibrium curves.

The transitional behaviour of both columns between different operating conditions was observed by means of the material balance. Fig. 18 shows the stationary condition at concentration factors 5 and 4. the progress of the more important

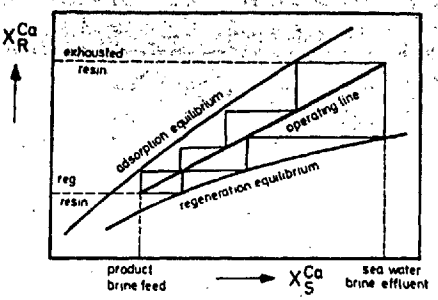

Fig. 17. Equilibrium diagram adsorption and regeneration.

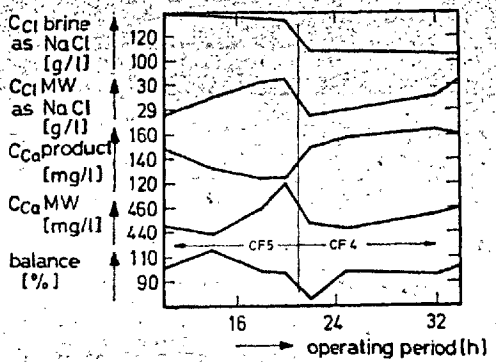

Fig. 18. Transitional behaviour.

concentrations and the balance in the zone of transition. The figures listed below refer to the stationary condition.

A particularly important factor determining the product quality, besides the number of stages, is the relation of the sea water throughput (Q) to the resin circulating speed (U), i.e. the pitch of the operating lines. Fig. 19 shows the stage efficiencies of the calcium exchange as a function of the quantity ratio (Q/U). A comparison of the figures obtained in the uniflow process and the fixed-bed test shows that the continuous countercurrent process results in a considerably improved product quality. Consumption of wash water is much lower in the case of the countercurrent process.

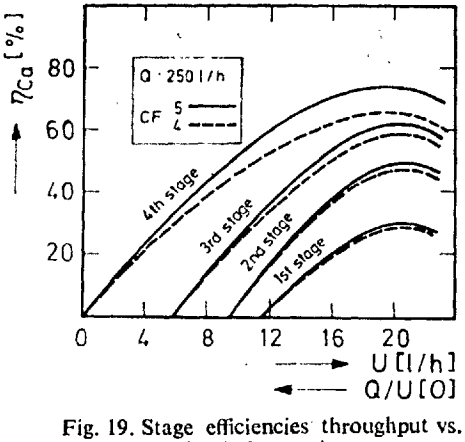

Fig. 19. Stage efficiencies throughput vs. circulation ratio.

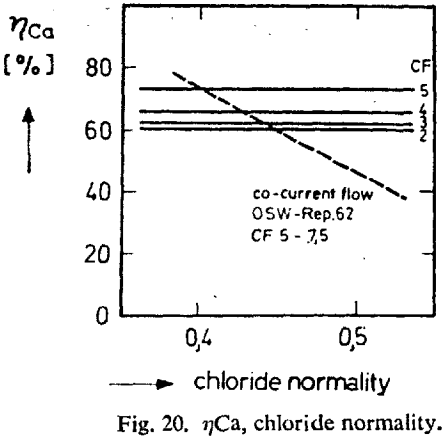

Fig. 20. ηCa, chloride normality.

There was no evidence suggesting that the efficiency of calcium exchange depended on the Na ion concentration, of the chloride ion concentration in sea water representative of it, with the operating conditions of the entire system being constant (Fig. 20). That is plausible; for while the exchange efficiency increases with decreasing chloride ion concentration in sea water, the regenerative effect of the

brine of constant concentration factor decreases. The two effects more or less appear to cancel each other out. The dependence of the uniflow charge stated in the OSW report 62 is probably due to constant concentration factors. Fig. 21 shows the relations between the calcium and the magnesium efficiencies. At higher concentration factors this relationship apparently changes in favour of the calcium efficiency.

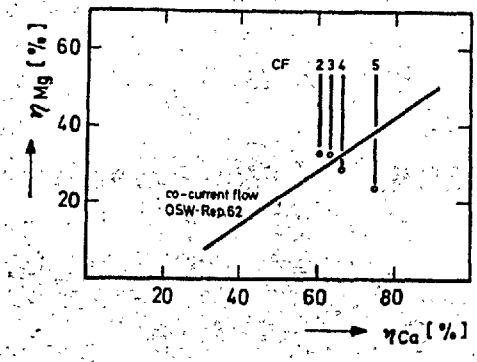

Fig. 21. Efficiencies ηMg, ηCa.

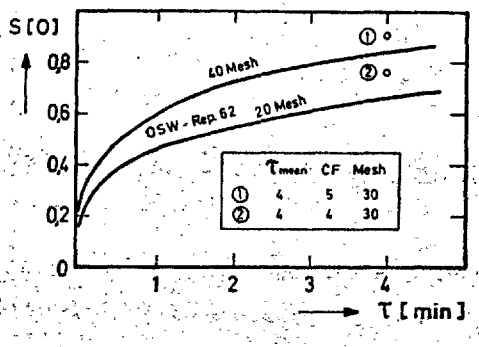

Fig. 22. Residence time tray efficiency.

As far as the ion exchange kinetics in the fluidized beds are concerned, comparatively high efficiencies could be achieved with a mean contact time of approximately 4 minutes per stage. Fig. 22 shows a number of experimental results obtained during continuous operation, and the dependence on the contact time measured intermittently in accordance with information released by the Dow Chemical Co.

4. SOLUBILITY OF CALCIUM SULPHATE AND COUNTERCURRENT ION EXCHANGE

The operating conditions of sea water desalination plants are determined by means of optimization calculations. The saturation temperatures at the optimum concentration factors are limits in such a programme. They can be found by comparing the exchange efficiencies with the saturation concentrations. Fig. 23 shows the saturation

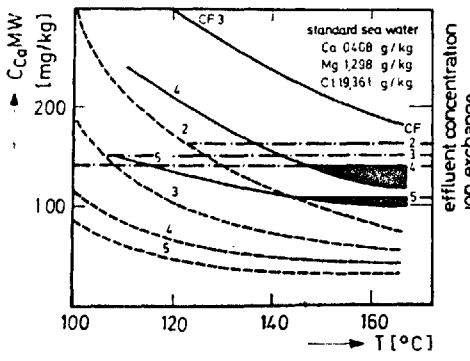

Fig. 23. Saturation temperatures.

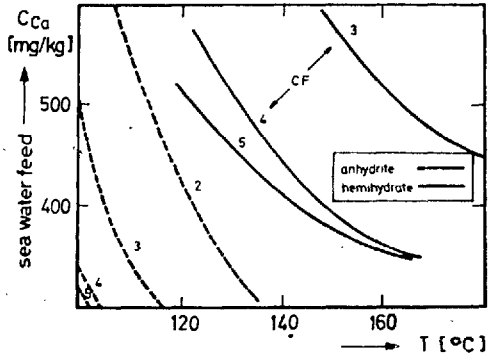

Fig. 24. Saturation temperatures vs. Ca content. of sea water

temperatures for the normal sea water concentration for various concentration factors. The saturation temperatures for different Ca ion concentrations in sea water are given in Fig 24. The graph in this figure indicates that the maximum temperature for sea water desalination plants operated in combination with ion exchange precleaning plant can be 160°C without reaching the saturation concentration of the hemihydate. If the operating temperatures do not exceed 120°C the Ca ion concentration remains below the anhydrite solubility limit.

REFERENCE

1. OSW, R and D Progress Report No. 62, Washington, D. C. (1962).